Self-Management, an Approach to Optimum Core Management of Thermal Reactors by Means of Ideal Burn-up Distributions

Thomsen, K. Ladekarl

Publication date:
1971

Document Version
Publisher's PDF, also known as Version of record

Risö Report No. 232

Danish Atomic Energy Commission

Research Establishment Risö

Self-Management, an Approach to Optimum Core Management of Thermal Reactors by Means of Ideal Burn-up Distributions

by K. Ladekarl Thomsen

November 1971

Sales distributors: Jul. Gjellerup, 87, Sölvgade, DK-1307 Copenhagen K. Denmark

Available on exchange from: Library, Danish Atomic Energy Commission, Risö, DK-4000 Roskilde, Denmark

U. D. C.
621.039.51

November, 1971 Risö Report No. 232

Self-Management, an Approach to Optimum Core Management of Thermal Reactors by Means of Ideal Burn-up Distributions

by

K. Ladekarl Thomsen

Danish Atomic Energy Commission
Research Establishment Risö
Reactor Physics Department

Abstract

In the multistage process, part of the decisions are separated from the remaining decisions by means of an internal optimality condition. This condition is either (1) minimum power form factor or (2) maximum fuel burn-up with limited power form factor. The external decisions regarding the power form factor at which the reactor is wanted to be operated, the number of the N concentric regions refuelled per cycle, and the enrichment of the reload fuel, are assumed given. The model is a one-dimensional, one-group model. The state of the fuel is described by the quantity $Q = \Sigma_a(k_\infty - 1) - DB_z^2$. The regions with lowest Q are refuelled. Fuel shuffling is performed as a synthesis of a "best fit" of the actual Q-distribution to an ideal Q-distribution, applied as a reference distribution. The ideal Q-distribution corresponding to a specific internal optimality condition is determined at equilibrium core conditions by simple iterative methods. The automated shuffling methods work without support from flux calculations. An absorber power shaping routine keeps the power shape fixed at the ideal shape.

This report was written in partial fulfilment of the requirements for obtaining the Ph. D. (lic. techn.) degree.

ISBN 87 550 0113 0

CONTENTS

Page

1. INTRODUCTION

Core management optimization concerns the optimization of fuel and absorber management which largely determines the power shape and fuel burn-up of a reactor. Fuel management is defined as the strategy for fuelling and refuelling the reactor. It includes decisions about the time of refuelling, the number and positions of fuel elements to be discharged, rearrangement of the remaining fuel elements and the enrichment of the fresh fuel that is loaded into the reactor. By absorber management we mean the operation of control absorbers such as control rods, soluble poison, and burnable poison.

This restricted definition of core management excludes the third constituent, which is management of the coolant flow. Even though the power shape is affected by the thermal and hydraulic relations, there are other factors which determine the optimum operation of the coolant.

There are strong economic incentives to invest research and development work in core management optimization. As a rule of thumb the capital investment in a large power reactor (~1000 MWe) is of the order of 1000 Mkr (M$ 130). Generally speaking capital constitutes 50-75%, fuel 15-40% and operation about 10% of nuclear energy costs. With improved power shape the reactor can be operated at a higher power level without violating the performance limits, thus reducing the capital costs per energy unit. Improved fuel burn-up will reduce the fuel costs. It is seen that even small improvements of power shape or fuel burn-up will result in large economic savings.

Formerly fuel management studies were based on one-dimensional calculations with fixed refuelling (or shuffling) schemes. In the search for the best refuelling scheme a number of different schemes were investigated, and the most profitable scheme with respect to power form factor and burn-up of the discharged fuel was chosen. A scheme which has found wide application for small to medium-sized power reactors is the three-zone out-in scheme, in which the fuel is loaded into the outer zone, shuffled inwards, and finally discharged from the central zone. For larger reactors this scheme gives bad power distributions with small power densities near the centre. In large reactors the scatter loading (often called salt-and-pepper) method, in which fuel elements of high and low irradiation are mixed among each other in a checkerboard pattern, is preferred. Very often the core is divided into a large central zone and a smaller outer zone. The power

shape may be flattened either by using a higher refuelling rate in the outer than in the inner zone or by using fuel of different enrichments in the two zones. The mixed scatter loading method is a variant in which the fresh fuel is loaded into the outer zone and shuffled to the inner zone in the next cycle, where it is mixed with highly irradiated fuel elements in a checker-board pattern.

Nowadays the refuelling schemes are investigated by means of two- or three-dimensional calculations, but one-dimensional calculations are still widely used in the search for profitable schemes, which requires a lot of fast survey calculations.

The development of large reactors has called for new methods in the optimization of the in-core fuel cycle. The "self-management" method is an attempt to solve the combined problem of fuel and absorber management optimization in thermal reactors. The work was started by B. Micheelsen with the development of the ONE-P programme (ref. 19), which used fixed shuffling schemes and a power flattening facility to keep the power flat by means of control absorber distribution. Later he started the development of a new programme ONE-SS, which included a preliminary version of the "irradiation flattening" method described in section 5.1[x].

This work was carried on in the present project with the development of the programmes IBU1 and SELMA1. The "self-management" method consists briefly in calculating an ideal burn-up distribution by means of IBU1 and using the ideal burn-up distribution as a reference distribution in the shuffling programme SELMA1. This programme includes a shuffling routine which automatically finds the "best fit" of the actual burn-up distribution to the ideal distribution. Further SELMA1 includes a new absorber power shaping routine which distributes the control poison during burn-up in such a way that a desired power shape is obtained. The ideal burn-up distribution satisfies one of the requirements (1) minimum power form factor or (2) maximum burn-up of the discharged fuel with limited power form factor.

---

[x] In that version the independent variable was the fuel burn-up. Later the convergence rate and normalization of the burn-up distribution to criticality has been improved by transformation of variables from burn-up to the "net production cross section".

2. GENERAL ASPECTS IN CORE MANAGEMENT OPTIMIZATION

Before describing the "self-management" method, which is the subject of this report, we shall review some general aspects of core management. First we consider the implications on reactor operation of different reactor designs and the problem of performance limits. Then the design of an optimum strategy is outlined in general terms. Finally we look at some previous approaches by other authors to the core management optimization problem.

2.1. Implications of Reactor and Fuel Design

At the start of a reactor the neutron production of the fuel is greater than the loss of neutrons by leakage and absorption in the fuel and moderator. The excess reactivity of the core is compensated by absorber materials. As burn-up proceeds, the amount of control absorber in the core is reduced. When all the poison has been withdrawn, the reactor gets subcritical, and the chain reaction cannot be maintained at a constant power level. Then some of the irradiated fuel elements have to be exchanged for new fuel, and the power production can proceed for another while. The refuelling process has to be repeated at regular intervals, so the life of a reactor can be regarded as a multi-stage process.

The main characteristics of this process are already determined at the assessment stage, at which it is decided whether refuelling is going to take place on-load or off-load, whether to use full-length or axially segmented fuel elements and whether to use radial and/or axial shuffling. Further the choice of initial core composition and type of control system influences the core management strategy.

Many of these questions, which concern the choice of reactor type, cannot be answered objectively. The answers depend on the importance assigned to the partly opposing requirements of minimum power cost, operating flexibility, and high availability and safety of the reactor.

On-load refuelling requires complicated equipment that works reliably at high temperature and pressure, whereas the equipment for off-load refuelling works at ambient temperature.

The on-load fuel management operations are performed at reduced power during the nights or weekends when the power demands are small. The increased costs and reduced reliability of complicated on-load refuelling equipment have to be balanced against the many merits. The capital to be invested in fuel and control system is reduced if the reactor is designed to

operate at small reactivities. The almost continuous on-load refuelling is very flexible for meeting variations in power need as well as for control of the overall power shape. The enrichment which is necessary to attain a desired fuel burn-up is smaller than with any batch refuelling.

In spite of these advantages most reactors in the world are refuelled off-load. The fuel is reloaded in batches of an order of magnitude of a third or a quarter of the core. The cycle time, which is the time between refuellings, is usually about one year, and the shut-down for refuelling is normally planned to take place in periods when the power consumption is small. However, the shut-down during refuelling reduces the availability of the reactor. In addition the large excess reactivity introduced with the fuel batches and the need for a more efficient control system imply higher capital costs. During a cycle the power shape can only be controlled by means of absorbers. High batch order reduces the enrichment that is necessary to attain a desired fuel burn-up, but has to be balanced against additional penalties of down-time. The limiting batch order corresponds to that of on-load refuelling.

Fuel shuffling constitutes a degree of freedom in reactor operation which can be used to get better control of power shape and fuel burn-up by appropriate mixing of irradiated and fresh fuel elements among each other. However, the more complex the shuffling pattern, the greater the expenses because of the need for more efficient shuffling machinery or increased down-time. Radial shuffling, which is most commonly used, has the advantage that it only requires full-length elements, which are cheaper than part-length elements. Axial shuffling can take place in the way used in the CANDU reactor, in which the fuel elements are pushed through the channels in opposite directions and at different rates in the different channels. More elaborate methods of axial shuffling would involve the discharge of complete channels and reloading of the segments in a different order. A rather simple possibility is axial inversion of full-length fuel elements.

Another factor with influence on the reactor and fuel design is the initial core composition, which presents a special problem, because it does not possess the spread of irradiations met in the equilibrium core. In fact the equilibrium core concept is an abstraction, since normal operation of a reactor throughout its life is a Utopia, but supposing the operation is normal and the same core management operations are repeated in each cycle, the state of the core approaches a state of equilibrium, called the equilibrium core. Normally the state of the core is pretty close to the equilibrium core already after the burn-up of one or two cores. An initial core composition

of fresh fuel at the reload enrichment all over the core is disadvantageous, partly because of its bad power distribution and discharge burn-up, and partly because of the investments in large excess reactivity and the equivalent amount of control poison.

The initial core can be improved in different ways. Frequently the initial core is composed of fuel elements of different enrichments distributed radially in such a way that a flat power distribution over the core is obtained. Of course axially segmented elements have the advantage that the power distribution can be flattened both axially and radially by placing fuel of the highest enrichment at the outer boundary of the cylinder as well as at the top and bottom. Instead of different enrichments we can use fuel containing burnable poison to solve the initial core problem, or we can simply start the reactor up with some empty fuel channels or channels with dummy elements.

A special, but rather doubtful (ref. 1) method to solve the problem of bad burn-up of the initial core is reinsertion in later cycles of partly irradiated fuel from the first cycle. Another method is that of fuel sharing between companion nuclear units that are started at a suitable time interval.

The implications of the design of the control system have been mentioned in different connections. Its major purpose of reactivity control can be fulfilled with soluble poison, whereas discrete absorbers are necessary for the purpose of power shaping. The different types of control systems are supposed to be well known. The efficiency of full-length control rods in power shaping is limited, because the rods are inserted from the top or bottom. More efficient power shaping would be possible with the use of part-length rods, which could be situated in the interior of the core in order to suppress local power peaks.

2.2. Performance Limits

In the operation of a reactor, care must be taken to ensure that the performance limits are not exceeded. The economic incentive to use the fuel and plant efficiently implies the desire to achieve high burn-up of the fuel at as high rating as possible without violating metallurgical criteria. These relate to such different effects as mechanical, thermal and radiation damage, can corrosion, fission product gas pressure, and melting.

The fuel elements are most seriously exposed to these effects since most of the heat generation takes place in the fuel itself. For the sake of fuel element integrity the maximum temperature of fuel and cladding is

restricted, as many of the damaging effects are functions of temperature. In water-cooled reactors melting of cladding will occur at excessive temperatures as a consequence of burn-out. The integral effect of can corrosion, which increases with temperature, is the limiting criterion in gas-cooled reactors. Anyway a limit on the maximum heat flux through the cladding surface must be evaluated for design purposes. This is in itself a very complicated task, as the maximum heat flux limit, besides being a function of the can temperature limit, strictly depends on the power distribution in the hottest channel as well as on the thermal and hydraulic parameters.

The maximum heat flux limit cannot be used directly in core management optimization, which at the present stage is performed by means of one- or two-dimensional models. These require the specification of a limit on the total power developed in the hottest channel, and this is done by relating the hot-channel power limit to the heat flux limit by means of the hot-channel factor concept (ref. 2). This concept, which relies on a series of approximations, allows for the spatial variation of the power development through a channel by the product of an axial power form factor for a "typical" power shape and a radial power form factor for the channel. In order to keep the maximum heat flux well below the upper limit in any situation, a lot of safety factors are introduced to account for deviations from the "typical" power shape. There are factors for deformation of the power shape as a consequence of partially inserted control rods and different constructional inhomogeneities. Other factors account for short-time operational variations in overall power shape and power level during burn-up, and still others are introduced because of manufacturing inaccuracy and computational uncertainty of the specific methods of treating the neutron flux and heat transfer problems.

Whether we use the conservative factor-product method or the statistical method, the combination of all the different factors constitutes the hot-channel factor. The hot-channel power limit is the maximum heat flux limit multiplied by the total surface area of all the fuel rods of an element and divided by the hot-channel factor. If the hot-channel power limit is divided by the mass of fuel in the element, we arrive at a limit on the average power density of the supercell. This hot-channel power density limit is usually specified as a performance limit in core management optimization calculations.

As a consequence of the integral damaging effects of corrosion, radiation damage, etc. the increasing brittleness puts an upper limit on the

burn-up of the fuel elements. Besides it is often forbidden to shuffle fuel elements of high burn-up because of increasing risk of handling damage, or it may be required to restrict highly burnt fuel to regions of low power density.

Two additional constraints of importance to core management optimization apply to the reactor itself. The reactor lifetime is restricted owing to wear-out of the structural materials or obsolescence of the design. The total power output of the reactor is limited by a design value, the nominal power, in order to match the reactor to the outer units of the plant.

Questions of safety and warranties of fuel and plant performance are closely related to the performance limits. Up till now suppliers have provided extensive warranties including fuel burn-up and operational safety. Of course such warranties require approval by the supplier of any change in the fuel management scheme that the operator may find preferable at the time of refuelling. Obviously the warranties have restrained the development and use of more elaborate techniques of fuel management. However, the situation is changing as the utilities build up staffs of nuclear engineers, which makes it possible for fuel management to become the responsibility of the utilities.

2.3. Ideal Core Management Optimization

In the design of an optimum operating strategy for a reactor the sequence of fuel management decisions may be considered as a multi-stage decision process. Similarly the absorber management decisions constitute a sequential process in the sense that the control rod pattern is changed at certain intervals. As burn-up proceeds between decisions, the reactor is maintained critical by moving the control system, so an additional condition is necessary regarding the coupling of the control absorbers between decisions. The coupling condition may for example be that criticality is maintained by insertion of all the control rods at equal speeds. Another example is control of the reactivity by means of soluble poison.

It is seen that the sequence of fuel and absorber management decisions together constitutes a multi-stage decision process (fig. 1). The input to box number j is the state x_{j-1} of the fuel at the end of the previous cycle and the state z_j of the fresh fuel. They may be given as matrices containing information about the composition (e. g. burn-up and enrichment) of the individual fuel elements. The set of decisions D_j includes all the fuel and absorber management decisions mentioned in the introduction. D_j determines the state of the core at the beginning of cycle number j. As D_j

further includes the cycle time, it is seen that the transformation of state x_{j-1} to x_j is given by D_j and the core burn-up relations. This can be written

$$x_j = f_1(x_{j-1}, D_j) . \tag{2.1}$$

Similarly the state y_j of burnt fuel discharged at stage j may be written

$$y_j = f_2(x_{j-1}, D_j) . \tag{2.2}$$

The energy production p_j during the cycle

$$p_j = f_3(x_{j-1}, D_j) \tag{2.3}$$

together with x_j and y_j constitute the output of stage j.

Besides x_{j-1} the input includes fresh fuel

$$z_j = f_4(D_j) \tag{2.4}$$

and manpower and materials for operation and maintenance,

$$o_j = f_5(D_j) . \tag{2.5}$$

In case of off-load fuel management a single fuel cycle may consist of several stages, since the control absorber pattern can be changed several times during the cycle. In the subcycles D_j only affects the control poison.

For a given reactor and fuel element design the optimum strategy is defined as the sequence of decisions $D_1, D_2 \ldots D_J$, which minimizes the production costs per energy unit without violating the performance limits. It is seen that for the optimum strategy the decisions at different stages are coupled via the state of the recycled fuel.

On the basis of the sequential model we shall now set up an idealized method to find the optimum core management strategy. In order to calculate the power production costs we have to evaluate the prices of z_j, y_j, and o_j by means of forecasts of fresh and spent fuel prices together with operating and maintenance costs. The net power production cost is the cost of z_j and o_j minus the value of the spent fuel y_j. In a realistic cost optimization the price of z_1 must include the capital costs of the whole plant as well as of the first core load, and the price of y_J must include the value of

the partly irradiated fuel of the last core as well as the costs of breaking up the reactor at the end of its life. The debit side of the balance sheet is the net power production costs for a sequence of decisions D_1, D_2, ... D_J, calculated by the "present worth" method, which requires a prognosis of the rate of interest during the reactor life. On the credit side the income depends on the total energy production of the reactor, so the "optimizer" must assume a certain utilization factor and availability (probability that the plant is available for power production at a given time) of the plant as a function of time. The power cost is assumed to be earned at the time of generation and reduced to "present worth". By requiring balance between debit and credit the unit energy cost is normalized.

Above we have implied the condition that the energy price remains constant during the life of the reactor. More generally we could assume an energy price policy, i. e. the unit energy price given as a function of time with one parameter free for the normalization. If the reactor is part of a power production system, the optimization is more complicated than for a single reactor, because the energy price policy and the forecast of the utilization of the reactor depend on the assumed variation and development in total power consumption by the grid, and on the past and future planning of the system.

The general optimization principle now is to calculate the unit energy cost for any possible sequence of decisions D_1, D_2, ... D_J that does not violate the performance limits, and select the sequence whose unit energy cost is minimum. Of course a complete optimization includes variation of the design parameters such as reactor size and fuel element design.

It might seem absurd to base an optimization on forecasts which reach many years into the future. In this connection, however, it should be remembered that the reduction to "present worth" assigns the highest weight by far to the plant costs and the first fuel loads. A much larger problem is the lack of suitable optimization methods which at the same time are realistic and sufficiently fast for use on present-day computers.

When the reactor is put in operation, the situation changes as guessing is gradually replaced by facts. Such unpredictable factors as refuelling dates, unscheduled shut-downs, unexpected changes in system capacity or load requirements, changing fuel prices and technology, reactor lifetime, rate of interest, improved computational techniques, etc. make it desirable to re-optimize the core management strategy continuously with feedback of operational data.

So far we have only considered fuel and absorber management optimization. This does not mean that the thermal and hydraulic relations are unimportant factors in core operation, but their influence on fuel and absorber management optimization is generally considered as secondary. The temperature and coolant mass distributions have some effect on the power shape, but in so far as the coolant flow through the individual channels can be varied separately by employment of different sizes of entry orifices, this is done with the purpose of improving the thermal - hydraulic performance, not for the sake of power shaping.

Reactivity control by means of varying void content is practised in boiling-water reactors. It could be included as a special example of the coupling condition between the control absorbers mentioned at the beginning of this section.

Coast-down operation, i. e. extension of the fuel cycle length at reduced power level, is a special feature which is generally excluded from theoretical optimization calculations. In practice, however, coast-down operation may be necessary or even desirable from an economic point of view, if it is compatible with the power requirements of the user.

2.4. Simplification of the Optimization Problem

As the optimization problem set up in the previous section is too large for present-day computer techniques, some simplifications are necessary. In fact the number of sequences to be compared is infinite as D_j includes decisions concerning the continuous variables, cycle time, fuel enrichment, and absorber pattern. In the following we shall deduce some qualitative results from the idealized model and introduce some hypotheses in order to discretize the problem.

In order to reduce the influence of capital costs on unit energy cost the total power output will have to be near the nominal power for as long time as possible. Any planned or unplanned shut-down because of refuelling, maintenance, or reduced power demands *increases* the capital part of the unit energy cost. Calculationally the reactor is supposed to operate at full power when in operation and out of power the rest of the time given by the utilization factor. Then the hot-channel power density limit can be transformed into a limit on the radial or XY power form factor, which is the ratio of peak to average power density in one- or two-dimensional geometry respectively.

The cycle time, i. e. the time between refuellings, is determined as the

time from refuelling until the reactivity or some equivalent quantity has reached some specified lower limit.

The fuel costs per energy unit are reduced by achieving an optimum combination of high burn-up and low enrichment without violating the burn-up limit. In practice this is usually consistent with achieving maximum permissible burn-up for as many fuel elements at as small enrichments as possible. As mentioned previously, the initial core may contain fuel of different enrichments. The enrichment of the replacement fuel in later cycles is either fixed or chosen among very few alternatives.

The reactor size is a very important parameter. If the reactor is small, the average power density must be high in order to achieve nominal power output. Consequently the power distribution over the reactor core must be rather flat without large peaks in order not to violate the form factor limit. However, as will be shown later a flat power distribution leads to rather bad burn-up of the fuel for a given enrichment, so perhaps a larger reactor will be better, since then the nominal power is achieved at a smaller average power density, which permits higher form factor and consequently larger burn-up.

In order to make the calculations practicable, we still have to introduce a lot of simplifications regarding the flux calculation, the number of free variables, and the coupling between decisions at different stages. Different authors have used different approaches, and it is difficult to see which of them is most profitable because in many cases the methods are tailored to special reactor types. Further the great differences of the various physical and economic (if any) models make comparison difficult.

In the next section we shall look at some approaches reported by other authors. We shall distinguish between two main cathegories of approach.

2.5. Previous Approaches

Several authors have applied the theory of dynamic programming to the fuel management problem. This method retains the sequential nature of the process with coupling between decisions at different stages. In all the dynamic programming references poison management is assumed to be separable from fuel management. A separate fuel management optimization, however, may only be fully justified for reactors with fixed control absorber pattern, e.g. reactors that are exclusively controlled by soluble poison. This is easily realized as the optimum refuelling decisions depend on the burn-up of the recycled fuel, which is partly determined by the absorber pattern via the power distribution.

Wall and Fenech (ref. 3) optimized the refuelling policy of a single-enrichment, three-zone, 1000 MWe PWR core. The state variable is a three-dimensional vector, whose components are the burn-up of the three zones. At each stage there are twenty-eight possible decisions which are the combinations of refuelling and shuffling of one, two, or three complete zones. The dynamic programming code uses precalculated predictions of the system behaviour during a cycle. These include end-of-cycle values of the zone irradiations, cycle length, and maximum power form factor given as polynomial functions of the fuel state at the start-of-cycle. The polynomials are least-squares fits to results from prior one-dimensional depletion calculations. The dynamic programming code calculates at each stage the power cost of a number of parallel sequences of decisions until that stage. Any time two or more sequences lead to similar end states, the sequence of minimum power cost is retained, while the others are eliminated. At the last stage the best sequence is chosen as the optimum policy. The results of a number of problems with different form factor and burn-up limits, but fixed reactor size are presented. As mentioned by the authors the conclusions regarding the optimum power form factor are obscured because the power level is specified as a fixed quantity instead of being a function of the form factor limit.

Stover and Sesonske (ref. 4) applied a similar technique to the optimization of a 1000 MWe BWR core with three-zone scatter-loading and no fuel shuffling. A number of discrete values are specified as the volume fractions of each zone which are allowed to be refuelled at each stage. The state of each fuel group is given by the U^{235} mass and the volume fraction.

Andersson (ref. 5) used up to four radial zones and discretized the fuel burn-up by introducing the "burn-up group" concept. The state of the core is given by the burn-up group of each of the zones. The optimization process proceeds backwards from the end-of-life. The transformation of the state vector between succeeding stages is treated statistically with a probability that a given state is transformed into another state. The model also gives a statistical treatment of uncertainties in fuel prices and cycle length.

Terney and Fenech (ref. 6) applied dynamic programming to poison management for a given fuel management scheme. The core was divided into two radial zones, and only three decisions were allowed at each stage, namely the three combinations of both, or one, of the control rod banks fully inserted and the other fully out. The objective was minimum power form factor.

The dynamic programming approaches suffer from loss of detail because the computing times restrict the application to problems with very few free variables. Further the refuelling decisions are confined to a very limited number of selected refuelling schemes. Nobody knows how close or far the best strategy achieved by these schemes is from a real optimum strategy.

The second category of approach need not reduce the number of free variables so drastically. Instead these approaches decouple part of the decisions D_j (cf. fig. 1) from the remaining decisions of the multi-stage process by introducing an additional condition which makes the optimum fuel and absorber distribution a function only of the state of the fuel at the moment of refuelling ("$x_{j-1} - y_j + z_j$" in fig. 1). The additional condition may be that the fuel and absorber distribution yield

(1) minimum power form factor or

(2) maximum fuel burn-up with limited power form factor.

As mentioned previously, the requirements of minimum form factor and maximum burn-up are non-compatible.

Melice (ref. 7) treated the fuel management problem of a three-zone mixed scatter-loaded PWR chemical-shim reactor by a method called the "semi-stationary method by optimization". The infinite multiplication factor k is used as a single variable to describe the fuel distribution over the core at any stage. In a cylindrical one-group model the optimal profile k(r) is derived analytically (with fixed zone boundaries). By introducing an "internal optimality condition", decisions D_j are separated into internal and external decisions. The internal decisions at each stage are decoupled from the remaining decisions of the sequence. The internal optimality condition is that at the start-of-cycle the optimal k-profile should be achieved (approximately) by shuffling. The external problem including decisions about the enrichments and numbers of fresh fuel elements fed into the core is treated by a sequential method. The author gives empirical rules for the synthesis of two-dimensional reloading patterns based on the one-dimensional optimal k-profile.

The ODYSSEUS code by Buckler (refs. 8 and 9) is a very realistic approach to the on-load core management problem in advanced gas-cooled reactors. The calculations are performed in two dimensions and two energy groups. A great number of different options are available. The element to be discharged is chosen by trial and error among highly irradiated elements in regions of low power. The element is "put back" if the form factor exceeds

a maximum limit, and an alternative is sought. Shuffling is possible. After each refuelling the power shape can be flattened by means of control rods, whose pattern is determined by an effective power shaping routine. The refuelling-time criterion is either on core reactivity or control rod insertion.

3. SELF-MANAGEMENT

In the following a new approach to the core management optimization is described. It belongs to the second category of approaches (cf. section 2.5), in which at each stage part of the decisions are decoupled from the remaining decisions of the multi-stage process by means of an internal optimality condition. The method is called "self-management", indicating that the selection of the detailed shuffling scheme and control absorber distribution at each stage is fully automated. Since the primary objective of the present study was to develop some basic optimization methods, a simple one-dimensional, one-group model was chosen. This model was found adequate for demonstration purposes and has the advantage of small computing times, which permits a great number of test calculations. It was the aim to retain as many general features as possible. Both on- and off-load management can be simulated, and a rather general shuffling scheme is implied. In this chapter the self-management method is explained in broad outline. The details will be considered in the following chapters.

The major part of the test calculations were performed with data for a BHWR 750 MWe design, a preliminary version of the BHWR-800 NORDIC STUDY (ref. 10). The reactor was designed for on-load fuel management, but both on- and off-load management is simulated in the calculations described in the following sections. The main data are given in table 1, and the core configuration is shown in fig. 2. The rest of the calculations were performed on the Yankee 392 MWe PWR reactor (ref. 11), the data of which are given in table 2.

3.1. The Reactor Model

The square lattice of fuel elements used in most reactors is inadequate for the one-dimensional model. The core is approximated by a cylinder and partitioned into N equivolume annular regions. A fuel region is defined as an annular volume in which the material constants D, Σ_a, etc. are independent of position, i.e. the regions consist of homogenized fuel of spatially constant enrichment, irradiation, etc. We adopt as an approximation

that all the regions contain equal amounts of fuel. The fuel between two consequtive region boundaries is called a batch. Fuel management operations, which include discharge, shuffling, and charge, are carried out batchwise in order not to violate the definition of a region.

In fig. 2 the core of the BHWR is partitioned into eighteen regions. It is seen that the region boundaries normally intersect the fuel elements, which gives rise to some difficulties in interpreting the results of a fuel management calculation. In the special case where there are many fuel elements, and the number of elements is an integer multiple of N, the fuel elements can be arranged in N groups in order of increasing distance from the core centre. Then the fuel management operations obtained as a result of calculations can be interpreted by identifying these groups with the fuel batches; but generally the batch movements cannot be transformed into fuel element movements. One only gets an impression of the directions and amount of fuel movements.

Therefore the value of one-dimensional calculations is mainly to estimate the performance with respect to power distribution and fuel burn-up for different modes of operation, different shuffling principles, etc. The investigations may be considered as preliminary studies for the development of a two-dimensional model. In two dimensions the individual fuel elements are supposed to take over the role of the fuel batches.

3.2. The Diffusion Equation

The steady-state, one-group diffusion equation, written in the form

$$\nabla \cdot D(\bar{r})\nabla\Phi(\bar{r}) - \Sigma_a(\bar{r})\Phi(\bar{r}) + k_\infty(\bar{r})\,\Sigma_a(\bar{r})\Phi(\bar{r}) = \lambda C(\bar{r})\Phi(\bar{r}) \qquad (3.1)$$

is reduced to one-dimensional cylinder geometry in the usual way by assuming cylindrical symmetry, separating the remaining two variables, r and z, and averaging the flux in the axial direction. The resulting equation is written in the following form

$$\nabla \cdot D(r)\nabla\varphi(r) + Q(r)\,\varphi(r) = \lambda C(r)\varphi(r)\,, \qquad (3.2)$$

where

$$Q(r) = \Sigma_a(r)\,(k_\infty(r) - 1) - D(r)\,B_z^2 \qquad (3.3)$$

is called the "net production cross section". The remaining symbols are:

$\bar{r}$	position vector	
$\Phi(\bar{r})$	neutron flux	
r	radius	
$\varphi(r)$	axial average neutron flux	
D(r)	diffusion coefficient	of fuel, moderator, and structural materials
$\Sigma_a(r)$	absorption cross section	
$k_\infty(r)$	infinite multiplication factor	
C(r)	absorption cross section of control poison	
λ	eigenvalue	
B_z^2	axial buckling.	

Equation (3.2) is solved numerically with the usual boundary conditions (no neutron current at the centre and extrapolation distance at the outer boundary of the reflector). The solution is either by traditional eigenvalue techniques or a power shaping method that distributes the control absorber C(r) in such a way that a specified power shape is obtained approximately. Details of the numerical methods are given in chapter 4. The power distribution is used in a simple interpolation burn-up routine, based on tabulations of one-group homogenized cell data given as functions of fuel burn-up in MWD/TU.

3.3. The State of the Fuel

For a given fuel type the net production cross section Q, the diffusion coefficient D, and the fission cross section Σ_f are given in a table as functions of the irradiation I. By introducing Q the diffusion equation (3.2) has got a very simple form, and a column is saved in the burn-up table (k_∞ and Σ_a are never used separately).

The burn-up tables for the BHWR were calculated by means of the point burn-up programme PBU (ref. 12), which is based on the heavy-water lattice programme TATAR (Ref. 13), utilizing the four-factor formula, two-group theory, and Westcott cross sections. The two-group constants obtained as a result of the PBU calculations were condensed to one energy group, and the net production cross section Q was calculated according to (3.3).

In fig. 3, Q is shown as a function of irradiation for a BHWR element with natural uranium and depleted uranium of different U^{235} contents. The

first term in (3.3) is the production minus the absorption cross section (hence the name "net production cross section"). The second, the axial leakage term, is rather small and almost independent of irradiation. The shape of Q vs. I is similar to the variation of the reactivity with xenon build-up in the start and a plutonium top at about 1500 MWD/TU. The variation of D and Σ_f with irradiation is shown in fig. 4.

For the 3.4% enriched PWR element of the Yankee reactor, Q vs. I is shown in fig. 5. In this case Q declines monotonically with irradiation. The burn-up table was calculated by the LASER programme (ref. 14).

The burn-up tables give a rather coarse description of the state of the core. For example, the void in the BHWR is accounted for simply by assuming a constant void content of 50%, and D is assumed independent of the control poison cross section C. Xenon is included in the cell data. As mentioned previously, this simple model was chosen for demonstration purposes. However, it should be stressed that the self-management method is not bound to this specific model. The optimization principles are thought to be sufficiently general to be applied with minor modifications in a more elaborate model.

If only one fuel enrichment is present in the core, the state of the fuel is completely specified in our model by a N-dimensional vector I_n, $1 \leq n \leq N$, whose components are the irradiations of the N fuel batches. For the initial core, in which fuel of different enrichments is allowed in the different regions, the state of the fuel is given by the 2N parameters (I_n, e_n).

3.4. Separation of the Decisions

In fig. 1 the state x_j of the fuel at the end-of-cycle j shall be taken as (I_n^j, e_n^j), $1 \leq n \leq N$. The decisions D_j are separated into internal and external decisions.

Internal decisions:

(a) Cycle time

(b) Selection of batches to be discharged

(c) Fuel shuffling

(d) Control poison distribution

External decisions:

(e) Number of regions N_d to be refuelled

(f) Enrichment e of fresh fuel

(g) Choice of internal optimality condition.

The work described in this report is mainly concerned with the internal decisions, which are decoupled from the multi-stage process by means of an internal optimality condition.

In chapter 8 it will be shown how the external decisions are thought to be optimized in an external sequential process which determines the number of regions to be refuelled and the enrichment of the fresh fuel at each stage. For the present we shall take these quantities as given in the following way:

The initial core is given by (I_n, e_n), specified as input. The number of regions N_d to be refuelled at later stages and the enrichment e of the fresh fuel are constant through the life of the reactor. On-load operation is simulated by putting $N_d = 1$, and off-load by giving N_d a larger value (e.g. $N_d = \frac{1}{3}N$).

The first internal decision concerns (a), the cycle time. The refuelling-time criterion is connected with the core average control poison cross section $\bar{C}$. The time of refuelling is determined as the time when $\bar{C}$ has reached a lower limit $\bar{C}_d$. The discharge limit $\bar{C}_d$ is specified as zero in off-load simulation. In on-load simulation $\bar{C}_d$ is given a value which permits restart in the xenon build-up period after shut-down.

The selection of batches to be discharged (b) is regarded as an internal decision. The N_d batches with the lowest net production cross section Q at the end-of-cycle are discharged. For the equilibrium core, in which only one enrichment is present, this is consistent with a highest burn-up criterion of the discharged fuel. The discharge criterion also applies to the first stages, in which the core is allowed to contain fuel of different enrichments. The criterion is considered reasonable as low Q means poor neutronics properties (e.g. if the choice is between two batches with equal burn-up, but different enrichments, the batch with the smaller enrichment will be discharged).

The fuel shuffling (c) and control poison distribution (d) are determined by an internal optimality condition. This condition is either

(1) minimum power form factor or

(2) maximum fuel burn-up with limited power form factor.

In fact (1) is a special case of (2), but they are separated because the numerical treatment of problem (1) is simpler than problems of type (2). The decision of the form factor limit is regarded as an external decision (g), and will be considered in chapter 8. So far the form factor limit is specified as input.

Even with our simple one-dimensional, one-group model it is impossible to carry out the N! eigenvalue calculations for all permutations of the N fuel batches, which would be necessary to decide which shuffling is best (for a given control poison distribution).

The fuel shuffling in the self-management method is determined by the condition that the radial Q-distribution after shuffling shall be the best fit to an ideal Q-distribution satisfying one of the internal optimality conditions.

In the next section we shall see how such ideal Q-distributions can be determined.

3.5. Ideal Fuel Distribution

We shall consider an equilibrium core situation at the time of refuelling. N_d regions are refuelled with fuel of enrichment e, and we are going to shuffle the fuel with the aim of fulfilling an internal optimality condition. Suppose this condition is of type (1), minimum power form factor.

Any fuel shuffling decision will change the burn-up distribution. If we adopt the convention that the batch index n corresponds to the region number which increases in order of increasing distance from the core centre, the burn-up distribution is given by the vector I_n, $1 \leq n \leq N$. In the following the index limits on the region number are omitted. It will be apparent from the context when I_n is a vector or burn-up distribution, and when it is the burn-up of region number n.

For the present we shall suppose that the control poison distribution over the core is given. Then the power form factor F is a function of I_n:

$$F = g(I_n). \tag{3.4}$$

The ideal Q-distribution is found by transformation of variables I_n to Q_n and search for the Q-distribution that makes F minimum.

In most reactors there is a one-to-one correspondence between Q and I. Then D and ν_f can be regarded as functions of Q, and the state of the fuel may be given by Q_n instead of I_n. In case Q is not a monotonous function of I (as for example in the BHWR, fig. 3), it is monotonized artificially by cutting off the part with small irradiations below the plutonium top.

The transformation of variables changes equation (3.4) into

$$F = f(Q_n). \tag{3.5}$$

The method used to calculate the ideal Q-distribution corresponding to minimum power form factor is a very simple iterative method. F is regarded as a continuous function of the N independent variables Q_n. The iterations start with a guess at the Q-distribution, and the power distribution is calculated. At the next iteration the components of Q_n are reduced in regions where the power density is greater than the average power density and increased in regions where the power density is smaller than the average over the core. Then a new flux-eigenvalue calculation is performed and so on, until the Q-distribution converges. At each iteration step the Q-distribution is normalized to a level that makes the reactor just critical at the specified control poison distribution ($\lambda \rightarrow 1$). The power distribution corresponding to the converged Q-distribution is very flat. In fig. 13 is shown a typical example of an ideal Q-distribution with minimum power form factor

A somewhat different and more involved iterative method is used if the internal optimality condition is of type (2), maximum fuel burn-up with limited power form factor. We shall not go in detail here as both methods are described in chapter 5. An example of the ideal Q-distribution corresponding to condition (2) is seen in fig. 17.

The ideal Q-distribution is calculated by means of a separate computer programme, IBU 1. The output is the ideal Q-distribution and the corresponding distributions of flux, power density, and control poison. In the following they will be marked by an asterisk (Q^*, φ^*, p^*, and C^*).

Actually the normalization of Q_n at each iteration means that the reactor is iterated critical on Q. Consequently the C^*-distribution is equal to the input specified control poison distribution. Of course the results depend on the shape and level of the poison distribution. Very often a uniform poison distribution is specified. Its level is determined by whether we wish to calculate the ideal Q-distribution corresponding to the beginning- or the end-of-cycle. If we choose a high poison level as representative of the start-of-cycle, the level of the ideal Q-distribution Q_n^* gets correspondingly high. Conversely, if $\overline{C}^* = \overline{C}_d$ (the discharge limit), the level of Q_n^* gets low corresponding to end-of-cycle.

The ideal distributions are used as references in the shuffling and absorber power shaping routines of the core management programme outlined in the next sections. The ideal Q-distribution is calculated prior to the core management calculations, and the same Q_n^* is used throughout the life of a reactor.

3.6. The Self-Management Method

At the start of each cycle the specific shuffling scheme that satisfies the internal optimality condition must be determined. After shuffling, the Q-distribution must resemble the ideal Q-distribution Q_n^*. A good deal of the work described in this report was devoted to the development of empirical rules suitable for fitting the actual Q-distribution to the reference Q_n^* in a fast and automatic (self-managing) way. Several different empirical rules for the synthesis of a "best fit" were devised and tested. An account of the best shuffling principles is given in chapter 7.

For the best fit of the Q-distribution to Q_n^*, the power shape p_n (from a flux-eigenvalue calculation) resembles p_n^* fairly well. The power shape may be further improved by the absorber power shaping routine which distributes the control poison with p_n^* as the target power shape. The control poison is redistributed at each burn-up step in order to keep the power shape constant during the cycle.

There are two different ways of using the ideal Q-distribution and the absorber power shaping routine as tools in the core management calculations. In the first way, the ideal Q-distribution Q_n^* refers to the beginning-of-cycle and in the second to the end-of-cycle (cf. section 3.5).

In the first case the shuffling rules can be applied directly, as the state of the fuel at the start-of-cycle is known at the shuffling time. The control poison is used to keep the power shape constant during the cycle. However, the method has the drawback that the Q-distribution that is good at the start-of-cycle will change during burn-up and move away from the ideal distribution towards the end-of-cycle. This is partly due to nonlinearity of Q vs. I (cf. fig. 3) and partly to uneven burn-up of the core, which is more pronounced the higher the power form factor is. The deviation of the Q-distribution from the ideal distribution at the end-of-cycle results in deviation of the power shape from p_n^*, and the power shaping routine is rather inefficient at the end-of-cycle, when the control poison is retired from the core.

In the second method an attempt is made to avoid the drawback of bad power shape at the end-of-cycle. This is done by rearranging the fuel at the start-of-cycle in such a way that the end-of-cycle Q-distribution fits Q_n^* which is here the ideal Q-distribution corresponding to end-of-cycle conditions. As the state of the fuel at the end-of-cycle is not known at the time of shuffling, we have to predict the end-of-cycle state. This is done by a prediction of the cycle time Δt_c and the assumption that the flux distribution is main-

tained constant equal to φ_n^* during the cycle. Then the irradiation at the end-of-cycle is predicted as

$$I_n^!(\Delta t_c) = I_n(0) + a\nu_{f,n}(0)\,\varphi_n^*\,\Delta t_c \,. \qquad (3.6)$$

In this expression the time is set to zero at the start-of-cycle. a is a normalization constant. $Q_n^!(\Delta t_c)$, which is the predicted net production cross section, is now obtained from the burn-up table. Then the shuffling procedure works on $Q_n^!(\Delta t_c)$, which is fitted to the ideal Q-distribution Q_n^*. The shuffling routine determines the shuffling scheme and thereby the burn-up distribution at the start-of-cycle $I_n(0)$.

Used in this second manner the shuffling routine gives a Q-distribution which may be rather far from ideal at the start-of-cycle. However, the power shaping routine is very effective at the start-of-cycle when the control poison level is high, so the power shape can be kept near p_n^*. After shuffling, burn-up proceeds from $I_n(0)$ with the correct power shape p_n as obtained from the power shaping routine. Towards the end-of-cycle the Q-distribution approaches the ideal distribution Q_n^*. This has the advantage that absorber power shaping becomes unnecessary as the control absorbers are withdrawn.

The success of this latter method depends on the ability of the power shaping routine to keep the power shape constant during the cycle. However, it seems to give better results than the former, and it is the method that was preferred in most of the calculations described in this report.

3.7. The Core Management Programme SELMA1

The various shuffling routines are included as options in the core management programme SELMA1. We shall now consider the proceeding of the internal decisions through the life of a reactor by means of the generalized flow diagram of SELMA1 (fig. 6).

The state of the initial core is given by I_n and e_n. Normally $I_n = 0$ at the start. For each enrichment a burn-up table is supplied. Further the ideal Q-distribution Q_n^* and the corresponding flux, power, and poison distributions are given. The region constants D, Q, and Σ_f are found by interpolation in the burn-up table and used in the eigenvalue-flux routine. After convergence we proceed along the path mp = 0 to the power density and form factor calculation. If the initial core contains more than one fuel type (enrichment), we go to the shuffling routine, where the cycle time Δt_c

is predicted and shuffling carried out according to one of the shuffling principles just mentioned*.

After shuffling we return to a new eigenvalue calculation. If we follow the path mp = 1, an absorber power shaping is performed. The resulting power distribution is now used in a burn-up step in the blocks below at the left in the diagram. If $p_n(t)$ is the average power density (MW/TU) of region number n at time t, the irradiation at the end of the time step Δt_b is

$$I_n(t + \Delta t_b) = I_n(t) + p_n(t)\,\Delta t_b \tag{3.7}$$

assuming that the change in power distribution during the time step is negligible.

The burn-up block is passed a number of times in each cycle. After each burn-up step the flux and power shaping calculations are repeated. Burn-up proceeds in time steps Δt_b of an input specified length until the control poison average $\bar{C}$ reaches the discharge limit $\bar{C}_d$. The last time step of the cycle is reduced by means of a prediction of the time when $\bar{C}_d$ is reached. As the decreasing rate of $\bar{C}$ is almost constant, the upper limit I_m to the average core irradiation $\bar{I}$, at which it is expected that $\bar{C} = \bar{C}_d$, is predicted as

$$I_m = \bar{I} + (\bar{C}_d - \bar{C})\,\frac{d\bar{I}}{d\bar{C}}. \tag{3.8}$$

Then the time τ until the next discharge is predicted as

$$\tau = \frac{I_m - \bar{I}}{\bar{p}}, \tag{3.9}$$

where $\bar{p}$ is the average power density. I_m and τ are currently adjusted. When τ becomes less than the input specified time step, the cycle is finished with a time step $\Delta t_b = \tau$. I_m is stored until the next cycle.

In the next pass through the question "time for next discharge?" the answer is "yes". Then the N_d regions with the lowest Q are refuelled, and a new eigenvalue-flux calculation performed. Now the answer to the question "time just after discharge?" is "yes", and fuel shuffling is carried out. The

* The shuffling principles were explained for a Q-distribution whose variation in Q_n was due to different burn-ups of the different regions, but they also work for the initial core where the variation in Q_n is due to different enrichments.

succeeding cycles proceed analogously to the first cycle. The calculations are finished when the integrated time exceeds the specified reactor life. The description of the block diagram was made in terms of the most general application. The coupling of the blocks may be varied in different ways (e. g. if mp = 2, the flux-eigenvalue routine is skipped).

The most important results from the calculations are the power form factor and discharge burn-up, which are plotted as functions of time in a lot of different cases (chapter 7).

4. SOLUTION OF THE DIFFUSION EQUATION

In section 3. 2 the diffusion equation was written in the form

$$\nabla \cdot D(r)\nabla\varphi(r) + Q(r)\,\varphi(r) = \lambda C(r)\,\varphi(r)\,, \tag{4.1}$$

where

$$Q(r) = \Sigma_a(r)\,(k_\infty(r) - 1) - D(r)\,B_z^2 \tag{4.2}$$

is the "net production cross section". The boundary conditions are:

$$\nabla\varphi(0) = 0 \tag{4.3a}$$

$$D(R)\nabla\varphi(R) = \delta\varphi(R), \tag{4.3b}$$

where R is the radius of the outer boundary of the reflector, and $\delta = D(R)/\lambda_{ex}$. If we assume a linear extrapolation distance $\lambda_{ex} = 0.71\,\lambda_{tr}$, we have $\delta = 0.467$.

In this chapter it is shown how the diffusion equation is solved numerically by traditional eigenvalue techniques. Besides an absorber power shaping method is described in which the control absorbtion cross section C(r) is distributed in such a way that a desired power shape is obtained approximately.

4.1. The Difference Equations

The fuel regions and the reflector are subdivided into meshes. D(r), Q(r) and C(r) are assumed constant meshwise. According to ref. 15 the set of finite difference equations is developed with the flux points in the middle of the meshes and linear approximation of the flux in each mesh

(cf. fig. 7). By integrating equation (4.1) over mesh number i it follows that

$$d_{i-1}\,\varphi_{i-1} - (d_{i-1}+d_i)\varphi_i + d_i\,\varphi_{i+1} + Q_i V_i \varphi_i = \lambda C_i V_i \varphi_i\,, \quad 1 \le i \le I \tag{4.4}$$

where

$$d_i = \frac{4D_i\,D_{i+1}\,r_i}{D_{i+1}(r_i - r_{i-1}) + D_i(r_{i+1} - r_i)} \tag{4.5}$$

$$Q_i = \nu_{a,i}(k_{\infty,i} - 1) - D_i B_z^2 \tag{4.6}$$

$$V_i = r_i^2 - r_{i-1}^2$$

r_i is the outer radius of mesh number i.

At the centre and the outer boundary of the reflector a pseudo-mesh is added. The leakage constants (4.5) and the leakage terms in (4.4) give the correct leakage through the boundaries if

$$d_o = 0 \tag{4.7a}$$

$$\frac{r_{I+1} - r_I}{D_{I+1}} = \frac{2}{\delta}\,, \qquad \varphi_{I+1} = 0. \tag{4.7b}$$

One of the quantities r_{I+1} and D_{I+1} may be chosen freely. For ease of computation $D_{I+1} = 1$. With this choice the leakage is correct even though the boundary condition (4.3b) is not fulfilled.

4.2. Eigenvalue Solution

In matrix form the difference equations (4.4) are written

$$(\bar{\bar{Q}} - \bar{\bar{D}})\bar{\varphi} = \lambda \bar{\bar{C}}\bar{\varphi}\,, \tag{4.8}$$

the symbols being self-evident by comparison with (4.4).

The outer iterations are performed according to

$$\lambda^{(m)} = \frac{\bar{\varphi}^{T,(m-1)}(\bar{\bar{Q}} - \bar{\bar{D}})\,\bar{\varphi}^{(m-1)}}{\bar{\varphi}^{T,(m-1)}\,\bar{\bar{C}}^{(m-1)}\,\bar{\varphi}^{(m-1)}}\,, \tag{4.9}$$

where m is the iteration step, and $\bar{\varphi}^T$ is the transposed flux vector. Actually (4.9) is a variational expression since the transposed flux is equal to the adjoint flux in this simple one-group, one-dimensional case. Therefore $\lambda^{(m)}$ converges very fast to the smallest eigenvalue λ_0 (supposing any critical control poison proportional to $\bar{\bar{C}}$ exists. If too many diagonal entries in $\bar{\bar{C}}$ are zero, $\lambda^{(m)}$ diverges).

Each eigenvalue iteration is succeeded by the adjustment[x]

$$\bar{\bar{C}}^{(m)} = \lambda^{(m)}\, \bar{\bar{C}}^{(m-1)} . \tag{4.10}$$

Consequently $\lambda^{(m)} \to 1$.

The inner iterations start at every iteration step m by splitting the diagonal matrix $\bar{\bar{Q}} - \bar{\bar{C}}^{(m)}$ into two new diagonal matrices $\bar{\bar{A}}^{(m)}$ and $\bar{\bar{B}}^{(m)}$, both of which are non-negative. The diagonal entries of $\bar{\bar{A}}^{(m)}$ and $\bar{\bar{B}}^{(m)}$ are

$$\left.\begin{aligned} A^{(m)}_{i,i} &= (Q_{i,i} - C^{(m)}_{i,i})\, V_{i,i} \\ B^{(m)}_{i,i} &= 0 \end{aligned}\right\} \quad Q_{i,i} > C^{(m)}_{i,i}$$

$$\left.\begin{aligned} A^{(m)}_{i,i} &= 0 \\ B^{(m)}_{i,i} &= (C^{(m)}_{i,i} - Q_{i,i})\, V_{i,i} \end{aligned}\right\} \quad Q_{i,i} \leq C^{(m)}_{i,i} \tag{4.11}$$

where $Q_{i,i}$, $C_{i,i}$, and $V_{i,i}$ are the constants from eq. (4.4).

Now by (4.8) and (4.11) we have

$$\bar{\varphi}^{(m)} = (\bar{\bar{D}} + \bar{\bar{B}}^{(m)})^{-1}\, \bar{\bar{A}}^{(m)}\, \bar{\varphi}^{(m-1)} \tag{4.12}$$

as the expression for the new flux iterate (only one inner iteration per outer iteration).

As $\bar{\bar{B}}^{(m)}$ is non-negative, $\bar{\bar{D}} + \bar{\bar{B}}^{(m)}$ is diagonally dominant. It is easily seen that among all the ways in which the matrix $\bar{\bar{Q}} - \bar{\bar{C}}^{(m)}$ can be split into two non-negative matrices, $\bar{\bar{A}}_1^{(m)}$ and $\bar{\bar{B}}_1^{(m)}$, subject to the condition $\bar{\bar{Q}} - \bar{\bar{C}}^{(m)} = \bar{\bar{A}}_1^{(m)} - \bar{\bar{B}}_1^{(m)}$, the splitting (4.11) is the one that makes $\bar{\bar{A}}_1^{(m)}$ minimum. It can be shown that under these circumstances the flux converges safely with the maximum convergence rate (ref. 16).

[x] This adjustment is only used in SELMA1, not in 1BU1, where (4.10) is replaced by $\bar{\bar{C}}^{(m)} = \bar{\bar{C}}$, and $\bar{\bar{C}}^{(m)}$ is replaced by $\lambda^{(m)}\, \bar{\bar{C}}^{(m)}$ in the following expressions.

The flux routine used in the present work is based on the principles outlined above. The matrix inversion problem (4.12) is solved by the direct method (ref. 17, p. 195). The convergence demand is that $\lambda^{(m)}$ satisfies the condition

$$\left| 1 - \lambda^{(m)} \right| < G \tag{4.13}$$

two consequtive times.

After convergence the power distribution is calculated by

$$p_i = a \Sigma_{f,i} \varphi_i \,. \tag{4.14}$$

The normalization constant a is found by requiring that the average power density over the core $\bar{p}$ is equal to a specified value.

The radial power form factor F is defined by

$$F = \frac{p_{i,\,max}}{\bar{p}} \,. \tag{4.15}$$

The flux routine is tested with the TWODIM programme (ref. 18), and the results are found in full agreement with the TWODIM results. With $G = 10^{-4}$ and a flat start flux, convergence is normally obtained after six to eight iterations, and the maximum relative flux change in the last iteration is about 0.1%. As an example the upper part of fig. 10 shows the power distribution in the core of the BHWR 750 MW for the burn-up distribution shown below and a uniform control poison distribution in the core. It is seen that the results of the coarse mesh calculation do not differ significantly from the fine mesh calculation. The rest of the figure is commented in the next section.

In fig. 10 and the following figures the distributions of power, burn-up, etc. are plotted on a volumetric scale instead of a linear radial scale. Then all the regions get equal weight in the visual impression of for example a power distribution. A linear scale would be disadvantageous because the central regions would seem to be more important than the outer regions.

4.3. Absorber Power Shaping

With eigenvalue techniques the flux and power distribution is calculated for a given control poison distribution. However, the inverse problem to find the control poison distribution that gives the power distribution a specified shape is of great practical importance. In the ONE-P programme

(ref. 19) power flattening was accomplished iteratively in a routine which alternates between the usual flux-eigenvalue calculation and adjustments of the poison distribution in order to suppress local power peaks. This method is analogous to the "irradiation flattening" techniques described in section 5.1.

In this section a more direct method developed after an idea by Crowther (ref. 20) is described. Later the method was found to have many features in common with the two-dimensional power shaping method applied in the latest version of the ODYSSEUS code (ref. 9).

4.3.1. Theory

Power shaping is accomplished by means of a control poison distribution which may be restricted to certain meshes called "control meshes". Each control mesh belongs to a "control domain" comprising one or several meshes. The control meshes and control domains must be specified in such a way that each control domain contains exactly one control mesh. Fig. 8 symbolizes a case with six control meshes numbered c_1, c_2, ... c_6. The domains are indicated by the dashed lines. The vertical arrows numbered f_1, f_2, ... f_6 indicate "fixpoints", i.e. meshes, in which we want the power density p to be equal to the specified reference power density p^*. In these fixpoints the flux is simply found as the power density divided by the fission cross section. In the general case with m control meshes and m fixpoints we have

$$\varphi_i = \frac{p_i^*}{\Sigma_{f,i}} \quad , \text{ m equations.} \tag{4.16}$$

Out of the I equations (4.4) we now select those in which $C_i = 0$ for the flux solution

$$d_{i-1}\varphi_{i-1} - (d_{i-1} + d_i)\varphi_i + d_i\varphi_{i+1} + Q_i V_i \varphi_i = 0, \quad \text{I-m equations.} \tag{4.17}$$

The solution of (4.17) proceeds in the way illustrated by arrows in fig. 8 From the centre to the first fixpoint f_1 the equations (4.17) are solved by the direct method, the recursion formulae of which are given in ref. 17, p. 195. The forward elimination - backward substitution techniques of this method are symbolized by the reversing arrow I. Now, the flux being known in all meshes $i \leq f_1$, φ_{f_1+1} directly results as the only unknown of (4.17) for $i = f_1$ This is repeated along arrow II, until the control mesh c_1 is reached. From c_1 onwards till f_2 we have to use the direct method again, since the differ-

ence equations of the control meshes are reserved for the purpose of finding the control poison cross sections. Along IV the simple method of II applies again. From c_2 we cannot go on because there is no fixpoint between c_2 and c_3. However, there are no control meshes between the fixpoints f_4 and f_5, so the direct method can be used to solve (4.17) along V. From f_4 we can now move towards the centre alternating between the two methods of solution until c_2 is reached. Then we move outwards from f_5 until (4.17) is completely solved.

Generally speaking we move outwards from the centre until we meet two control meshes without any fixpoints between them. Then we jump to the next two fixpoints without any control meshes between them or to the reactor boundary and solve (4.17) inwards. After that, we move outwards in the same way as before, ending at last on the outer boundary. It is seen that the flux can always be found directly from the l equations (4.16) and (4.17).

The remaining difference equations, i.e. the equations for the control meshes,

$$d_{i-1}\varphi_{i-1} - (d_{i-1}+d_i)\varphi_i + d_i\varphi_{i+1} + Q_i V_i \varphi_i = C_i V_i \varphi_i, \quad \text{m equations,} \quad (4.18)$$

are written without a λ in the control absorber term as the problem is not an eigenvalue problem. The values of C_i are determined by (4.18). They are the control poison cross sections that make the power distribution equal to the reference power distribution in the fixpoints.

Before the method is complete, two problems must be solved. The first one is that C_i may turn out to be negative. The second one is to determine the positions of the fixpoints.

These problems are overcome by iteration in the way described by the block diagram of fig. 9. If the control poison cross section of a mesh is negative in one iteration, it is returned to zero, and the relevant equation (4.18) is converted to the form (4.17). At the same time the flux is released all over the corresponding domain, omitting the relevant equation (4.16). The fixpoint may be said to be passive now. The fixpoints are chosen so as to make the (unnormalized) power density $p_i = p_i^*$ in the fixpoints and $p_i \neq p_i^*$ in all other meshes. Oviously this condition leads to excellent power flattening if $p_i^* = 1$ for all i because then the fixpoints will be the mesh-points with maximum power density.

The block diagram starts with $C \neq 0$ only in the control meshes. The control meshpoints are arbitrarily chosen as fixpoints. Then the flux, power and poison distributions are calculated as described above. Now, if

$C < 0$ in any mesh, we put $C = 0$ and return to the flux calculation. In the flux calculation all the fixpoints corresponding to control meshes with $C = 0$ are made passive in the way just described. If $C \geq 0$ in all meshes, we search for new fixpoints based on the power densities of the last iteration. The fixpoint of each domain is chosen as the meshpoint in which $p - p^*$ is maximum within the domain. If $p - p^* > 0$ in a fixpoint, this indicates that the fixpoint has shifted to a new mesh during the last iteration, and consequently a new iteration is necessary. One could imagine that $p - p^* > 0$ in the fixpoint of a domain, whose control poison $C = 0$ from a previous iteration. In this case we put $C = 1$ in this control mesh before returning to the flux calculation in order to be able to control the power in this domain. The calculations are terminated when $p = p^*$ in all active fixpoints. Finally the flux and power density is normalized in the same way as described in the previous section.

As the flux problem (4.17) is solved without relaxation techniques, the solution is mathematically exact apart from rounding errors in the computer. Therefore it can be used as a reference in investigations of convergence of the eigenvalue method in a problem where the poison distribution resulting from the power shaping method is used as input in the flux routine described in the previous section. Conversely, the eigenvalue-flux solution can be used to check that the flux routine of the power shaping method works correctly.

Because of the direct nature of the power shaping method only about three or four iterations are normally necessary, so it is still faster than the eigenvalue-flux routine.

Of course the method must give up when the reactor is subcritical, as the poison of all the control meshes then tends to be negative; but otherwise it is very reliable and has worked satisfactorily in several thousand cases.

Originally the power shaping method was designed only for power flattening ($p^* = 1$). Used as a power shaping routine with another reference power distribution p^* the method has the drawback that the average of the normalized power density over a domain is generally different from the average of the reference power density. The difference is most pronounced if there are only a few broad domains. Probably the power distribution would fit better to the reference distribution in this case if eqs. (4.16) were replaced by the requirement that the average of p should be equal to the average of p^* in each control domain. Of course the fixpoints would then have to be chosen in another way than scheduled above. However, this has not been tried. Another extension of the method would be to impose an upp

limit on C, which can easily be done in the same way as with the lower limit $C \geq 0$.

4.3.2. Examples

For the burn-up distribution of fig. 10, which was used in the example illustrating the eigenvalue method, power flattening calculations ($p^* = 1$) give the power distributions shown below in the same figure. In the coarse mesh case all the core meshes were specified as control meshes, and consequently each domain only contained one mesh. As a result the control poison was distributed in six mexhes. The poison distribution is shown as the hatched areas, and it is seen that the power density is equal to the maximum value in these six meshes. The power flattening has reduced the form factor from 1.193 to 1.108.

For the fine mesh case one mesh in the middle of each region was specified as a control mesh, and the boundaries of the eighteen domains were laid on the region boundaries. As a result the poison was distributed in four meshes. Of course the absorption cross sections C are higher than in the previous case as the meshes are smaller; but the distribution and the average poison cross section over the core $\overline{C}$ are largely the same. The power density has equal maximum values in the four poisoned domains, and the power form factor is reduced from 1.208 in the flux-eigenvalue calculation to 1.118 by power flattening.

The burn-up distribution in fig. 10 is representative of the type of calculations simulating on-load refuelling with minimum power form factor as the internal optimality condition. The case is from the equilibrium core at the start-of-cycle, but can be taken as representative of the whole cycle, which is short in on-load operation.

In fig. 11 is shown another case with only three meshes specified as control meshes. The corresponding domains are indicated by Roman numerals. The unflattened power distribution is obtained from a flux-eigenvalue calculation with equal poison in the three control meshes and the remaining meshes without any poison. The results from the eigenvalue calculation and the power flattening calculation are shown. The form factor is reduced from 1.74 to 1.14. In this case the burn-up distribution is representative of off-load operation (one third of the core refuelled per cycle) at the start-of-cycle when the control poison level is high.

As an example of power shaping fig. 12 shows the result of a case with all the core meshes specified as control meshes. Before power shaping a usual eigenvalue calculation with uniform poison distribution gives the power

distribution with a form factor of 2.11. Then power shaping is performed with the reference power distribution p^* taken as the power distribution corresponding to one of the ideal Q-distributions from section 5.2. The form factor of the reference power distribution is 1.50. The power is shaped very efficiently, the resulting power form factor being 1.509. Fig. 12 presents one of the most successful examples of power shaping at the start-of-cycle in a case with off-load refuelling. This time the internal optimality condition was maximum fuel burn-up.

5. IDEAL BURN-UP DISTRIBUTIONS

The ideal burn-up distributions satisfying the internal optimality conditions of minimum power form factor or maximum fuel burn-up with limited power form factor are determined on the basis of a continuous model where the state of the fuel is given by the N continuous variables Q_n, $1 \leq n \leq N$. The ideal Q-distribution is found by minimization of an object function which is a function of Q_n. The control poison distribution is kept constant during the calculation. In section 5.1 the power form factor is the object function. In section 5.2, where the aim is to find the Q-distribution that gives maximum fuel burn-up another function of Q_n is shown to be the object function.

5.1. Minimum Power Form Factor

The power form factor F is regarded as a continuous function of the net production cross sections Q_n of the N regions

$$F = f(Q_n). \tag{5.1}$$

We want to determine the Q-distribution that makes F minimum and makes the reactor just critical for a specified control poison distribution C_i. The method which is used may be called "irradiation flattening", indicating that the irradiation distribution or rather the Q-distribution is corrected iteratively until the power distribution is flat.

5.1.1. The Power Flattening Method

The iterative method used to solve this power flattening problem starts with a guess at the Q-distribution. The Q-distribution is then corrected successively in steps. At every iteration step Q_n is reduced in regions where the power density is greater than the average power density, and increased in regions where the power density is smaller than the average power density over the core.

The range of permissible Q-values is restricted to values covered by the burn-up curve. For other reasons, which will be discussed later, it is desirable to make the Q-limits dependent on the region number. The upper Q-limit is specified as Q_n^u.

At every iteration step an eigenvalue calculation with proper values of D and Σ_f in the diffusion equation gives the power distribution p_n and eigenvalue λ (cf. footnote section 4.2) corresponding to Q_n. p_n is the average power density for all meshes of region number n. From $Q_{n,k}$, where k is the iteration number, we get to the next iterate $Q_{n,k+1}$ by means of the two-term correction

$$Q_{n,k+1} = Q_{n,k} - \Delta Q'_{n,k} - \Delta Q''_{n,k} . \tag{5.2}$$

The first correction $\Delta Q'_{n,k}$ flattens the power shape, and the second $\Delta Q''_{n,k}$ gives a normalization of the Q-distribution.

The first correction $\Delta Q'_n$ (iteration index k omitted) is given by the expression

$$\Delta Q'_n = a\left(\frac{p_n}{\bar{p}'} - 1\right), \tag{5.3}$$

where a is a constant with the same dimension as Q, and $\bar{p}'$ is the average power density over regions for which $Q_{n,k} < Q_n^u$.

If $\Delta Q'_n$ calculated by means of (5.3) makes $Q_n - \Delta Q'_n > Q_n^u$, (5.3) is replaced by

$$\Delta Q'_n = Q_n - Q_n^u . \tag{5.3a}$$

Now the normalization term $\Delta Q''_n$ is determined by

$$\Delta Q''_n = (\lambda - 1)\,\bar{C} - \frac{1}{N}\sum_{n=1}^{N} \Delta Q'_n , \tag{5.4}$$

where $\bar{C}$ is the average control poison cross section over the core. $\Delta Q''_n$, which is equal for all regions, changes the level of the Q-distribution with the exception of regions where the upper limit Q_n^u is exceeded. In such regions Q_n is returned to Q_n^u in the same way as before by an expression similar to (5.3a).

The normalization makes the level of the Q-distribution converge towards a value that makes the reactor just critical at the specified control poison distribution C_i. The change of the level by (5.3) is balanced by the second term in (5.4). The first term is explained by reference to the diffusion equation (4.1). It is seen that Q(r) and $\lambda C(r)$ may be changed additively by the same amount without disturbing the neutron balance. If $(\lambda-1)C(r)$ is subtracted, the right-hand side becomes C(r). As $\Delta Q'_n + \Delta Q''_n$ has a shape which is generally different from the shape of the control poison distribution C_i, the eigenvalue will not become exactly 1, but during the iterations $\lambda \to 1$.

It is seen from (5.3) that the net production cross section is decreased in regions where the power density is too high, and increased in regions where the power density is smaller than the average power density. The iterations are converged when $p_n = \bar{p}'$ in all the regions where $Q_n < Q_n^u$. In regions where $Q_n = Q_n^u$, the net neutron production of the fuel $Q_n \varphi_n$ cannot be increased, and the converged p_n gets smaller than $\bar{p}'$ in such regions. This is the reason why the power density of these regions is not included in $\bar{p}'$, as $\Delta Q'_n$ would then not converge towards 0.

5.1.2. Examples

The examples given in this chapter are all for the BHWR 750 MW. The burn-up table for natural uranium is used (cf. figs. 3 and 4). As Q is not a monotonous function of I, it is monotonized artificially by cutting off the part of the curve below the plutonium top at 1550 MWD/TU. The rest of the curve, which is monotonous, is used.

In fig. 13 the ideal Q-distribution is shown for a case with uniform control poison distribution C. The control poison level is the end-of-cycle value $\bar{C} = \bar{C}_d$ corresponding to on-load operation of the reactor. With $\bar{C}_d = 3 \times 10^{-5}$ cm^{-1}, which corresponds to a reactivity of about 1%, the reactor can be restarted until about twenty minutes after shutdown and then not until sixty hours later because of xenon build-up.

It is seen that the ideal Q-distribution has $Q \sim C$ in the central regions. Here the net neutron production by the fuel is balanced by the absorption of the control poison, and there is no leakage. In the outer regions Q attains its upper limit, Q^u. In these regions the fuel must yield a net neutron production which balances the absorption of the control poison as well as the leakage out of the reactor. It is seen that the power density is kept flat except in the outer regions, where $Q = Q^u$. The power form factor is 1.082. The shape of the Q-distribution and power density seems to be in good agreement with the optimal k-profile derived analytically by Melice (*ref.* 7).

The reason for making the upper Q-limit Q_n^u dependent on the region number is that the ideal Q-distribution is used as a reference distribution (Q^*) in the shuffling routine of the programme SELMA1 (cf. section 3.6). For the equilibrium core, which is reached after a long time, there is a spread of irradiations from fresh fuel up to high irradiations. The Q^u-values are chosen as the values corresponding to the smallest irradiations in the equilibrium core. As the ideal Q-distribution shown in fig. 13 was wanted to be the end-of-cycle distribution, the Q^u-values were chosen as representative of the end-of-cycle state of the equilibrium core. By the time the ideal Q-distribution is calculated, the state of the equilibrium core is not known, so it is necessary to make a guess at Q_n^u. Later it may be necessary to recalculate the ideal Q-distribution with new Q_n^u-values, if the first guess appears to be bad. Generally, however, with a little experience the first guess is sufficiently good, because the power shape is not very sensitive to changes of Q_n in the outer regions.

In fig. 13 it is seen that the greatest values of Q_n^u are placed nearest to the reflector. In another case the consequence of inverting the Q^u-distribution in the six outermost regions (Q_{18}^u interchanged with Q_{13}^u and so on) was investigated. The resulting ideal Q-distribution was slightly decreased relative to that in fig. 13 (most pronounced in region 12). The change in power distribution was scarcely detectable. This indicates that it is not very important what shape Q^u is given, especially if the unflattened part of the reactor only includes a few of the outer regions.

In fig. 14 the control poison distribution is specified as a three-mesh distribution. The average value $\overline{C}$ is again equal to 3×10^{-5} cm^{-1}. Again the power is completely flat in the central regions where $Q_n < Q_n^u$. One might suspect the Q-distribution not to be converged. However, investigations have shown that the result is the same for different start guesses of Q_n.

The cases of figs. 13 and 14 were calculated by means of the ALGOL programme IBU1 on a Burroughs B6500 computer. The necessary number of iterations depends on the value of α and the start guess of Q_n. In the examples, $\alpha \approx 2 \times 10^{-4}$ cm^{-1} was found to be about the largest value giving convergence. With this value and a good start guess at Q_n a sufficiently good convergence is obtained after 10 iterations, while a bad start guess (e.g. uniform Q-distribution) requires 20-30 iterations. A case with 18 regions in the core (25 meshes in the flux calculation) and 30 iterations takes 8 seconds of processing time on the computer.

5.2. Maximum Fuel Burn-up

As burn-up optimization is generally contradictory to power flattening, an optimization of the discharged fuel burn-up with a constraint on the power form factor of the core is of great interest. A large discharge burn-up is achieved by shuffling the fuel in such a way that the cycle time becomes maximum.

Let us consider the equilibrium core, which is reached when the initial state of the core is forgotten. The development of the eigenvalue λ with time is illustrated in fig. 15. The peaks correspond to the times just after discharge. During the cycle the eigenvalue decreases until it reaches the lower limit, when a new refuelling is performed. The high eigenvalue just after discharge can be further increased by appropriate shuffling. On the basis of the working hypothesis that the decreasing rate of the eigenvalue is independent of the shuffling scheme used, it is seen that high eigenvalue leads to long cycle time and consequently high discharge burn-up. The Q-distribution Q_n and λ are changed, but $\sum_{n=1}^{N} Q_n$ is not changed by shuffling. The shuffling which makes λ maximum leads to maximum discharge burn-up

5.2.1. The Object Function

Now, returning to the continuous model, we cannot use λ directly as the object function and then optimize λ, because during the iterative search for the optimum Q-distribution we want to normalize the Q-distribution to a level which makes the reactor just critical at the specified control poison distribution ($\lambda \to 1$ as in section 5.1.1).

Instead we shall search for the just critical Q-distribution, which has minimum average net production cross section $\overline{Q}$ over the core. This corresponds to high average burn-up of the equilibrium core and consequently high discharge burn-up. With this new formulation the problem of maximizing the eigenvalue with constant $\overline{Q}$ is converted into the problem of minimizing $\overline{Q}$ with constant eigenvalue.

The ideal Q-distribution is found by minimizing the object function

$$J = \frac{1}{N} \sum_{n=1}^{N} (Q_n - \lambda C_n), \tag{5.5}$$

where C_n is a constant distribution as in section 5.1.1[*].

[*] The control poison is allowed to vary meshwise. C_n is the average control poison cross section for region number n.

It is seen that $J = \overline{Q} - \lambda\overline{C}$. The object function is considered as a continuous function of Q_n in the N-dimensional Q-space. The iterative method which is used in the search for the ideal Q-distribution is based on the hypothesis that $\overline{Q}$ decreases when Q_n is moved in the opposite direction of the gradient of J.

This hypothesis is a matter of experience. According to the explanation given in section 5.1.1, the neutron balance equation (4.1) makes J rather stable with respect to changes in Q_n. If Q_n is changed in one of the central regions, the resulting change in λ will be larger than at a change of Q_n in one of the outer regions. As a consequence λ may be kept constant if Q_n is increased a little in a central region and decreased by a larger amount in an outer region. This change leads to a decrease in $\overline{Q}$ and J. As a rule the components of grad J are negative in the central regions and positive in the outer regions, so our hypothesis is confirmed.

The iterative method, which is described in the next section, cannot be proved to converge towards the Q-distribution with minimum $\overline{Q}$, but in the Appendix it is shown under some simplifying assumptions that $\overline{Q}$ converges towards $\overline{Q}_{min}$ in a case with only two regions. Besides the example serves as an illustration of the method.

The method is complicated a little by the constraint on the power form factor

$$F \leq F_m \,, \tag{5.6}$$

which must be satisfied by the ideal Q-distribution.

5.2.2. Minimization of the Object Function

As in the power flattening method we come from $Q_{n,k}$ to $Q_{n,k+1}$ by means of the two-term correction

$$Q_{n,k+1} = Q_{n,k} - \Delta Q'_{n,k} - \Delta Q''_{n,k} \,. \tag{5.7}$$

The first correction $\Delta Q'_{n,k}$ moves the point $Q_{n,k}$ in the N-dimensional Q-space in the opposite direction of grad J. By means of the second correction $\Delta Q''_{n,k}$ the Q-distribution is normalized to criticality.

Iteration step number k starts with an eigenvalue calculation. The resulting eigenvalue is denoted λ_0. The corresponding power distribution is p_n. Then the gradient of J is calculated. The n'th component of grad J is found by giving the net production cross section of region number n an increment dQ_n and calculating the eigenvalue, which is denoted λ_n. The

eigenvalue is seen to be changed by $d\lambda_n = \lambda_n - \lambda_o$. The change of J

$$dJ_n = \frac{1}{N} dQ_n - d\lambda_n \overline{C} \tag{5.8}$$

divided by dQ_n is the finite difference expression of the n'th component of grad J

$$\frac{dJ_n}{dQ_n} = \frac{1}{N} - \frac{d\lambda_n}{dQ_n} \overline{C} . \tag{5.9}$$

It is seen that N+1 eigenvalue calculations are necessary at iteration step number k[x].

The explanation of the *corrections* $\Delta Q'_n$ and $\Delta Q''_n$ at a certain iteration step is given by reference to fig. 16, where the imagined distribution of Q_n, the components of grad J according to (5.9), and the *power densities* are shown. There are four characteristic conditions of the different regions:

(I) In regions 5 and 6 the upper Q-limit Q^u is attained.

(II) In regions 10, 11, and 12 the lower Q-limit Q^l is attained.

(III) In regions 1, 3, 7, 8, and 9, $Q^l < Q < Q^u$, and $p < \bar{p}F_m$.

(IV) In regions 2 and 4, $Q^l < Q < Q^u$, and $p > \bar{p}F_m$.

First we consider the regions of types III and IV. In regions 7, 8, and 9 the correction $\Delta Q'_n$ is calculated as

$$\Delta Q'_n = \beta \frac{dJ_n}{dQ_n} , \tag{5.10a}$$

where β is a constant with the same dimension as Q.

In regions 2 and 4 the constraint on the form factor is violated. In such regions $\Delta Q'_n$ is calculated as

$$\Delta Q'_n = \gamma \left(\frac{p_n}{\bar{p}} - F_m \right) , \tag{5.10b}$$

where γ is a constant, and $\bar{p}$ is the average power density over the all regions of the core.

---

[x] The calculation of $d\lambda_n$ could be speeded up by means of perturbation theory, but this was not done because the eigenvalue calculations are very f[illegible] in one dimension and one group.

In regions 1 and 3 the power density is smaller than the limiting value $\bar{p}F_m$ and the component of grad J is negative, so it is seen that irrespective of which of expressions (5.10a) or (5.10b) is used, Q_n will be increased. If p_n is only slightly smaller than $\bar{p}F_m$, (5.10a) will increase Q_n too much, whereas the increase by (5.10b) will give a soft variation, which is a necessary condition for convergence of the calculations. The decision whether to use (5.10a) or (5.10b) is automated by calculating $\Delta Q'_n$ by both expressions and always choosing the greater of the two (making Q_n the smaller). This is done for all the regions. In this way we get no conflict with what was said for the remaining regions of types III and IV.

The Q-limits are tackled in a similar manner as the upper Q-limit in the power flattening routine (cf. (5.3a)). In region 5, Q_n will tend to be increased, irrespective of which of the expressions for $\Delta Q'_n$ is chosen, but Q_n is not allowed to exceed Q_n^u. For region 6 the gradient is positive, so Q_n moves downwards. None of regions 10, 11, and 12 are changed as they are not allowed to exceed the lower limit Q_n^l.

The principle in the normalization is the same as in the power flattening method (section 5.1.1), but there is the difference that the Q-level is only changed by $\Delta Q''_n$ in regions where $Q_n^l < Q_n - \Delta Q'_n < Q_n^u$ and $\Delta Q'_{n,a} < \Delta Q'_{n,b}$ ($\Delta Q'_{n,a}$ and $\Delta Q'_{n,b}$ are short for $\Delta Q'_n$ calculated from (5.10a) and (5.10b) respectively). In fig. 16 the normalization is only performed in regions 6, 7, 8, and 9. The number of regions N1 satisfying these inequalities are counted, and then the normalization term is calculated from the expression

$$\Delta Q''_n = \frac{1}{N1} \sum_{n=1}^{N} ((\lambda-1)\, C_n - \Delta Q'_n) , \qquad (5.11)$$

which corresponds to (5.4) multiplied by N/N1. After the normalization the iteration step is finished, and we can proceed to the next iteration step.

The choice of Q_n^u and Q_n^l follows the directives given for Q_n^u in the power flattening method (section 5.1.2). Q_n^l are taken as the smallest values expected in the equilibrium core. There are no problems with the application of Q_n^l since experience has shown that Q_n always attains the lower Q-limit in the outer regions. The smallest Q^l-values are applied in the outermost regions where grad J is largest. As for Q_n^u it cannot be predicted in what region the upper Q-limit is attained. By some trivial logics, which shall not be elaborated here, the highest Q^u-value is always applied in the innermost of the regions for which Q_n attains the upper Q-limit, in the next region the second largest Q^u-value, and so on.

Another trivial problem had to be solved before the method worked satisfactorily. The arrows in fig. 16 show the direction of the corrections by $\Delta Q'_n$. The contributions to $\Delta Q''_n$ from $\Delta Q'_n$ for the central regions, where p_n is close to $\bar{p}F_m$, largely eliminate each other, so the change in the Q-level by $\Delta Q'_n$ is largely due to the regions beyond the regions with maximum of Q. The normalization re-establishes the Q-level, and since grad J is larger in the outer than in the inner regions, it is seen that the slope of the Q-distribution in regions 6, 7, 8, and 9 gets still steeper for each iteration, ending up with a Q-distribution where $Q = Q^u$ in some regions (maybe 5, 6, and 7), and $Q = Q^l$ in the outer regions (from number 7 outwards). In the next iterations the normalization does not work because N1 = 0. In this case $\Delta Q''_n$ is calculated with N1 = 1, and region number n, where the normalization is performed, is taken as one of the neighbour regions to the boundary between the zones $Q = Q^u$ and $Q = Q^l$. In this way the normalization amounts to moving this boundary outwards or inwards until the Q-distribution is just critical.

Having recognized that the iterations always end up with this type of problem, a method could be suggested in which the cumbersome calculation of grad J is avoided if Q_n is bound to the lower limit Q_n^l in some outer regions and to the upper limit Q_n^u in some intermediate regions. The boundary between these two zones should be moved in the way described above. In the central zone the power shape should be flattened by means of (5.10b). Applied in a two-dimensional model this method would save much computer time. Of course it would be reassuring to have a routine to calculate grad J after convergence of the iterations for control purposes, especially if the method is developed in multi-group theory, because the introduction of more than one energy group might influence the conclusions based on the present one-group model.

5.2.3. Examples

The examples for the BHWR 750 MW shown in figs. 17 and 18 present the most typical features of ideal Q-distributions corresponding to maximum discharge burn-up at a form factor limit $F_m = 1.50$ and 1.20 respectively. Both are end-of-cycle distributions for on-load simulation. The control poison distribution is uniform with an average cross section $\overline{C} = 3 \times 10^{-5}$ cm^{-1} as in the previous examples.

The Q-limits are a little different in the two cases because the discharge burn-up (obtained by SELMA1) gets higher when the form factor is high. As in the case with power flattening one is obliged to make a guess at

Q_n^u and Q_n^l if they are not known from previous SELMA1 calculations. This might seem difficult, but in fact it is rather easy with a little experience to get sufficiently good Q-limits. Some guidelines will be given in connection with the description of the different shuffling principles.

It is seen from the figures that the ideal Q-distributions have a shape in the central part which is similar to the shape found in the power flattening example, fig. 13. The difference is that Q attains the lower Q-limit in the outer regions. Obviously the small neutron production in the outer regions makes the leakage out of the reactor minimum. The deficit of neutrons in the outer regions is balanced by the excess production in the regions with high Q. As the form factor is constrained, Q is suppressed in the central regions where $Q \sim C$, resulting in flat power distribution. By comparison of figs. 17 and 18 it is seen that the most typical difference is the shift of the boundary between the zones with $Q = Q^u$ and $Q = Q^l$. By increasing F_m, this boundary moves towards the centre. For decreasing values of F_m the boundary moves towards the reflector. For $F_m = 1.08$, which was the value found by the power flattening method in section 5.1, the zone with $Q = Q^l$ disappears, and the Q-distribution becomes the same as found by the power flattening method (fig. 13). The value of the object function for $F_m = 1.08$, 1.20, and 1.50 is $J = 7.62 \times 10^{-5}$, 2.62×10^{-5}, and -2.29×10^{-5} cm^{-1} respectively.

In the development of the method for minimizing J it was tacitly assumed that J has only one minimum within the domain of definition in the Q-space. Actually J behaves very properly. The minimum found by the IBU1 programme always belongs to the boundary of the domain of definition, and it has not been possible to locate any other minimums by choosing various start guesses of the Q-distribution. With a reasonable start guess at the Q-distribution it is not necessary to recalculate grad J at every iteration step. The computing time for the Q-distribution in fig. 17 was 19 seconds of processor time. The number of iterations was 30, and grad J was recalculated 6 times. The constants were $\beta = 10^{-3}$ cm^{-1} and $\gamma = 10^{-4}$ cm^{-1}.

The routine was investigated on various other examples. One of these was a case with only three control meshes. The routine behaved completely as expected with peaks in Q around the control meshes in the same way as in fig. 14, but still with $Q = Q^l$ in the outer regions. The power density was kept flat in all the central regions.

6. DIRECT SHUFFLING OPTIMIZATION

The most direct way to find the optimum shuffling scheme at a certain stage of the multi-stage process would be to carry out the N! flux-eigenvalue calculations for all possible permutations of the N fuel batches in the core and then choose the permutation with the

(1) smallest power form factor or

(2) highest critical control poison level and a power form factor less than F_m.

Condition (2) corresponds to high discharge burn-up as explained in section 5.2 (Highest critical control poison corresponds to highest eigenvalue, cf. (4.10) with footnote).

It would be very desirable to be able to perform such calculations, not only for a single stage, but for a sequence of stages sufficiently long to obtain equilibrium core conditions*. There are two reasons for making such calculations. First they could indicate whether the ideal Q-distributions found in the previous chapter are right or wrong, and secondly they could be used to deduce some rules for fitting the actual Q-distribution to the ideal Q-distribution by shuffling. However, the search among all the N! permutations is not practicable except for very small values of N because of excessive computing times.

In this chapter somewhat different search techniques are used. At each stage (after refuelling of N_d regions) a large number of trial interchanges of batches in pairs is performed, and for each trial interchange a full flux-eigenvalue calculation is carried out. The best interchange according to one of the internal optimality conditions (1) or (2) above is made permanent. This procedure is repeated I times, resulting in L batch interchanges at each stage. With a moderate value of L it is possible to come through a whole sequence of stages within a reasonable time, and the number of trial interchanges is still large enough for the aim set by the internal optimality condition to be fulfilled quite well.

---

* The equilibrium core concept was defined in terms of fixed shuffling schemes, but it is also used when the shuffling scheme varies from stage to stage. If only the same shuffling principle is used consistently all over the sequence, the evolution of power form factor and discharge burn-up with time will on the average approach steady values which are the equilibrium values.

6.1. Shuffling Optimization Based on Many Trial Interchanges

The shuffling routine, which is based on this direct optimization method, is considered in detail in this section. It is included as an option in the SELMA1 programme in parallel with the fast shuffling routines described in chapter 7. First, however, we shall consider the methods for prediction of the cycle time and the end-of-cycle state of the fuel. These methods are also applied in the fast shuffling routines.

6.1.1. Prediction of Cycle Time

For the reasons given in section 3.6 we want to perform the shuffling in the way that makes the burn-up distribution optimal towards the end-of-cycle. For this purpose a prediction of the cycle time Δt_c is necessary. Only a coarse estimate of Δt_c is needed, as it is only used to predict the burn-up of the fuel at a time towards the end-of-cycle, not necessarily at the discharge time itself.

If there is only one fuel enrichment present in the core, which is the case as soon as the initial fuel load is discharged, the prediction of the cycle time is made in the same way as the determination of the last burn-up time step of each cycle. Then we have

$$\Delta t_c = \frac{I_m - \bar{I}(0)}{\bar{p}} \quad , \tag{6.1}$$

where I_m is approximately the average core irradiation at the discharge of the previous cycle (cf. section 3.7), and $\bar{I}(0)$ is the actual value of the average core irradiation.

If the initial core contains fuel of different enrichments, the cycle time is predicted by calculating how long time the actual fuel in the core would have to be irradiated in an imagined constant flux distribution φ_n^* before $\bar{Q}$ reached $\bar{Q}^*$. φ_n^* and $\bar{Q}^*$ are the flux and average Q for the relevant ideal Q-distribution (at end-of-cycle). Since Q is not a linear function of I, it is clear that the value found for Δt_c depends on how the fuel is distributed in the core. It was found that the small routine, which calculates Δt_c by an iterative interpolation method, gave sufficiently good estimates when the enrichment distribution of the initial core was made up intuitively, guided by the ideal Q-distribution. As for the second and later cycles the fuel is not rearranged just after discharge, before the prediction of Δt_c.

6.1.2. Prediction of the End-of-Cycle State

The burn-up distribution at the end-of-cycle is predicted by assuming

that the flux may be maintained constant equal to φ^* throughout the cycle. During the search for the optimal shuffling scheme the batches are interchanged in pairs. Suppose that the batches of regions number j and k are interchanged. Then the irradiations for these batches at the end-of-cycle are predicted as

$$I'_j(\Delta t_c) = I_k(0) + a\Sigma_{f,k}(0)\varphi^*_j\Delta t_c \qquad (6.2a)$$

$$I'_k(\Delta t_c) = I_j(0) + a\Sigma_{f,j}(0)\varphi^*_k\Delta t_c \qquad (6.2b)$$

For the remaining batches we have

$$I'_n(\Delta t_c) = I_n(0) + a\Sigma_{f,n}(0)\varphi^*_n\Delta t_c \qquad \begin{cases} 1 \leq n \leq N \\ n \neq j, k \end{cases} \qquad (6.2c)$$

In these expressions the time is set to zero at the start-of-cycle. a is a normalization constant giving the correct power level.

6.1.3. The Shuffling Routine

The search technique consists in stepping regions numbers j and k through the values $1 \leq j < N$, and $j < k \leq N$. For each new value of j and k the end-of-cycle state is predicted and a flux-eigenvalue calculation is carried out for the predicted end-of-cycle burn-up distribution. The resulting average control poison cross section and power form factor are compared with the values from previous trial interchanges, and the optimal interchange according to internal optimality condition (1) or (2) is remembered. After each eigenvalue calculation bathces j and k are put back into their original regions before the next trial interchange. After completion of the search the pair of batches which gave optimum conditions of power form factor and average control poison cross section are interchanged permanently, and a search for a new pair of batches to be interchanged is initiated.

When L interchanges have been performed, or when the fuel distribution cannot be further improved by interchange of any two batches, the shuffling is stopped. If the number of interchanges is L, the total number of flux-eigenvalue calculations per shuffling is seen to be $\frac{1}{2}LN(N-1)$. During the shuffling a single fuel batch may have participated in several interchanges.

Therefore the shuffling is finished with a determination of the simplest shuffling scheme which leads to the same result.

The result of the shuffling is a new $I_n(0)$-distribution, which is now burned in steps as described in section 3.7.

It is seen that, although φ^* is used for the prediction of the burn-up at the end-of-cycle, the shuffling is in principle performed independently of the ideal Q-distribution Q^*, so if the Q-distribution found at the end of a late cycle, when the equilibrium state is reached, is in agreement with the ideal Q-distribution calculated by IBU1, this is taken as a support of the theory in chapter 5.

6.1.4. Results

In the following a series of cases calculated by the SELMA1 programme are described. When nothing is specially mentioned, the results were obtained for the BHWR 750 MWe reactor with natural uranium fuel in the initial core as well as in the equilibrium core. In all the cases in this chapter the core is partitioned into 18 regions. The flux calculation is performed with 22 meshes in the core and 3 in the reflector. The power shaping routine is normally used with all the meshes of the core as control meshes (22 control domains). Later in the present and the following chapter a few cases are given to illustrate the effects of varying numbers of regions, different enrichments in the initial core, and reduction of the number of control domains.

6.1.4.1. On-Load Simulation. On-load is simulated by setting the number of batches discharged per cycle $N_d = 1$ and using the discharge criterion $\bar{C}_d = 3 \times 10^{-5}\ cm^{-1}$.

The core history obtained in a case with minimum power form factor as the internal optimality condition is shown in fig. 19. The maximum number of batch interchanges per cycle L was 5. As explained in connection with the flow diagram of SELMA1 (fig. 6) each eigenvalue calculation is succeeded by an absorber power flattening calculation[x], and the burn-up calculation is based on the power distribution from the power flattening calculation. The form factors of both of the power distributions are shown as functions of time in fig. 19. The form factor from the eigenvalue calculation (with uniform control poison distribution in this case) is an expression of the performance of the shuffling routine, while the form factor from power flattening expresses

[x] The term power flattening is used when $p^* = 1$ in the power shaping routine. The term power shaping is used when p^* is specified as the power shape corresponding to the ideal Q-distribution (cf. section 4.3.1)

the combined effects of shuffling and power flattening. It is seen that the eigenvalue calculation gives a form factor about 1.9 for the initial core. For comparison the form factor for a bare, infinite homogeneous cylinder is 2.316. The power flattening is very effective for the initial core as long as the control poison level $\overline{C}$ is high. At the end of the first cycle and in the next few cycles it is difficult to keep the power shape flat. This part of the curves shall later be referred to as the "initial transient". After a few cycles the form factors attain on the average a steady value. The average form factor is 1.18 for the eigenvalue calculations and 1.10 for the power flattening method.

The average control poison cross section $\overline{C}$ is seen to decrease with time between the refuellings, and it is seen that the decreasing rate is rather constant except in the first cycles. The power flattening method gives somewhat lower values of $\overline{C}$ than the eigenvalue method, because the control poison is mainly distributed in the inner part of the core where the power is flat. Here the poison is more effective than in the outer part where the power density is low. The discharge criterion is applied on $\overline{C}$ from the eigenvalue calculation, and it is seen that the automatic determination of the burn-up step Δt_b works satisfactorily for the equilibrium core, whereas it is less good in the cycles after the first discharge.

The burn-up of the discharged fuel is seen to be small for the first batches discharged. In later cycles the discharge burn-up increases. After 514 days batch No. 18 is discharged as the last batch of the initial core. The next batch discharged has a much lower burn-up, because it has not been irradiated for more than the 313 days from the end of the first cycle.

Although the state of the fuel is not yet in equilibrium, the sequence of cycles is sufficiently long for the Q-distribution at the end of the last cycle after about 600 days to be compared with the ideal Q-distribution from the IBU1 calculation (which was not used in the shuffling routine). This is done in fig. 20. Of course the actual Q-distribution cannot be expected to be a smooth curve as was the case with the ideal Q-distribution Q^*. However, it is seen that the Q-distribution on the average corresponds fairly well to Q^*. Below in the same figure the corresponding power distributions are compared. The actual power distribution p is that obtained from the eigenvalue calculation. A similar comparison was made for several of the cycles with as good agreement as in fig. 20, so it is concluded that the ideal Q-distribution found by the irradiation flattening method is adequate as a reference Q-distribution in the fast shuffling routines described in chapter 7.

The core history shown in fig. 21 was obtained with the internal optimality condition (2), highest critical control poison level, and $F_m = 1.50$. It is seen that the objective of getting higher discharge burn-up is fulfilled. The average burn-up of the first eighteen batches (first core) discharged is 8697 MWD/TU to be compared with 7414 MWD/TU for the first eighteen batches of fig. 19. The discharge burn-up gets more stable than in fig. 19, but the irradiation time is too short to conclude that equilibrium has been attained.

The power form factors are seen to be a little higher than 1.50. The end-of-cycle form factor from the eigenvalue calculation is of special interest since the objective of the shuffling routine is to achieve optimum conditions at the end-of-cycle. It is seen that the end-of-cycle values are very close to 1.50. It is interesting that the form factor approaches F_m, although the form factor condition is only $F \leq F_m$. The power shaping routine is seen to give more stable form factor values than those obtained by the eigenvalue routine. The power shaping routine is seen to give the higher control poison level. This is because most of the poison is distributed in the outer regions, where it is less effective than in the inner regions because of low power density near the reflector.

In fig. 22 the Q-distribution at the end of the last cycle in fig. 21 is compared with two ideal Q-distributions from the IBU1 programme. It is seen that the agreement is better with the ideal Q-distribution with a form factor $F = 1.40$ than that with $F = 1.50$. That it must be so is understood from the fact that the actual power distribution p cannot be smooth like p^*, and since the power peaks are not allowed to exceed the plateau of p^* with $F = 1.50$, its average value over the central regions must necessarily be somewhat smaller. Consequently the fast shuffling routines which fit the actual Q-distributions to the ideal Q-distribution must be expected to give somewhat higher form factors than the power form factor of the ideal distribution.

In table 3 the maximum and average values of form factors and discharge burn-ups derived from figs. 19 and 21 are given as case 1 and case 3 respectively. Case 2 is another example with the form factor limit $F_m = 1.25$.

In the evaluation of form factors the equilibrium period was generally reckoned from the time when about twenty-five batches had been discharged ($N = 18$). At about that time the steady state as regards the form factor was found to commence in cases with long irradiation times, calculated with the application of the fast shuffling routines (chapter 7).

Since full equilibrium is not obtained in the present cases, the evaluated equilibrium form factors must be taken with some reservation. From a theoretical point of view the most interesting figures are the equilibrium values of the maximum end-of-cycle form factor, obtained by the eigenvalue routine, and the average and maximum form factors from power shaping, which give an impression of the performance of the shuffling routine and the absorber power shaping routine.

The discharge burn-ups were found to be best represented by the average discharge burn-up per full core discharged. In the present cases only one full core was discharged. The average discharge burn-up for the first core load is seen to increase with increasing F_m. The maximum discharge burn-up given in each case is an expression of the spread of irradiations. In almost all the cases investigated the maximum was found at the discharge of one of the last batches of the initial core load.

In all of the cases the computing time on the B6500 was 53 seconds processor time per cycle with L = 5.

6.1.4.2. Off-Load Simulation. Off-load management is simulated by discharging one third of the core per cycle (N_d = 6) and using the discharge criterion $\overline{C}_d = 0$.

The core history in a case with minimum power form factor is shown in fig. 23. The maximum number of batch interchanges per cycle L is 10. Burn-up proceeds in steps of thirty days. The power form factor from the eigenvalue calculation is seen to be large at the beginning of some of the cycles, but at the beginning-of-cycle the power flattening is very effective. Towards the end-of-cycle as power flattening gets inefficient, the eigenvalue form factor decreases to a rather low value. For the equilibrium core the maximum end-of-cycle form factor is 1.24, and the average form factor with power flattening is 1.12. The discharge burn-ups shown below in the figure are the average burn-ups of the six batches discharged simultaneously. All the characteristic values from fig. 23 are given in table 3, case 4.

In fig. 24 the Q-distribution from the end of the last cycle is compared with the ideal Q-distribution with minimum form factor. It is seen that $Q^* = 0$ in the central regions, because C^* was specified as zero in the IBU1 calculation.

In fig. 25 is shown a case with minimization of the form factor at the start-of-cycle. The calculations were performed by formally setting $\Delta t_c = 0$ in expressions (6.2a-c) and then in other respects making the same calculations as for fig. 23. At the start-of-cycle the form factors are

excellent, but the end-of-cycle values are higher than in fig. 23. For the equilibrium core the form factors from power flattening have an average of 1.13 and a maximum of 1.30. The form factor increases because the power density decreases in the central regions owing to faster burn-up than in the outer regions. The case illustrates the advantage of using end-of-cycle optimization.

The initial core with only one enrichment is seen to give a high initial form factor transient and require a high control poison level. Further the burn-up of the initial fuel load is bad. In fig. 26 is shown the results from a case where the initial core is composed of 6 batches with natural uranium, 4 with 0.66% U^{235}, 6 with 0.6% U^{235}, and 2 with 0.5% U^{235}. In later cycles the reload fuel is natural uranium (0.712%). As a result the form factors are improved and the control poison level reduced. The discharge burn-ups are not very informative as they are average values for differently depleted fuel (table 3, case 5).

The Q-distribution from the end of the first cycle is compared with the ideal Q-distribution in fig. 27. With the given composition the range of Q-values in the initial core is not as broad as in the equilibrium core (cf. fig. 24), so the agreement cannot be expected to be much better than in the figure.

The core history shown in fig. 28 is from a case with the internal optimality condition (2), which gives maximum fuel burn-up with limited power form factor. Again the power form factor from the eigenvalue calculation is rather haphazard at the start-of-cycle, but at the end-of-cycle the form factor gets close to $F_m = 1.50$. In this case the power shaping routine does not do its task of keeping the form factor close to F_m throughout the cycle very well. As mentioned in chapter 4, the power shaping routine was first made for power flattening only and later extended to include power shaping. This extension is expected to be improved by some further work.

In fig. 28 the initial core was composed of 8 batches with natural uranium and 10 batches with 0.6% U^{235}. This composition was too stiff for the Q-distribution at the end of the first cycle to get in accordance with the ideal Q-distribution Q^*. In another case with four enrichments (the same as in fig. 26) in the initial core, the accordance with Q^* was better, but still not satisfactory. Because of the strong non-linearity of Q vs. 1 (fig. 3) it was difficult with this special reactor type to make a composition of the initial core which at the same time possessed a large range of Q-values and did not get subcritical immediately after start-up. It is now realized that slightly enriched uranium fuel should have been tried together with natural

and depleted uranium. However, further work had to be given up because of shortage of time.

As the reload fuel is natural uranium, the discharge burn-up for the equilibrium core in fig. 28 is comparable with the discharge burn-up from the case with minimum form factor. The values taken from fig. 28 are given in case 6 of table 3. The equilibrium discharge burn-up is seen to be about 520 MWD/TU higher than in case 4.

6.2. Reduction of the Number of Trial Interchanges

When the core is refuelled, large perturbations are introduced in the N_d regions where burnt fuel is exchanged for new fuel. Obviously one of the batches to be interchanged must be searched for in these regions. This idea is the basis for the reduction of the number of trial interchanges.

6.2.1. The Search Technique

In the search for the first pair of batches to be interchanged j is stepped through the numbers of those regions that have just been refuelled (N_d numbers). For each j-value, k is stepped through the remaining region numbers ($N-N_d$ numbers). In any other respect the best pair of batches to be interchanged permanently is determined in the same way as described in section 6.1. In the second search j is stepped through N_d+1 numbers, namely the numbers of the N_d regions that were refuelled and the region whose fuel was just interchanged with the fresh fuel from one of these regions. k is now stepped through the $N-N_d-1$ numbers of hitherto unchanged regions. By continuing the search in this way, a new batch is involved in the shuffling for each new search. The shuffling is finished when the number of batch interchanges is L, or when no further improvement is possible. The total number of trial interchanges per cycle is seen to be reduced to $N_d(N-N_d) + (N_d+1)(N-N_d-1) + \ldots\ldots + (N_d+L-1)(N-N_d-L+1)$.

6.2.2. On-Load Calculations with Few Trial Interchanges

A few on-load examples shall be given for comparison with cases 1 and 3 from section 6.1.4.1.

The case with form factor minimization in fig. 29 is seen to give slightly higher form factors than found in case 1 (fig. 19). The discharge burn-up has not yet become stable after more than two full cores' irradiation time, and some weak periodic variation is also seen for the form factors. (At the start of discharge some details are missing in the figure, because six batches were discharged at very small time intervals). Fig. 29 corresponds to case 7 in table 3.

In case 8 only one pair of batches is allowed to be interchanged per cycle. As a result the form factor increases to as high values as 1.37 with eigenvalue calculation and 1.24 with power flattening. Because of the increase in form factor it is not surprising that the discharge burn-up is increased relative to case 7.

The core history with maximum burn-up and $F_m = 1.50$ is shown in fig. 30, which corresponds to case number 9 in table 3. The results are seen to be largely as good as those of case 3 (fig. 21). The average discharge burn-ups for core 2 given in cases 9 and 10 must be taken with the reservation that they are only based on the first fifteen batches of core 2. Case number 10 corresponds to case 9 with the difference that only one batch interchange is allowed per cycle.

The computing time on the B6500 was about 15 seconds processor time per cycle in cases 7 and 9.

6.3. Fixed Shuffling Schemes

The SELMA1 programme includes an option which uses fixed, input-specified shuffling schemes. The results of a case with a three-zone out-in scheme and another case with a mixed scatter loading scheme are given as cases 11 and 12 in table 4. The refuelling schemes are given below the table. In case 12 the two refuelling schemes are applied alternately in every second cycle. The discharge conditions correspond to off-load refuelling.

In the case with three-zone out-in the form factors from the eigenvalue calculation are tolerable. In the equilibrium core the power density is low at the centre, but not extremely low as the reactor is not very large. In the mixed scatter loading case a high power peak arises at the centre in every second cycle, when batch number 13 is reloaded into region number 1. In both of the cases the form factor is reduced by absorber power flattening. It is noted that the equilibrium discharge burn-up is about 250 MWD/TU higher in case 11 than in case 12.

The two cases should be compared with case 4 (and case 18 which shall be treated later). It should be remembered that the use of fixed shuffling schemes has the disadvantage that deviations in refuelling time or from the fixed scheme will bring the state of the core out of equilibrium, which gives rise to excursions of the power form factor from the steady state value. In that respect the self-management methods are more flexible.

Case number 13 is a special case of some theoretical interest, since the eighteen-zone in-out scheme was expected to give absolutely maximum

discharge burn-up. This expectation was based on the results from two other calculations.

The first case was an IBU1 calculation with burn-up optimization where the form factor limit was removed (in practice by giving F_m a very high value). The resulting ideal Q-distribution was a simple two-zone distribution with $Q = Q^u$ in a central zone and $Q = Q^l$ in an outer zone. The usual central zone with flat power distribution completely disappeared (cf. section 5.2.3). The eighteen-zone in-out scheme gives an equilibrium core in which the highest Q-value is also at the centre, and with radially decreasing Q.

The other case was calculated with SELMA1 using the direct shuffling optimization method with $F_m = 1.00$. The results clearly pointed in the direction of the eighteen-zone in-out scheme as the optimal shuffling scheme. All the batch interchanges moved fuel with higher irradiation outwards and fuel with lower irradiation inwards. Because of the limitations of the search technique, however, the resulting scheme did not become a pure in-out scheme, but the results were very close to those given in table 4, case 3, for the pure scheme.

Surprisingly the equilibrium discharge burn-up of 9325 MWD/TU from case 13 appeared not to be the maximum obtainable discharge burn-up. In a later case (17) as high a value as 9623 MWD/TU was obtained.

A further investigation showed that the fundamental hypothesis (cf. section 5.2.1) that the decreasing rate of the eigenvalue (here control poison level) is independent of the shuffling scheme becomes invalid in this extreme case. At moderate form factors the hypothesis is a good approximation, but at the excessive form factors in case 13 the decreasing rate of the control poison level is very high. This can be illustrated by the following decreasing rates of the average control poison cross section $d\bar{C}/dt$ obtained for three on-load cases with SELMA1:

Min. power form factor:	0.90×10^{-6} cm^{-1} day^{-1}
Max. discharge burn-up with $F_m = 1.50$:	1.18×10^{-6} cm^{-1} day^{-1}
Eighteen-zone in-out:	3.67×10^{-6} cm^{-1} day^{-1}

The values are equilibrium core values at end-of-cycle obtained by using small burn-up steps (5 days).

Even though the poison level is made highest by eighteen-zone in-out shuffling, $\bar{C}$ decreases so fast that the cycle time becomes shorter than in the case with $F_m = 1.50$.

7. FAST SHUFFLING METHODS

The fast shuffling methods which shall be considered in this chapter rely on empirical rules for fitting the predicted Q-distribution at the end-of-cycle to one of the ideal Q-distributions calculated by IBU1. In the previous chapter it was shown that the end-of-cycle Q-distributions obtained by direct shuffling optimization were in good agreement with the ideal Q-distributions, although the distributions are in principle obtained independently of each other. Inversely, a shuffling method that makes a good fit of the end-of-cycle Q-distribution to the ideal Q-distribution must be supposed to achieve optimum conditions in the core.

All the fast shuffling methods are designed to make their decisions, exclusively on the basis of the Q-distributions, rendering flux calculations in support of the decisions superfluous. The minimum integrated Q-deviations method, which shall be described first, is clearly the most reliable fitting method. It gives even better results for the equilibrium core than the direct method. However, it has the drawback that it requires almost all of the batches of the core to be moved at each shuffling. Consequently the method is not suitable for on-load purposes. In the search for feasible on-load methods a lot of different fitting rules were devised and tested. The most promising methods shall be described.

The work was concentrated on solving the equilibrium core problem. The ideal Q-distributions correspond to equilibrium conditions because of the way the limits Q^u and Q^l are chosen. The same ideal Q-distribution is used throughout the reactor life from the very start. During the approach to equilibrium, therefore, the actual distribution of the fuel cannot be expected to be fully optimal.

The few investigations of initial cores containing different enrichments give good prospects of optimizing the initial core too by means of the self-management method. But as long as the method for optimization of the external decisions, especially those concerning the enrichments, is not developed, it cannot be said whether the ideal Q-distribution corresponding to equilibrium core conditions is adequate for the initial core too, or whether some other ideal Q-distribution(s) with other Q^u- and Q^l-values apply better to the initial core. The answer to that question depends on the width of the range of Q-values in the initial core, which is to be found by the external optimization.

7.1. The Minimum Integrated Q-Deviations Method

It appears from the figures in which the end-of-cycle Q-distributions from direct shuffling optimization were compared with the ideal Q-distributions that the single Q_n-values may deviate quite much from Q_n^*, but the integrated Q-deviations $\left|\sum_{r=1}^{n}(Q_r-Q_r^*)\right|$ seldom become greater than the greatest value of $|Q_m-Q_m^*|$ for arbitrary region numbers m and n. This observation is the basis of the present method which is designed to minimize the integrated Q-deviations at the end-of-cycle.

7.1.1. Prediction of the Q-Deviations at the End-of-Cycle

Like all of the other fast shuffling methods the present method works on the predicted end-of-cycle Q-values $Q_n'(\Delta t_c)$ obtained by interpolation in the burn-up table for the predicted burn-up $I_n'(\Delta t_c)$ as obtained from (6.2a-c). For the sake of abbreviation the argument Δt_c shall be omitted in the following.

The predicted end-of-cycle Q-distribution Q_n' and the ideal Q-distribution Q_n^* generally have somewhat different levels. Before the shuffling the level of Q_n^* is shifted to the level of Q_n' by adding the amount $\overline{Q}' - \overline{Q}^*$ to Q_n^*. The resulting distribution is denoted q_n^*.

$$q_n^* = Q_n^* + (\overline{Q}' - \overline{Q}^*) . \tag{7.1}$$

The predicted Q-deviations at the end-of-cycle are now given by

$$\Delta Q_n = Q_n' - q_n^* . \tag{7.2}$$

This elaboration might seem trivial, but it is done because q_n^* is calculated before the shuffling, whereas ΔQ_n has to be recalculated every time a fuel batch is moved to another region, partly because q_n^* is different in the new region, and partly because Q_n' changes as a consequence of the change in φ_n^*, cf. (6.2a-b). The recalculation of ΔQ_n is implied any time the Q-deviation is used in the expressions of the different shuffling routines.

7.1.2. The Shuffling Method

The shuffling method is now simply to search for the fuel distribution with

$$\min_{1\le n\le N} \left|\sum_{r=1}^{n}\Delta Q_r\right| , \tag{7.3}$$

understood in the way that the search starts with n = 1 and moves outwards until n = N. For the arbitrary region number n the search for the "best" fuel batch to be allocated to that region is carried out among all the batches belonging to regions with numbers greater than, or equal to n. Suppose that batch number j is found to satisfy (7.3) best for region number n, ($j \geq n$). Then batches n and j are interchanged, and the search can be continued with region number n + 1. The total number of trial interchanges is seen to be $\binom{N}{2}$.

By starting the search at the centre the number of options becomes largest for the central region and is reduced outwards. This has the advantage that the Q-deviations become smallest at the centre which is the place where the power shape is most sensitive to deviations from Q^*.

The batch number j to be allocated to region number 1, (n = 1) is required to satisfy the additional condition

$$\Delta Q_{j,1} \langle \Delta Q_1 \wedge \Delta Q_{j,1} \rangle -3\Delta Q_1 \quad \text{if } \Delta Q_1 \geq 0,$$

and (7.4)

$$\Delta Q_{j,1} \rangle \Delta Q_1 \wedge 3\Delta Q_{j,1} \langle -\Delta Q_1 \quad \text{if } \Delta Q_1 \langle 0 ,$$

where ΔQ_1 is the Q-deviation before the interchange, and $\Delta Q_{j,1}$ is the Q-deviation according to (7.2) recalculated for batch number j at position n = 1. In plain talk the additional condition for region number 1 prefers negative to positive Q-deviations by a factor of three. This condition was introduced because of the experience that a high positive ΔQ_1 gives a large power peak at the centre. The same condition is introduced in the on-load shuffling methods which are described later.

7.1.3. Burn-up Giving Zero Integrated Reactivity

In fuel management it is common practice to use the burn-up I_o giving zero integrated reactivity as a standard of reference for evaluation of the obtainable burn-up of a given reactor with a given refuelling scheme. This quantity is defined in terms of the reactivity curve $\rho(I)$ for the point burn-up model by the expression

$$\int_0^{I_o} (\rho(I) - \rho_o)\, dI = 0, \tag{7.5}$$

where ρ_o is the reactivity at which the reactor is refuelled. I_o may be interpreted as the obtainable burn-up for a hypothetical reactor with con-

tinuous refuelling and homogeneous mixing-up of fresh and irradiated fuel in the core, and with a refuelling rate adjusted to give constant reactivity ρ_o of the reactor.

The reactivity curve ρ (I), and I_o corresponding to $\rho_o = 0$ are given in addition to the cross sections as results from the PBU programme (ref. 12). The result for the BHWR 750 MW reactor was $I_o = 10592$ MWD/TU. This value of I_o is used as the standard of reference in the off-load calculations. For the on-load cases the discharge criterion $\overline{C}_d = 3 \times 10^{-5}$ cm^{-1} must be transformed into the corresponding reactivity. For the point burn-up model the connection between the excess reactivity and the corresponding critical control poison cross section is given by the relation

$$C = k_\infty \Sigma_a \rho \quad . \tag{7.6}$$

The corresponding values of ρ and $k_\infty \Sigma_a$ making $C = 3 \times 10^{-5}$ cm^{-1} were found at 5050 MWD/TU, where $\rho = 0.90\%$. This reactivity was applied as ρ_o in (7.5), which then gave $I_o = 9445$ MWD/TU. This value is used as the standard of reference in the on-load cases.

The entry denoted α in tables 5 and 7 is the discharge burn-up ratio, defined by

$$\alpha = \frac{I_{eq}}{I_o} \quad , \tag{7.7}$$

where I_{eq} is the equilibrium average discharge burn-up. The calculated α-values shall be commented later.

7.1.4. On-Load Results for the BHWR 750 MWe

The results from a series of calculations for the BHWR 750 MWe reactor performed by means of the minimum integrated Q-deviations method are given in table 5. Most of the problems are the same as those treated by the direct optimization method so only a few remarks shall be spent on the single cases, except for new effects. For general remarks concerning the table and the accompanying figures the reader is referred to chapter 6. With the present method the computing time is reduced to 1.8 seconds processor time per cycle (about 0.3 seconds for the shuffling alone), which facilitates the computation of long core histories. The irradiation times were made sufficiently long for full equilibrium to be established.

The first four cases, 14 to 17, simulate on-load refuelling. Three of the corresponding form factor histories are shown in fig. 31, and the curves

in fig. 32 show the discharge burn-ups versus discharge number from the start-of-life. It is seen that the form factors from the eigenvalue calculation make some initial transients and then approach steady values somewhat higher than the ideal form factors, as might be expected on the basis of the discussion of fig. 22. The power shaping routine is seen to work satisfactorily in all of the cases. From fig. 32 it is seen that the approach to equilibrium of the discharge burn-ups occurs a little later than for the form factors. The initial transient of the burn-ups is seen to be smaller relative to the steady value, the larger F_m is made. As a rule the average discharge burn-up of the third core can be used as the equilibrium value. The equilibrium discharge burn-up is increased by 18% at $F_m = 1.50$ relative to the burn-up at minimum form factor ($F_m = 1.08$). The values of α are quite high in the on-load cases in which the refuelling approaches the continuous refuelling model. There is no contradiction in the fact that $\alpha > 1$ in case 17, because the fuel is not mixed homogeneously. On the contrary the fresh fuel is placed in the interior part of the core where the flux level is high, and the highly irradiated fuel is placed near the reflector where the flux is low (cf. fig. 17).

In cases 15, 16, and 17 the shuffling schemes become cyclic in the equilibrium state. In case number 14 the shuffling is still non-cyclic at cycle number 81, at which the calculation was stopped. In table 6 the shuffling schemes obtained from the SELMA1 calculations are given. For case 14 the last three shufflings are given. In case 16 two slightly different shuffling schemes were applied alternately in every second cycle from cycle number 61 and on. In case 17 four schemes were applied alternately. The cyclicity will be recognized in fig. 32.

In fig. 33 the Q-distribution taken from one of the equilibrium core cycles of case 14 is shown together with the ideal Q-distribution. It is seen that the best approximation to Q^* is achieved at the centre because of the special search technique of the shuffling routine.

The burn-up spectra given in fig. 37 are equilibrium burn-up spectra from each of the cases 14 to 17. They are obtained from the burn-up distribution in the equilibrium core at the end-of-cycle by arranging the fuel batches in one of the last cycles in order of increasing burn-up. The single points are connected with smooth curves in order to facilitate the survey. At low form factor the burn-up spectrum becomes almost linear. At increasing form factor the burn-up spectrum becomes distorted because in the last cycles before discharge the fuel is placed in the regions with low power densities.

The burn-up spectra may be utilized for the determination of values of Q^u and Q^l for IBU1. In the present investigation the behaviour of the reactor was of course known from many previous cases, so there were no problems with the determination of the Q-limits corresponding to equilibrium core conditions. Actually large freedom is alllowed in the choice of Q-limits without significant deterioration of the results from SELMA1. The following directives can be suggested for the choice of Q-limits for other reactors:

(1) Determine I_o from the reactivity curve $\rho(I)$ obtained from the point burn-up or cell calculation.

(2) Select the burn-up spectrum shape corresponding to the desired form factor limit F_m.

(3) Guess a value of α, taking into account the refuelling method, form factor limit F_m, reactor size, etc.

(4) Draw a new burn-up spectrum on the basis of these ingredients. The burn-up values at the low end are used for the determination of Q^u by entering the burn-up curve Q vs. I as determined from the point burn-up or cell data, and the burn-ups at the high end of the burn-up spectrum are used for the determination of Q^l in a similar manner.

Case number 21 in table 5 corresponds to case 14. The difference is that only three meshes are used as control meshes simulating banks of control rods. The ideal Q-distribution used as the reference distribution in this case was that shown in fig. 14. In the SELMA1 calculation the eigenvalue calculations were performed with equal poison in the three control meshes, and the remaining meshes clean of poison (in contradistinction to the previous cases, where the control poison distribution was uniform). The absorber power shaping routine worked with three control domains as described in chapter 4. The performance is seen to be nice with slightly higher form factors and lower discharge burn-up than in case 14.

7.1.5. Off-Load Results for the BHWR 750 MWe

Case number 18 in table 5 is an off-load simulation with minimum form factor. The corresponding fig. 34 exhibits very stable operation in the equilibrium state. It is seen by comparison with case 4 that the form factor from power flattening is smaller in the present case. This is supposed to be the reason why the equilibrium discharge burn-up is smaller. The value of α is significantly lower at off-load than at on-load simulation. The re-

fuelling scheme, which is given in table 6, becomes cyclic from cycle number 10.

In case number 19 the initial core is composed of the same four enrichments as were used in case 5. The form factors given in table 5 are the initial values, i. e. taken over the first three cycles. It is remarkable that this case ends up with the same shuffling scheme in the equilibrium state as the previous case, and that cyclicity occurs before. In this case too the integrated Q-deviations method gives better results than the direct method.

In case 22 the control poison is restricted to three control meshes in the same way as in the on-load case (21). The results should be compared with those of case 18. Generally higher form factors lead to higher discharge burn-up, but on the other hand the discrete poison distribution seems to lower the obtainable burn-up. The latter effect seems to have been prevailing in this case. The large initial transient is found at the end of the first cycle where the control poison level is zero, making power flattening impossible.

The core history shown in fig. 35 is from case 20. In this case the power shaping is working satisfactorily in contradistinction to case 6. The undesirable peaks at end-of-cycle are due to a limitation of the shuffling method in connection with the strong non-linearity of Q as a function of I (fig. 3). One of the Q-distributions at end-of-cycle is shown in fig. 36 in order to illustrate the bad fit to Q^* in this case. It is seen that the problem arises with region number 18, where Q gets much too high. This is explained by reference to expressions (7.1-3). q_n^* was calculated before the shuffling for the shuffling problem (7.3) to come right (at the termination of the search there is no choice for region number n = N, because the search is always carried out among the regions $j \geq n$). However, as a consequence of the recalculation of Q'_n and ΔQ_n any time a batch is moved, the level $\overline{Q}'$ is changed currently during the shuffling on account of the non-linearity of Q vs. I. A detailed study of the present case has shown that the level $\overline{Q}'$ increases because the shuffling makes the predicted irradiations I'_n of the fresh fuel shift from one side of the maximum on the Q vs. I curve to the other, keeping Q'_n almost constant for these batches, whereas the batches that are moved from regions with high power density to the outer regions with low power density get a high increase in Q'_n. This is the reason why the shuffling problem (7.3) does not come right at the termination, when n = 18.

Although the power peak is found near the centre, the maldistribution of Q_n is thought to have the responsibility. With a better fit to the ideal Q-distribution the cycle time would probably become longer (giving higher burn-up), and as the power peak is on fast return (cf. fig. 35), the form factor might then attain a lower value at the end-of-cycle. However, the problem is very complicated as any change in the shuffling method interferes with the equilibrium core burn-up spectrum as well as the cycle time.

The answer to the question why the same problem (with opposite sign) did not arise in case 18, is firstly that the power differences are not so large for the various regions, and secondly that the predicted irradiations I'_n for the fresh fuel do not move around the plutonium top when the fuel is shuffled, but at slightly higher irradiations.

When the detailed mechanism had been realized, the defect could have been remedied by recalculating q^*_n after the shuffling and repeating the shuffling immediately afterwards with the new and probably better level of q^*_n. However, this was not done. The problem is expected to disappear in cases with enriched uranium fuel, where Q as a function of irradiation does not possess the strong non-linearity.

In fig. 38 the burn-up spectra from the off-load cases 18 and 20 found analogously to the on-load spectra are shown.

7.1.6. Extension to 1165 MWe

The minimum integrated Q-deviations method as well as the direct shuffling optimization method were tested in a series of cases calculated for a hypothetical BHWR 1165 MWe reactor. The size of this reactor was chosen by proportioning the core of the BHWR 750 MWe reactor up in radial direction in the volumetric ratio 28/18. In this way the core radius became 525.0 cm. The core height, reflector thickness, average power density, etc. were the same as for the BHWR 750 MWe (cf. table 1), and the same burn-up tables (for natural uranium) were assumed (cf. figs. 3 and 4). The core was partitioned into 28 regions, each of which got the same volume as the regions in the 750 MWe reactor.

The intention with these calculations was primarily to test the methods on a very large reactor and the effect of increasing the number of regions, and secondly to get an impression of the dependence of the burn-up ratio a on the reactor size.

The performance of the two shuffling methods was found to be very similar to the performance in the 750 MW cases. The results from two on-load cases are given in table 7. Unfortunately, case 24 was too short

for the equilibrium discharge burn-up to be determined. It is expected to be very close to 10000 MWD/TU. However, the α-values are clearly seen to be increased as might be expected on account of the reduced influence of the leakage of neutrons out of the reactor on the reactivity.

7.1.7. Yankee Calculations

A few calculations were carried out for the Yankee reactor (ref. 11) with the purpose of testing the self-management method on a light-water reactor. The net production cross section Q as a function of burn-up was given in fig. 5, and the main plant data are seen in table 2. The reactor was too small for getting physically very interesting results. However, it is found interesting that the IBU1 programme, which calculates the ideal Q-distributions, gave as good convergence as in the heavy-water examples.

The ideal Q-distribution with minimum power form factor is shown in fig. 39. The upper Q-limit Q^u corresponds to the equilibrium core burn-up spectrum as obtained by SELMA1. It is seen that Q attains its upper limit everywhere, except in the three central regions, where the power shape is flattened. On application of the ideal Q-distribution as the reference distribution in SELMA1, the results given in table 8, case 25, were obtained. The shuffling scheme ended up as a pure three-zone out-in scheme in the equilibrium state. The absorber power shaping routine keeps the form factor low for most of the cycle, but towards the end-of-cycle the form factor increases to 1.41 when the control poison is removed. In case 26 the three-zone out-in scheme was applied with the routine using fixed refuelling schemes. In that case the absorber power flattening routine was not used. This case gives a somewhat higher discharge burn-up.

It is seen that the size of the Yankee reactor is near the lower limit of the range of applicability of the self-management method. The degeneration of the ideal Q-distribution gave rise to some trouble. The upper Q-limits Q^u had to be recalculated two times. In the first run with IBU1 the upper Q-limit was specified everywhere as the maximum Q, corresponding to zero burn-up. That gave a form factor as low as 1.03 with flat power distribution in twelve of the eighteen regions constituting the core. The Q-distribution was of the type shown in fig. 13 for the BHWR. On application of this first distribution as the reference distribution Q^* in SELMA1 an equilibrium core burn-up spectrum was obtained. On the basis of this spectrum new Q^u-values were determined and specified for a new IBU1 run. The whole procedure was repeated still once more, until there was reasonable accordance between the Q^u-values based on the equilibrium core burn-up

spectrum from the last SELMA1 calculation and those used in the previous IBU1 calculation.

Out of the six batches discharged at the end of an equilibrium core cycle the burn-up of the most irradiated batch is largely of the same magnitude as the burn-up of 10800 MWD/TU, at which Q crosses zero in fig. 5. It is supposed that IBU1 cannot be used for a smaller reactor than that giving a highest burn-up corresponding to $Q = \overline{C}_d$ (the discharge limit $\overline{C}_d = 0$ in this case).

7.2. The Sum of Least Squares of Integrated Q-Deviations Method

In this method the number of batch moves in the core per shuffling is reduced. First the same search technique was tried as was used in the direct shuffling optimization method with L successive searches, each one resulting in a pair of batches being interchanged. The "best" pair of batches to be interchanged was taken as the batches of those regions, j and k, that minimized the integrated Q-deviations from regions numbers 1 to j and from 1 to k. Actually this method gave a promising improvement of the Q-distribution at the interchange of the first pair of batches, but the batches interchanged next spoiled the good result from the first interchange if they belonged to regions with smaller numbers than j and k from the first interchange.

It was learnt from this example that the whole shuffling had to be performed at once. In the sum of least squares of integrated Q-deviations method, which shall now be described, the number of batches involved in a shuffling is permanently three, one of which is always the batch with fresh fuel. The shuffling method is designed for on-load refuelling only ($N_d = 1$).

7.2.1. The Shuffling Method

Suppose that region number n was refuelled. The search for two other batches j and k is then carried out among all of the other regions of the core, stepping j and k through the values $1 \leq j \leq N$ and $1 \leq k \leq N$ with the exception of j = n, k = n, and k = j. For each pair of numbers j and k the shuffling scheme n → k → j → n is tried[x]. The trial shuffling that gives minimum of the expression

---

[x] The resulting refuelling scheme is: Fresh fuel → k → j → n → discharge. Since both of the numbers j and k are stepped through the same values, the different shuffling scheme n → j → k → n is also tried.

$$\sum_{n=1}^{N} \left(\sum_{r=1}^{n} \Delta Q_r \right)^2 w_n \qquad (7.8)$$

and satisfies the additional condition (7.4) is taken as the "best" shuffling. By trial shuffling is meant a preliminary shuffling for the calculation of (7.8), after which the three batches are put back into their original regions. The Q-deviations ΔQ_r are given by expressions (7.2). The weight function w_n must be specified by the user. After completion of the search the shuffling that gave minimum of (7.8) and satisfied (7.4) is performed permanently. It is seen that the number of trial shufflings is (N-1) (N-2).

7.2.2. Results

The results from three of the cases calculated with this method are given in table 9. Cases 27 and 28 use the ideal Q-distribution with minimum form factor. In case 27 the weight function w is made constant all over the core, and in case 28 the weight function is given the distribution shown below the table. In this case the central regions are given very high weight with the consequence that the integrated Q-deviations become smaller for the central regions than for those far from the centre. It is seen that the form factors were only slightly improved. The same problem was also calculated with still another weight function, but without any significant change in the results.

Cases 27 and 28 should be compared with cases 7 and 8 in table 3. Unfortunately no results are available for the direct shuffling optimization method with L = 2, which would have been the correct reference case. However, the form factors from the eigenvalue calculation are slightly smaller in case 28 than in case 8, but higher than in case 7, indicating that the present shuffling method is acceptable in the minimum form factor case. The form factors from power flattening are better than those of case 8 as well as of case 7. The equilibrium discharge burn-up is seen to be slightly higher than in case 14, table 5.

Case 29 is of the burn-up optimization type with $F_m = 1.40$. As discussed in section 6.1.4.1 in connection with fig. 22 the form factors might be expected to be slightly higher than F_m, no matter how well the actual Q-distribution was fitted tc the ideal Q-distribution by shuffling. This justifies the comparison of case 29 with cases 9 and 10, calculated with direct shuffling optimization at $F_m = 1.50$. Even on this basis of reference the form factors obtained by shuffling in case 29 are pretty high. However,

the power shaping routine gives acceptable form factors. As the target power shape p^* in case 29 is different from p^* in cases 9 and 10, the results of these three cases cannot be used directly for estimating whether the performance of the power shaping routine is better when used in connection with the present shuffling method than in connection with the direct shuffling optimization method, but there seems to be an indication to that effect.

7.3. The Three-Region Q-Deviations Method

The previous methods involve an integration in radial direction and may for that reason give rise to some trouble if the methods are going to be transferred to a two-dimensional model because of possible difficulties in defining paths of integration.

Contrary to these previous methods the three-region Q-deviations method relies on an evaluation of the state of each of the two fuel batches interchanged at a time, each one evaluated in connection with the fuel of its two neighbour regions. The analogy to this method in two dimensions is clearly seen to be the evaluation of the state of a fuel element in connection with its nearest surroundings. Whether the method is fit for use in two dimensions is difficult to say for the present.

The method was developed in a number of variants, the best of which is described. The search technique is the same as was used in the direct shuffling optimization method with few trial interchanges.

7.3.1. The Shuffling Method

A shuffling consists of L searches, each one resulting in a pair of batches being interchanged (cf. section 6.2.1). At each of the L searches j is stepped through the numbers of the N_{ℓ} regions which were refuelled, and the regions which were involved in the present shuffling previously. For each j-value k is stepped through all of the hitherto unchanged regions (the remaining regions). The "best" pair of batches j and k to be interchanged is taken as those giving minimum of the expression

$$S_{j,k} + S_{k,j} - S_{j,j} - S_{k,k} \tag{7.9}$$

and satisfying the additional condition (7.4). The three-region Q-deviation sums are given by

$$
\begin{aligned}
S_{j,j} &= \left| \Delta Q_j + \tfrac{1}{2} (\Delta Q_{j-1} + \Delta Q_{j+1}) \right| w_j \\
S_{k,k} &= \left| \Delta Q_k + \tfrac{1}{2} (\Delta Q_{k-1} + \Delta Q_{k+1}) \right| w_k \\
S_{j,k} &= \left| \Delta Q_{j,k} + \tfrac{1}{2} (\Delta Q_{k-1} + \Delta Q_{k+1}) \right| w_k \\
S_{k,j} &= \left| \Delta Q_{k,j} + \tfrac{1}{2} (\Delta Q_{j-1} + \Delta Q_{j+1}) \right| w_j
\end{aligned}
\qquad (7.10a)
$$

except for the boundary regions, where (7.10a) is replaced by

$$
\begin{aligned}
S_{1,1} &= \left| \Delta Q_1 + \Delta Q_2 \right| w_1 \\
S_{j,1} &= \left| \Delta Q_{j,1} + \Delta Q_2 \right| w_1
\end{aligned}
\qquad (7.10b)
$$

and

$$
\begin{aligned}
S_{N,N} &= \left| \Delta Q_N + \Delta Q_{N-1} \right| w_N \\
S_{j,N} &= \left| \Delta Q_{j,N} + Q_{N-1} \right| w_N .
\end{aligned}
\qquad (7.10c)
$$

In these expressions ΔQ_j is the Q-deviation for batch number j before the interchange, given by (7.2), and $\Delta Q_{j,k}$ is the Q-deviation recalculated for batch number j in region number k. The sums are multiplied by a weight function w_j for region number j.

The "best" pair of batches j and k according to (7.9) are interchanged, and the search for a new pair of batches to be interchanged is initiated. After L batch interchanges, or when no further improvement is possible, the shuffling is finished.

It is seen from expressions (7.10a) that if the Q-deviation of a batch is balancing the average Q-deviation of the two neighbour batches, the corresponding sum S becomes zero. This is supposed to be a "good fit". By minimizing (7.9) it is seen that the shuffling method searches for the two batches j and k which on being interchanged "improve" the fit more than any other pair of batches.

7.3.2. Results

The results obtained by the three-region Q-deviations method are given in table 10. All of the cases except case 37 are on-load cases. Cases number 30 through 33 are with form factor minimization. Cases 34 through 36 are of the burn-up optimization type with $F_m = 1.40$. It is seen by comparison of case 30 with 31 that it is rather unimportant at form factor minimization whether the weight function w is made constant or given the distribution (d) that is shown below the table, whereas the form factors are somewhat lower in case 35 with the distribution (d) than in case 34 with $w = 1$ everywhere. This is the reason for using the distribution (d) in the remaining on-load cases. Comparison between cases 31 through 33 leads to the conclusion that no significant deterioration occurs at form factor minimization when the number of batch interchanges per shuffling L is decreased from 10 to 3, whereas the increase in form factor is serious at going from 3 to 1. At $F_m = 1.40$ the deterioration already occurs at $L = 3$. Finally, case number 37 shows that the method is inadequate for off-load purposes.

Unfortunately the comparison of the results from the three-region Q-deviations method with those from the sum of least squares of integrated Q-deviations method (table 9) is rendered difficult, because no results had been obtained with the present method for $L = 2$. The need for such cases could not be foreseen as the method of section 7.2 was the very last method developed, and time did not allow new runs with the other methods. The form factors from case 32 are seen to be smaller than those of case 28. For case 36 the maximum form factors from eigenvalue calculation are higher than for case 29. As these results are obtained for $L = 3$, the method of section 7.2 seems to be preferable as regards the form factor. The discharge burn-ups only show small variation from one method to another. In the cases with $F_m = 1.40$ only the burn-ups of the two first cores are given, because the computations were stopped when just under 50 batches had been discharged.

The computing time per cycle was (in seconds processor time) 2.39, 1.71, and 1.56 for $L = 10$, 3, and 1 respectively.

7.3.3. Remarks on Variants of the Method

Two variants of the method described in section 7.3.1 shall be briefly commented on here. In a version where the three-region expressions (7.10) for the sums S in (7.9) were replaced by the single region expressions

$S_{j,j} = |\Delta Q_j|$, $S_{j,k} = |\Delta Q_{j,k}|$, etc., Q often became higher than Q^* in several adjoining regions, giving rise to high unwanted power peaks. It was consequently found necessary to use at least three regions in the evaluation of whether the fit of Q to Q^* in a given region was good or bad.

In another variant of the three-region method expressions (7.10) were replaced by

$$S_{j,j} = |\Delta Q_{j-1} + \Delta Q_j + \Delta Q_{j+1}| \, w_j$$

and the analogous expressions. It appeared that this expression gave the two neighbour regions too high weight relative to region j itself. The form factors (from the eigenvalue calculation) generally became ten or twenty per cent higher than those in table 10.

A possibility that has not been utilized in the SELMA1 programme is "putting back" of the batches shuffled, returning to the time of shuffling and trying again with another shuffling, if the form factor during the succeeding cycle exceeds a certain limit. If such a facility were introduced in combination with the fast shuffling methods, it should only be used to avoid the emergence of extraordinarily high form factors, like those found now and then in the core histories, especially in cases with few batches interchanged per shuffling. In this manner probably only a few "putting-back" operations would be required during the computation of a whole core history.

8. EXTERNAL DECISIONS

In this chapter some ideas of how to approach the problems concerning the external decisions are outlined. This account does not pretend to solve this difficult problem, but a possible extension of the self-management method which might be of interest is pointed out. The external decisions concern the number of regions $N_{d,j}$ to be refuelled and the enrichment e_j of the fresh fuel loaded into the reactor at cycle number j. Further the choice of the internal optimality condition is regarded as an external decision. The internal optimality condition is given by the form factor limit F_m (which defines a specific ideal Q-distribution) together with the specification of which of the fast shuffling methods we want to use. The optimum value of F_m should be determined.

The intention is to separate the external decisions further in the following way. For a given internal optimality condition (F_m) we shall search for the sequence of decisions D_1, D_2, ... D_J giving minimum fuel cycle cost per energy unit. In this chapter the symbol D_j denotes the external decisions $N_{d,j}$ and e_j only, in contradistinction to the notation in chapter 2 and 3. The fuel cycle cost per energy unit is here defined as the costs of fuel and other variable costs per energy unit produced.

8.1. Suggestion for Determination of a Near to Optimum Sequence

The suggestion is to develop a third computer programme to supplement the two other programmes IBU1 and SELMA1. This third programme should be designed for the computation of a number of parallel core histories based on different sequences of external decisions D_1, D_2, ... D_J. Let us for the present suppose that the SELMA1 programme was declared as a procedure in this new programme. Further the programme should include an economic model for the calculation of the fuel cost as a function of the decisions D_j and the discharge burn-ups obtained from the SELMA1 "procedure". Other variable costs could be computed by simple expressions. The real time should be related to the irradiation time (the time in SELMA1) by means of a utilization factor and by taking into account the possible down-time for refuelling. On the basis of the real time and the rate of interest the fuel cycle costs should be reduced to the "present worth". The integrated power production should be calculated as being proportional to the irradiation time.

If the fuel cycle cost of cycle number j is c_j and the integrated power production is P_j, we want to determine the sequence of decisions, D_1, D_2, ... D_J, which gives

$$\min\left(\frac{\sum_{j=1}^{J} c_j}{\sum_{j=1}^{J} P_j}\right). \qquad (8.1)$$

At each stage j decision D_j is supposed to be a choice among very few (fixed) values of the number N_d of regions refuelled and of enrichments e (all of the N_d fuel batches are getting equal enrichment). If, for example, there are two possible values of N_d and three possible values of e, there are six possible decisions at stage number j for a given sequence D_1, D_2, ... D_{j-1}. As the number of possible sequences rises exponentially with stage number j (with the exponent six in the example), it is necessary to exclude non-profitable sequences. The suggestion is to retain at any stage a moderate number of most profitable, parallel sequences and drop the rest. The most profitable sequences at stage number j should be chosen according to

$$\min\left(\frac{\sum_{i=1}^{j} c_i}{\sum_{i=1}^{j} P_i}\right). \qquad (8.2)$$

In this way we always follow the most powerful branches on the "dicision tree". Such exclusion of non-profitable sequences might of course theoretically lead to exclusion of some sequences which at later stages would appear to be profitable, but in practice this is thought to be very unlikely.

The optimum value of F_m is supposed to be found parametrically. The most profitable sequence of decisions D_1, D_2, ... D_J should be found for different values of F_m (different ideal Q-distributions). It is seen to be an indirect function of F_m. Further the fixed costs (mainly capital) are a function of F_m. The optimum value of F_m should be determined as the value giving minimum unit energy cost, i. e. fixed and variable "present worth" costs over the whole life of the reactor, divided by the total energy produced.

8.2. Modification of the Fuel Management Procedure

In the outline of the suggested programme the fuel management procedure was taken as the whole SELMA1 programme in order to facilitate the exposition. However, there are good reasons to believe that SELMA1 may be modified significantly for the present purpose in order to reduce the computing time. Since the power shape during the whole life of the reactor is kept very near to the ideal power shape p_n^*, it might appear to be a sufficiently good approximation to assume constant flux and power shapes, $\varphi_n = \varphi_n^*$ and $p_n = p_n^*$, throughout the life of the reactor. φ_n^* and p_n^* are the distributions corresponding to the ideal Q-distribution found by IBU1. In this manner the very time-consuming flux calculations by the eigenvalue method and the absorber power shaping method could be completely avoided.

The shuffling method should be the minimum integrated Q-deviations method, which gave the best performance with power shapes very near to p_n^*. The burn-up and discharge routines should be used unchanged.

In SELMA1 the determination of the cycle length was based on the critical control poison level $\overline{C}$ (cf. section 3.7). In the modified version this method must be replaced by another method. The method used for the prediction of the cycle time Δt_c based on the Q-level (cf. section 6.1.1), could also be used for the final determination of the cycle time in the modified version.

Of course a detailed testing of the modifications suggested should be made by means of the complete SELMA1 programme in order to investigate the effects of the approximations.

8.3. Estimate of Computer Requirements

The shuffling routine alone was previously found to use about 0.3 seconds processor time per cycle. On stripping the SELMA1 programme of the most time-consuming parts, the total computing time per cycle will presumably be brought down to roughly 0.5 seconds. The cost calculations are thought to be very fast. Suppose that the programme is used in off-load simulation and that the number of cycles $J = 20$. Then it will be possible to calculate e.g. 100 branches on the "decision tree" per cycle. In that case the total computing time will be about $0.5 \times 20 \times 100 = 1000$ seconds processor time. The storage requirement will be rather small as only 2 N words are required for the storage of burn-up and enrichment of the fuel of N regions making $2 \times 18 \times 100 = 3600$ words in the 18 region case. Further about the same space will be required for the storage of the 100 core histories $D_1, D_2, \ldots D_J$.

9. SUMMARY AND MAIN CONCLUSIONS

The core management problem was approached for a one-dimensional, one-group model. The multistage decision process was separated into internal and external decisions by means of an internal optimality condition. This condition is either (1) minimum power form factor or (2) maximum fuel burn-up with limited power form factor. Only the internal problem was treated. The external decisions regard the power form factor F_m at which the reactor is wanted to be operated, the number of regions refuelled per cycle, and the enrichment of the reload fuel. In the approach to the internal decision problem these quantities are supposed to be given.

The state of the fuel is described by the "net production cross section" Q. The first internal decision concerning the time of refuelling is based on the critical control poison level. When the minimum poison level is reached, the fuel with lowest Q is exchanged for fresh fuel. The fuel shuffling is performed as a synthesis of a "best fit" of the actual Q-distribution to an ideal Q-distribution, applied as a reference distribution. The ideal Q-distribution corresponding to a definite internal optimality condition specified by F_m is determined at equilibrium core conditions. By means of the absorber power shaping routine the power shape is kept fairly constant during the whole cycle, the target power shape being the ideal power shape with form factor F_m.

Three different shuffling methods based on simple empirical fitting rules are described. All the shuffling decisions are exclusively based on the Q-distributions without support from flux calculations. The minimum integrated Q-deviations method is clearly the most suitable method for off-load simulation. It shows very stable performance with form factors slightly higher than the ideal form factor, except in a single case where a power peak arises at the end-of-cycle, presumably because of the strong non-linearity of Q as a function of irradiation for the natural uranium fuel of the specific reactor (BHWR 750 MWe) used in most of the test examples. The method has given promising results in a case with four enrichments in the initial core. Applied on the Yankee reactor the method gave the pure three-zone out-in scheme as a result. The method is supposed to be unsuitable for smaller reactors. Despite the large number of fuel batches being shuffled per cycle the method has been applied for on-load simulation for the BHWR, and it gave an 18% increase in discharge burn-up on going from minimum form factor to $F_m = 1.50$. At $F_m = 1.50$ a discharge burn-

up ratio $a > 1$ was found. Only cost calculations can show which value of F_m is optimum. For a very large reactor (BHWR 1165 MWe) the form factor was kept as stable as for the smaller reactor, and the discharge burn-up increased.

The two other fast shuffling methods described are only suitable for on-load simulation. The number of fuel batches being shuffled per cycle can be limited, but as a consequence the form factors get larger than with the minimum integrated Q-deviations method.

It has been found advantageous to apply the self-management method with optimization of the Q-distribution at the end-of-cycle under the definite assumption that the control absorbers were allowed to be used for power shaping. However, detailed power shaping is not possible in all reactors. If the control absorber distribution is required to be kept fixed, the ideal Q-distribution should be determined corresponding to start-of-cycle conditions and the shuffling rules applied on the start-of-cycle Q-distribution.

Certainly a good deal of work is still required, but as a general conclusion the self-management method has proved suitable for use in one dimension and one energy group. The processor time used by the integrated Q-deviations method on the Burroughs B6500 computer was 0.3 seconds per cycle in a case with the number of regions $N = 18$. According to the expression $\frac{1}{2} N(N-1)$ for the number of trial interchanges the processor time per cycle in a case with $N = 100$ is estimated to be about 10 seconds. On the basis of these facts there seems to be good prospects for the method if developed in two-dimensional geometry.

ACKNOWLEDGEMENTS

The author is much indebted to B. Micheelsen for having got the opportunity to continue the work that he started with the ONE-SS programme. Thanks are also due to the other members of the Reactor Physics Department of Risö for their valuable assistance and advices, especially to G. K. Kristiansen and K. E. Lindstrøm Jensen, as well as the entire computer group.

The work was made possible by a grant from the Danish Atomic Energy Commission, which is gratefully acknowledged.

REFERENCES

1) D. J. Bauhs, W. D. Leggett, and D. A. Nordman, Core Management and Fuel Cycle Costs. Proc. Amer. Power Conf. 31, (1969) 164-73.

2) S. Glasstone and A. Sesonske, Nuclear Reactor Engineering, (D. van Nostrand Co., Inc., Princeton, N. J., 1963) 830 pp.

3) I. Wall and H. Fenech, The Application of Dynamic Programming to Fuel Management Optimization, Nucl. Sci. Eng. 22 (1965) 285-297.

4) R. L. Stover and A. Sesonske, Optimization of BWR Fuel Management Using an Accelerated Exhaustive Search Algorithm, J. Nucl. Energy 23 (1969) 673-682.

5) G. Andersson, On the Theory of Reactor Operation Optimization, Parts I and II, AE-RFR-555 (1966) and AE-RFR-678 (1967).

6) W. B. Terney and H. Fenech, Control Rod Programming Optimization Using Dynamic Programming, Nucl. Sci. Eng. 39 (1970) 109-114.

7) M. Melice, Pressurized Water Reactor Optimal Core Management and Reactivity Profiles, Nucl. Sci. Eng. 37 (1969) 451-477.

8) A. N. Buckler, ODYSSEUS, A Two-Group Two-Dimensional Fuel Cycle Computer Programme Suitable for Advanced Gas-Cooled Reactors. Part A, TRG-Report-976(W), (1965) 13 pp.

9) A. N. Buckler, ODYSSEUS 6-A Comprehensive Fuel Management Code for AGR's. AEEW-R 652 (1970) 31 pp.

10) Danish Atomic Energy Commission 1969/70, Fourteenth Annual Report (1970) 13-14. Detailed report is to be published.

11) H. W. Graves, R. F. Janz, and C. G. Poncelet, The Nuclear Design of the Yankee Core. YAEC-136 (1961) 88 pp.

12) J. Pedersen, Risö, Denmark, internal report (1967).

13) O. Kalnæs, H. Neltrup and P. L. Ølgaard, A Recipe for Heavy-Water Lattice Calculations. Risö Report No. 81 (1964) 43 pp.

14) C. G. Poncelet, LASER - A Depletion Programme for Lattice Calculations based on MUFT and THERMOS. WCAP-6073 (1966) 104 pp.

15) A. Hassitt, A Computer Program to Solve the Multigroup Diffusion Equations. TRG Report 229 (1962) 39 pp.

16) G. K. Kristiansen, Risö, Denmark, personal communication, 1969.

17) R. S. Varga, Matrix Iterative Analysis (Prentice-Hall, Inc., Englewood Cliffs, N. J., 1962) 322 pp.

18) K. E. Lindstrøm Jensen, Development and Verification of Nuclear Calculation Methods for Light-Water Reactors. Risö Report No. 235 (1970) 161 pp.

19) B. Micheelsen, Risö, Denmark, internal report (1968).

20) R. L. Crowther, Burn-up Analysis of Large Boiling-Water Reactors. In: Fuel Burn-up Predictions in Thermal Reactors. Proceedings of a panel held in Vienna, 10-14 April, 1967. (IAEA, Vienna, 1968) 173-89.

21) R. V. Meghreblian and D. K. Holmes, Reactor Analysis (McGraw-Hill Book Company, Inc., New York, 1960) 808 pp.

APPENDIX

We shall consider a two-region case with the net production cross sections Q_1 in the inner and Q_2 in the outer region. The situation is shown in the two-dimensional Q-space in fig. A1, where it is assumed that the eigenvalue varies linearly with the position (Q_1, Q_2). Suppose we are at position A. According to the principles given in section 5.2 we move a step from A in the direction of -grad J. Then the Q-distribution is normalized, whereby we arrive at point B on the line $\lambda = 1$. For simplicity it is assumed that the normalization move hits the line $\lambda = 1$ exactly. The normalization moves the point in a direction 45° to the axes (equal changes of Q_1 and Q_2). From B we move in the direction of -grad J at the point B and so on until we get to the forbidden region where $F \rangle F_m$ (or until we reach one of the limits on Q).

We want to show that this procedure leads to the point on the line $\lambda = 1$ where $\overline{Q}$ is minimum. This is done under the assumption $0^\circ \langle \alpha \langle 45^\circ$ in accordance with the experience that the change of the eigenvalue is faster in direction Q_1 than in direction Q_2 (cf. the remarks in section 5.2.1). Under this assumption it is seen that the point on $\lambda = 1$ where $\overline{Q} = \frac{1}{2}(Q_1 + Q_2)$ is minimum, is at the lower end of $\lambda = 1$. The aim therefore is to show that a step from point B in the direction of -grad J together with a normalization move 45° to the axes will lead to a point D below B.

In fig. A2 the situation around point B is considered. In order to determine the direction of grad J the variation of $\overline{Q}$ and $\lambda\overline{C}$ by a displacement q from B to B' in the direction θ must be known. It is seen that the variation of $\overline{Q}$ is

$$\Delta\overline{Q} = \frac{1}{2}(\Delta Q_1 + \Delta Q_2) = \frac{1}{2}q(\sin\theta - \cos\theta). \qquad (A.1)$$

The variation of $\lambda\overline{C}$ is assumed to be proportional to the distance from the line $\lambda = 1$

$$\Delta\lambda\overline{C} = c\sin(\theta - \alpha). \qquad (A.2)$$

c is the proportionality constant. From $J = \overline{Q} - \lambda\overline{C}$ it is seen that

$$\Delta J = \frac{1}{2}q(\sin\theta - \cos\theta) - c\sin(\theta - \alpha). \qquad (A.3)$$

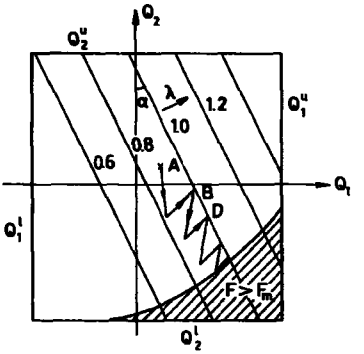

Fig. A1.

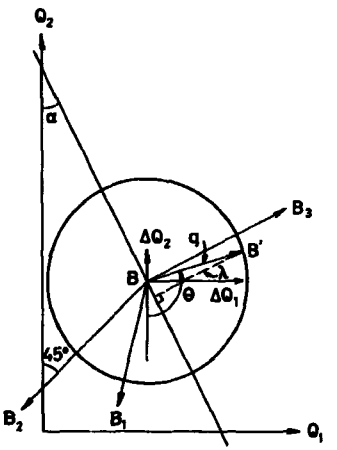

Fig. A2.

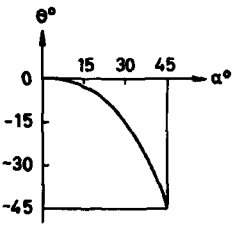

Fig. A3.

The direction of -grad J is given by the value of θ, for which

$$y = \frac{\Delta J}{q} = \frac{1}{2}(\sin\theta - \cos\theta) - \frac{c}{q}\sin(\theta - \alpha) \qquad (A.4)$$

is minimum. This value is found in the usual way.

$$y = (\frac{1}{2} - \frac{c}{q}\cos\alpha)\sin\theta - (\frac{1}{2} - \frac{c}{q}\sin\alpha)\cos\theta \qquad (A.5)$$

$$\frac{dy}{d\theta} = (\frac{1}{2} - \frac{c}{q}\cos\alpha)\cos\theta + (\frac{1}{2} - \frac{c}{q}\sin\alpha)\sin\theta = 0 \qquad (A.6)$$

$$\operatorname{tg}\theta = -\frac{\frac{1}{2} - \frac{c}{q}\cos\alpha}{\frac{1}{2} - \frac{c}{q}\sin\alpha} . \qquad (A.7)$$

We do not know the value of $\frac{c}{q}$, but it is required by the neutron balance equation that any change in Q_n is accompanied by a change in λ of such a magnitude that $\Delta\lambda\overline{C}$ becomes almost equal to $\Delta\overline{Q}$. The change of J results as a small quantity compared with $\Delta\overline{Q}$ and $\Delta\lambda\overline{C}$. For these reasons it is of special interest to find the direction of -grad J in the case $\frac{1}{2}q = c$.

1°. $\frac{c}{q} = \frac{1}{2}$:

$$\operatorname{tg}\theta = -\frac{1-\cos\alpha}{1-\sin\alpha} . \qquad (A.8)$$

This equation has two solutions corresponding to the minimum and the maximum of y. For the minimum value the variation of θ with α in the interval $0^\circ < \alpha < 45^\circ$ according to (A.8) is shown in fig. A3.

The angle between the line $\lambda = 1$ and the direction of -grad J is $\alpha - \theta$. It is seen that for small values of α, the angle $\alpha - \theta$ is small, and consequently the convergence is good. For $\alpha \to 45^\circ$ we get $(\alpha - \theta) \to 90^\circ$. The arrow BB_1 in fig. A2 indicates the direction of -grad J. Even though the convergence is bad for large values of α, point D in fig. A1 will always get to be below B, since $\theta > -45^\circ$.

In case $c \neq \frac{1}{2}q$, it can be shown that point D still gets below B. We shall consider the two limiting cases:

2°. $\frac{c}{q} \to 0$:

$$\operatorname{tg}\theta \to -1 \qquad (A.9)$$

y is minimum for $\theta = -45^{\circ}$. The direction of -grad J is indicated by BB_2 in fig. A2.

3°. $\frac{c}{q} \to \infty$:

$$\operatorname{tg} \theta \to - \cot \alpha \qquad (A.1C)$$

y is minimum for $\theta = \alpha + 90^{\circ}$. The direction of -grad J is indicated by BB_3 in fig. A2.

These results could have been seen directly as they correspond to $J = \overline{Q}$ in case 2°, and $J = -\lambda\overline{C}$ in case 3°.

Case 3° seems to indicate that the definition of the object function J could have been avoided since a move in the direction of $\operatorname{grad}\lambda$, indicated by BB_3, and the subsequent normalization move 45° to the axes also leads to a point on $\lambda = 1$ below B. This suggests the use of the statistical weight (ref. 21) instead of grad J in (5.10a), cf. footnote in section 5.2.2.

Table 1

BHWR 750 MWe (version 2). Main plant data

Reactor thermal power	MWt	2450
Net electric output	MWe	750
Average power density	MW/TU	21.85
Core diameter	cm	842.7
Core height	cm	442
Radial reflector (to moderator tank)	cm	41.3
Axial reflector, top and bottom	cm	100.5
Number of fuel elements		542
Number of refuelling channels		2
Number of control rods		60
Square lattice pitch	cm	30.4
Number of fuel rods per cluster		36
Fuel enrichment	w/o U^{235}	0.712
Fuel pellet diameter	mm	13.43
Can thickness	mm	0.55
Shroud inner diameter	mm	172.7
Shroud thickness	mm	1.2

Table 2

Yankee Core I (PWR). Main plant data

Nominal power output	MWt	392
Average power density	MW/TU	18.75
Average core diameter	cm	190.75
Active core height	cm	233.40
Number of fuel assemblies		76
Number of fuel rods		23142
Fuel rod pitch	cm	1.0719
Fuel rod outside diameter	cm	0.8636
Fuel rod stainless-steel cladding thickness	cm	0.0533
Fuel pellet diameter	cm	0.7468
Fuel enrichment	w/o U^{235}	3.4
Number of Ag-In-Cd control rods		24
Number of Zr shims		8
Average power density	MW/TU	18.75

Table 3

BHWR 750 MWe. Results from direct shuffling optimization

Search technique			Many trial interchanges						Few trial interchanges			
Case No.			1	2	3	4	5	6	7	8	9	10
Nc. of batch discharges per cycle N_d			1	1	1	6	6	6	1	1	1	1
No. of initial core enrichments			1	1	1	1	4	2	1	1	1	1
Max. no. of batch interchanges L			5	5	5	10	10	10	5	1	5	1
Discharge condition $\bar{C}_d(10^{-5}cm^{-1})$			3	3	3	0	0	0	3	3	3	3
Form factor aim F_m			Min.	1.25	1.50	Min.	Min.	1.50	Min.	Min.	1.50	1.50
Radial power form factor	Max. initial transient (power shaping)		1.25	1.29	1.64	1.70	1.23	1.63	1.26	1.23	1.77	1.91
	Equilibrium core, Eigenvalue	Average	1.18	1.27	1.52	1.35	1.30[a]	1.58	1.19	1.25	1.50	1.51
		Max.	1.24	1.31	1.70	1.83	1.76[a]	2.11	1.27	1.37	1.61	1.56
		Max. end-of-cycle	1.15	1.26	1.50	1.24	1.23[a]	1.50	1.20	1.37	1.50	1.50
	Equilibrium core, Power shaping	Average	1.10	1.24	1.55	1.12	1.13[a]	1.55	1.11	1.15	1.56	1.60
		Max.	1.14	1.29	1.59	1.24	1.23[a]	1.70	1.15	1.24	1.60	1.68
Discharge burn-up (MWD/TU)	Max. for single batch		9640	9580	9920	9805	9514	10231	9885	9381	10165	10453
	Core number 1, average		7414	8103	8697	7076	6085[b]	6593[b]	7470	7467	8763	8834
	Core number 2, average		-	-	-	7580	-	8081[b]	8153	8359	9307	9088
	Equilibrium, average		-	-	-	7839	-	8357	-	-	-	-

a) initial core values

b)

Table 4

BHWR 750 MWe. Results by fixed shuffling schemes

Refuelling method				3-zone out-in	Mixed scatter loading	18-zone in-out
Case No.				11	12	13
Discharge condition $\bar{C}_d(10^{-5}cm^{-1})$				0	0	3
Radial power form factor	Max. initial transient (power flattening)			1.70	1.70	6.03[x]
	Equilibrium core	Eigenvalue	Average	1.31	1.40	5.93
			Max.	1.33	1.80	6.03
		Power flattening	Average	1.16	1.13	-
			Max.	1.29	1.27	-
Discharge burn-up (MWD/TU)	Max. for single batch			8823	9197	12065
	Core number 1, average			6970	6976	6130
	Core number 2, average			7584	7408	9300
	Equilibrium, average			7825	7572	9325

x) No power flattening

Refuelling schemes

Region No.	1	2	3	4	5	6	7	8	9	10	11	12	13	14	15	16	17	18
	gets fuel from region no. (0 indicates fresh fuel)																	
3-zone out-in	7	8	9	10	11	12	13	14	15	16	17	18	0	0	0	0	0	0
Mixed scatter loading (2 schemes applied alternately)	13		14		15		16		17		18		0	0	0	0	0	0
		13		14		15		16		17		18	0	0	0	0	0	0
18-zone in-out	0	1	2	3	4	5	6	7	8	9	10	11	12	13	14	15	16	17

Table 5

BHWR 750 MWe. Results obtained by the minimum integrated Q-deviations method

Case No.				14	15	16	17	18	19	20	21	22
No. of batch discharges per cycle N_d				1	1	1	1	6	6	6	1	6
No. of initial core enrichments				1	1	1	1	1	4	1	1	1
Discharge condition $\overline{C}_d(10^{-5}cm^{-1})$				3	3	3	3	0	0	0	3	0
No. of control meshes				22	22	22	22	22	22	22	3	3
Ideal power form factor F_m				1.08	1.20	1.40	1.50	1.07	1.07	1.50	1.07	1.07
Radial power form factor	Max. initial transient (power shaping)			1.23	1.29	1.52	1.64	1.70	1.18	1.68	1.30	2.09
	Equilibrium core	Eigenvalue	Average	1.14	1.28	1.52	1.61	1.35	1.35[a]	1.86	1.13	1.37
			Max.	1.20	1.31	1.58	1.66	1.53	1.59[a]	2.11	1.19	1.59
			Max. end-of-cycle	1.14	1.26	1.48	1.56	1.14	1.18[a]	1.71	1.15	1.20
		Power shaping	Average	1.09	1.22	1.42	1.52	1.10	1.11[a]	1.54	1.12	1.15
			Max.	1.09	1.22	1.42	1.52	1.14	1.18[a]	1.71	1.16	1.20
Discharge burn-up (MWD/TU)	Max. for single batch			9223	9735	10035	10038	9368	8858	8798	9376	9208
	Core number 1, average			7207	8072	8442	8572	7053	5986[b]	7414	7079	7184
	Core number 2, average			7899	8994	9496	9616	7416	7496[b]	8282	7848	7413
	Equilibrium, average			8124	9046	9464	9623	7580	7580	8270	7945	7558
α				0.86	0.96	1.00	1.02	0.72	0.72	0.78	0.84	0.71

a) initial core values

b) depleted uranium

Refuelling schemes for equilibrium core found by the minimum integrated Q-deviations method

Case No.	Cyclic from cycle No. (if cyclic)	Region No.																	
		1	2	3	4	5	6	7	8	9	10	11	12	13	14	15	16	17	18
		gets fuel from region No.																	
14	81 still non-cyclic (last 3 shufflings given)	-	5	-	2	7	4	9	6	12	8^{x}	-	14	15	0	18	17	16	13
		2	3	5	1	7	4	9	6	12	8^{x}	0	13	11	17	14	18	15	16
		3	1	5	2	7	4	9	6	12	8^{x}	18	13	14	0	16	15	-	11
15	27	2	3	5	1	7	4	9	6	10	12	0	14	11	13	16	18	15^{x}	8
16	61 (bi-cyclic)	2	3	5	1	7	4	8	10	0	11	9	14^{x}	6	18	-	13	16	17
		2	3	5	1	7	4	8	10	0	11	9	18	6	16	14	15	12^{x}	13
17	50 (quadro-cyclic)	2	4	1	6	3	7	9	0	10	8	17^{x}	5	12	13	14	18	16	15
		2	4	1	6	3	7	9	0	10	8	17^{x}	5	12	13	14	15	16	-
		2	4	1	6	3	7	9	0	10	8	17^{x}	5	12	13	14	15	18	16
		2	4	1	6	3	7	9	0	10	8	17^{x}	5	12	13	14	-	18	15
18	10	11^{x}	13	9^{x}	14	8^{x}	15	6^{x}	16	17	4^{x}	18	2^{x}	0	0	0	0	0	0
19	8	11^{x}	13	9^{x}	14	8^{x}	15	6^{x}	16	17	4^{x}	18	2^{x}	0	0	0	0	0	0
20	10 still non-cyclic (last shuffling given)	9	0	8	0	7^{x}	0	0	0	0	6	2	18	11^{x}	12^{x}	10^{x}	1^{x}	3^{x}	4

^{x} discharged regions. 0 fresh fuel. - unchanged.

Table 7

BHWR 1165 MWe (28 regions). Results obtained by the minimum integrated Q-deviations method. On-load ($N_d = 1$, $\overline{C}_d = 3 \times 10^{-5} cm^{-1}$)

Case No.				23	24
Ideal power form factor F_m				1.07	1.40
Radial power form factor	Max. initial transient (power shaping)			1.20	1.49
	Equilibrium core	Eigenvalue	Average	1.14	1.57
			Max.	1.19	1.65
			Max. end-of-cycle	1.15	1.50
		Power shaping	Average	1.08	1.43
			Max.	1.09	1.43
Discharge burn-up (MWD/TU)	Max. for single batch			10017	10540
	Core number 1, average			7670	9047
	Core number 2, average			8516	9980
	Equilibrium, average			8728	-
α				0.93	≥ 1.06

Table 8

Yankee 392 MWe PWR. Results obtained by the minimum integrated Q-deviations method and three-zone out-in. Off-load (N_d = 6, $\overline{C}_d$ = 0)

Case No.				25	26
Shuffling method				Min. integr. Δ Q	Three-zone out-in
Ideal power form factor (Min.)				1.35	-
Radial power form factor	Max. initial transient (power flattening)			1.88	2.10[x]
	Equilibrium core	Eigenvalue	Average	1.42	1.38
			Max.	1.44	1.42
			Max. end-of-cycle	1.41	1.36
		Power flattening	Average	1.29	-
			Max.	1.41	-
Discharge burn-up (MWD/TU)	Max. for single batch			11322	11131
	Core number 1, average			9024	9097
	Core number 2, average			9051	9264
	Equilibrium, average			9110	9280

[x] No power flattening

Table 9

BHWR 750 MWe. Results obtained by the sum of least squares of integrated Q-deviations method. On-load simulation ($N_d = 1$, $\overline{C}_d = 3 \times 10^{-5} cm^{-1}$)

Case No.				27	28	29
Form factor aim F_m				1.08	1.08	1.40
Weight function w[a)]				1	d	d
Radial power form factor	Max. initial transient (power shaping)			1.23	1.23	2.46
	Equilibrium core	Eigenvalue	Average	1.21	1.21	1.60
			Max.	1.41	1.37	1.81
			Max. end-of-cycle	1.35	1.29	1.71
		Power shaping	Average	1.10	1.10	1.44
			Max.	1.13	1.13	1.49
Discharge burn-up (MWD/TU)	Max. for single batch			9446	9541	10286
	Core number 1, average			7302	7318	8793
	Core number 2, average			7938	7971	9578
	Equilibrium, average			8186	8213	-

a) w is either 1 for all regions (1) or has the distribution (d):

Region No.	1	2	3	4	5	6	7	8	9	10	11	12	13	14	15	16	17	18
w	30	15	8	5	4	4	3	3	3	3	3	3	3	3	2	2	1	1

BHWR 750 MWe. Results obtained by the three-region Q-deviations method

Case No.			30	31	32	33	34	35	36	37
No. of batch discharges per cycle N_d			1	1	1	1	1	1	1	6
Max. No. of batch interchanges L			10	10	3	1	10	10	3	30
Discharge condition $\overline{C}_d$ (10^{-5} cm^{-1})			3	3	3	3	3	3	3	0
Form factor aim F^m			1.08	1.08	1.08	1.08	1.40	1.40	1.40	1.07
Weight function w[a)]			1	d	d	d	1	d	d	1
Radial power form factor	Max. initial transient (power shaping)		1.23	1.23	1.23	1.27	1.52	1.55	1.71	2.04
	Equilibrium core, Eigenvalue	Average	1.17	1.17	1.19	1.35	1.55	1.52	1.60	1.42
		Max.	1.28	1.29	1.26	1.83	1.71	1.63	1.97	2.29
		Max. end-of-cycle	1.23	1.23	1.26	1.75	1.59	1.54	1.75	1.61
	Equilibrium core, Power shaping	Average	1.09	1.09	1.10	1.15	1.43	1.44	1.44	1.12
		Max.	1.10	1.10	1.13	1.28	1.44	1.47	1.47	1.61
Discharge burn-up (MWD/TU)	Max. for single batch		9256	9340	9442	9883	9783	10264	9918	9445
	Core number 1, average		7238	7268	7325	7426	8499	8510	8736	7009
	Core number 2, average		7943	7910	8120	8160	9472	9479	9326	7455
	Equilibrium, average		8130	8120	8287	8492	-	-	-	7630

a) w is either 1 for all regions (1) or has the distribution (d):

Region No.	1	2	3	4	5	6	7	8	9	10	11	12	13	14	15	16	17	18
w	16	9	7	5	4	4	3	3	3	3	3	3	3	3	2	2	1	1

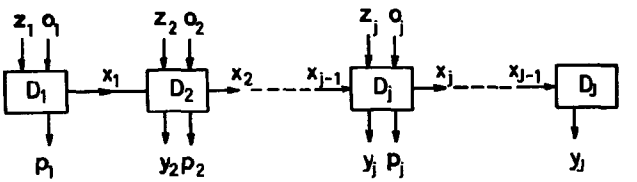

Fig. 1. Reactor life regarded as a multistage decision process.

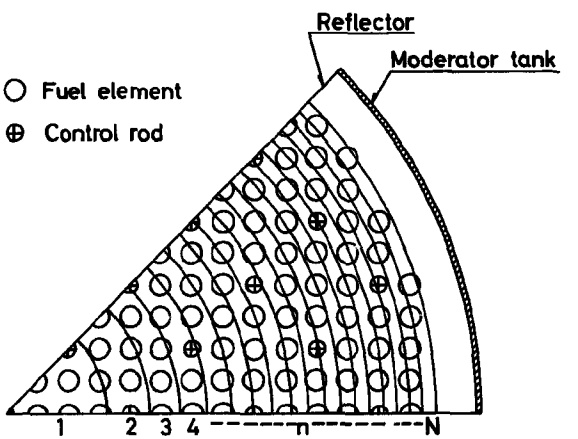

Fig. 2. BHWR 750 MW. Core configuration and fuel region partitioning.

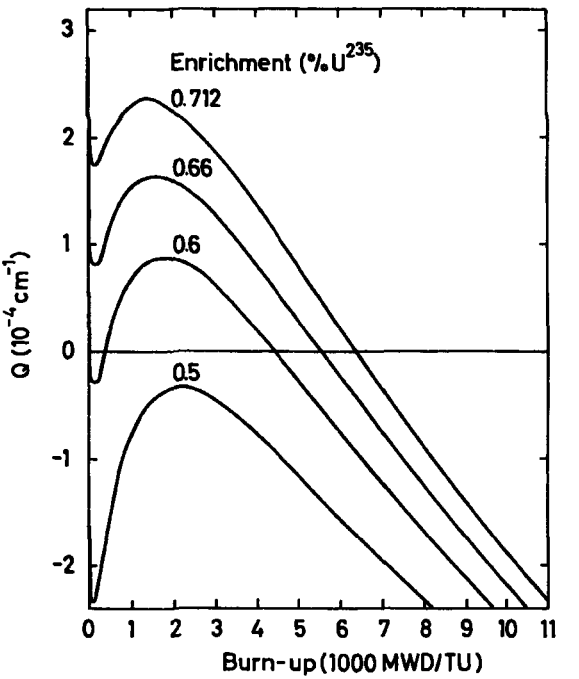

Fig. 3. BHWR 750 MW. Net production cross section Q vs. burn-up for different enrichments.

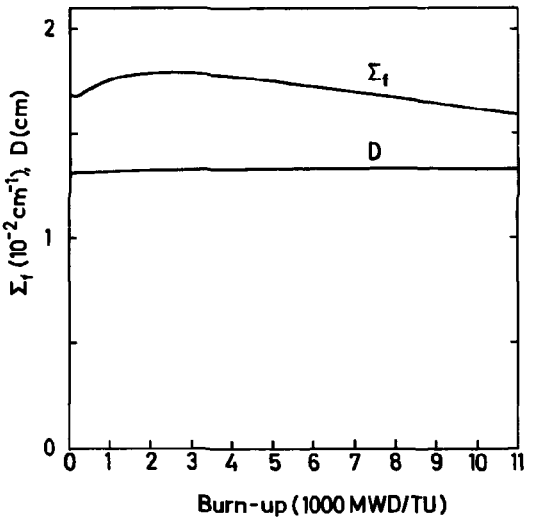

Fig. 4. BHWR 750 MW. Fission cross section $^{1}_{f}$ and diffusion coefficient D vs. burn-up for nat. U.

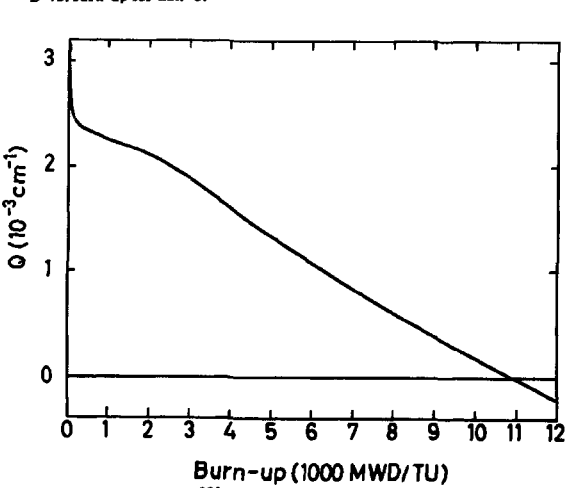

Fig. 5. Yankee, 3.4% U^{235}. Net production cross section Q vs. burn-up.

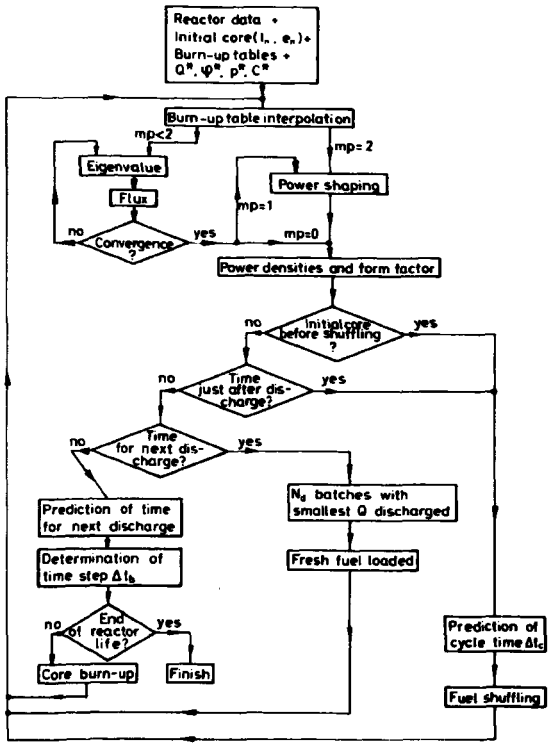

Fig. 6. Generalized flow diagram of SELMA1.

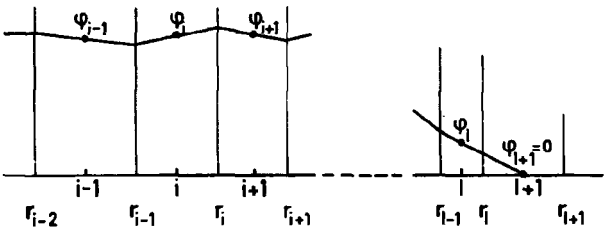

Fig. 7. Mesh description.

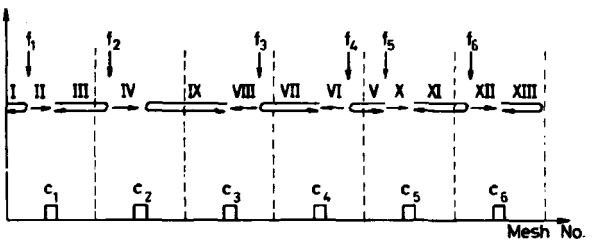

Fig. 8. Illustration of flux calculation in power shaping routine.

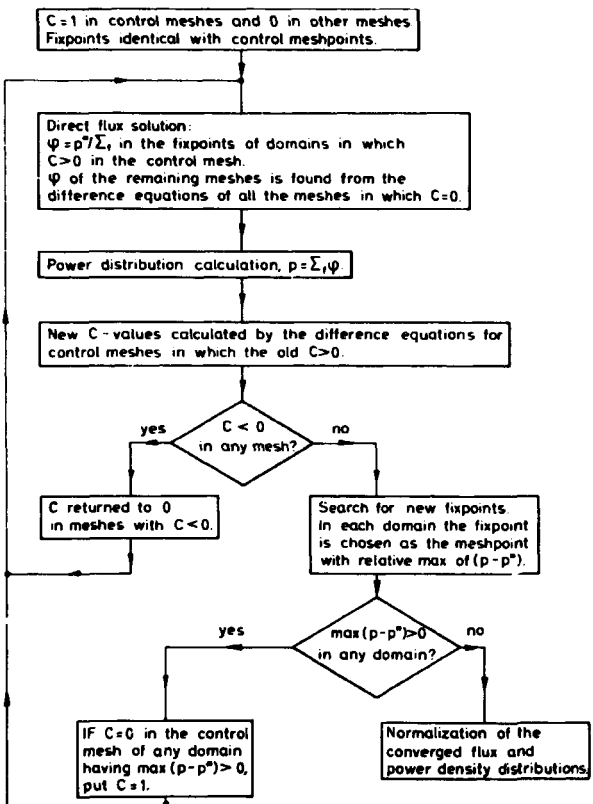

Fig. 9. Block diagram of the power shaping routine.

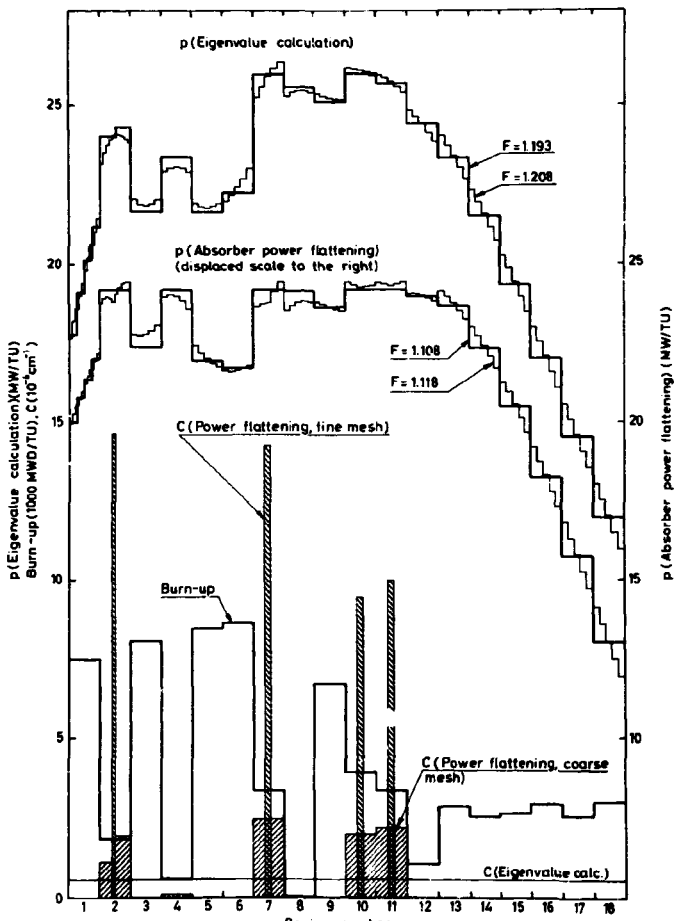

Fig. 10. Power distributions p and control poison cross sections C obtained from traditional eigenvalue calculations and absorber power flattening. Both fine and coarse mesh representation of the core.

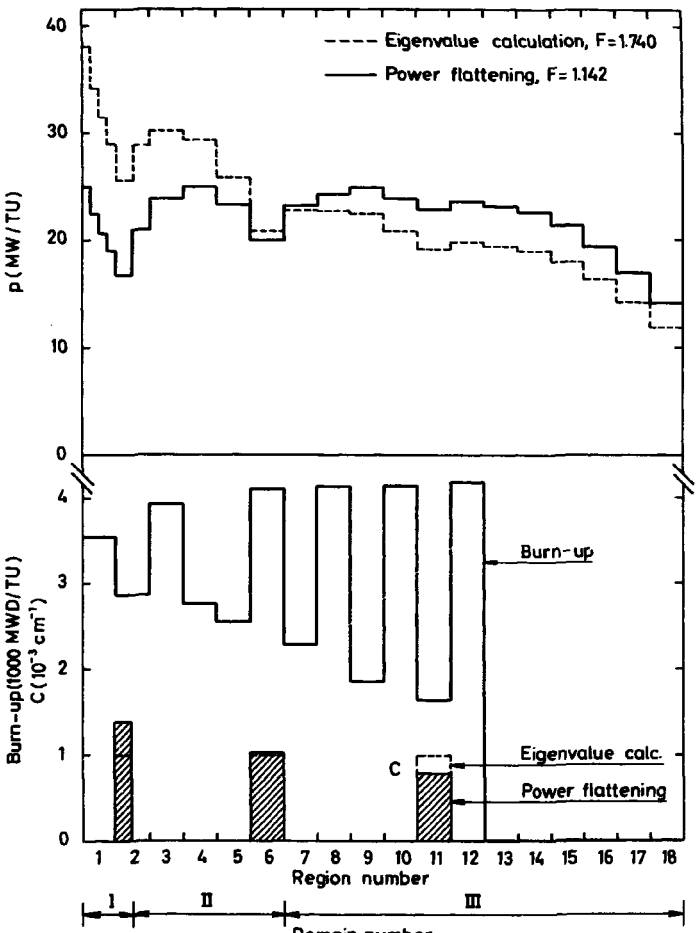

Fig. 11. Power distributions p and control poison cross sections C from eigenvalue calculation and absorber power flattening.

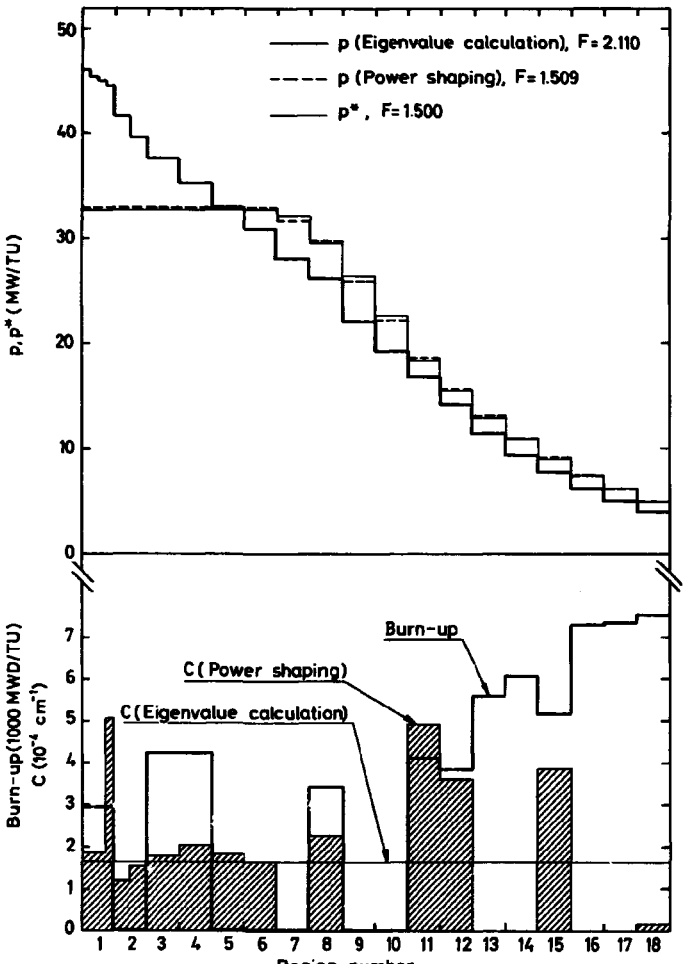

Fig. 12. Power distributions p and control poison cross sections C from eigenvalue calculation and absorber power shaping. Target power p*.

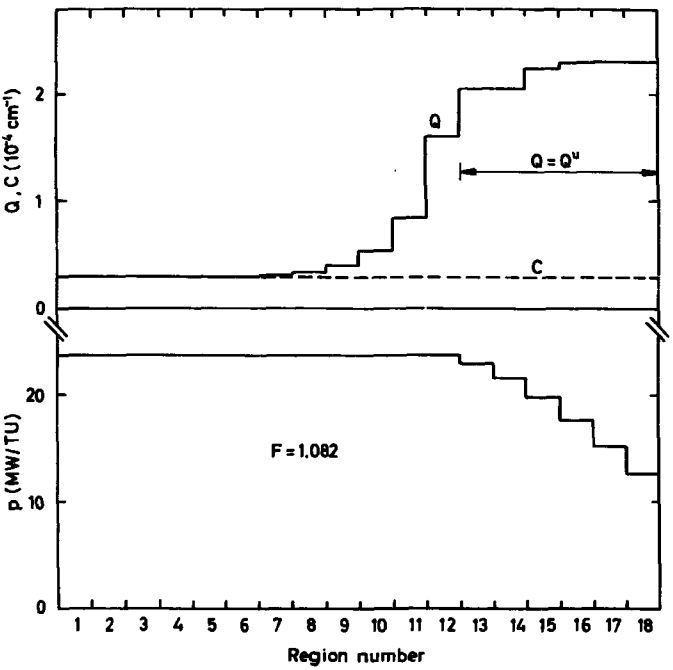

Fig. 13. Ideal Q-distribution with flat power shape p. Upper limit Q^u reached in unflattened part. Uniform control poison distribution C.

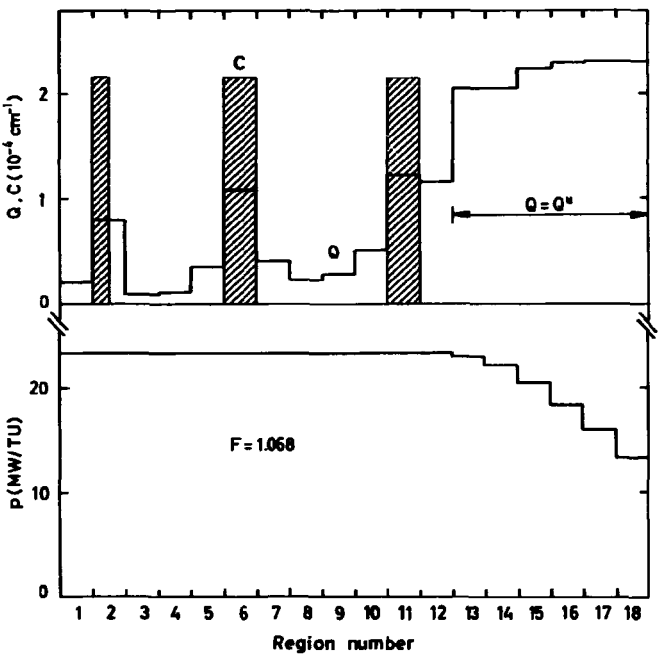

Fig. 14. Ideal Q-distribution with flat power p for the control poison C restricted to three meshes.

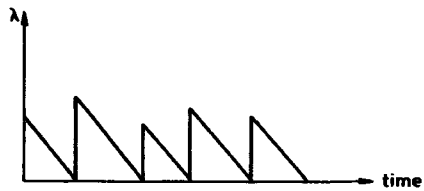

Fig. 15. Development of eigenvalue with time.

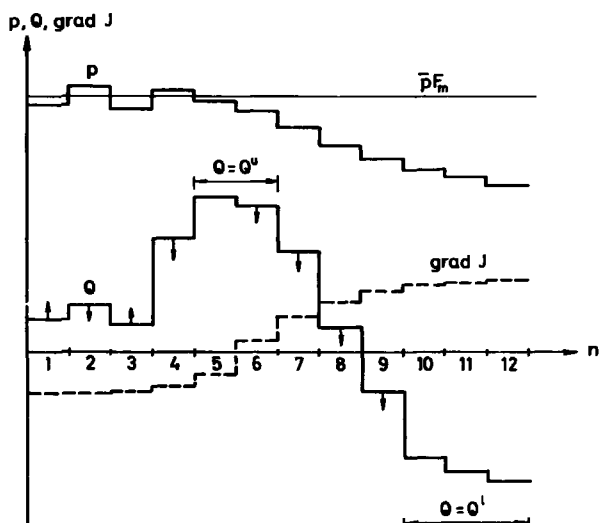

Fig. 16. Illustration of iteration step number k in the search for the ideal Q-distribution giving maximum discharge burn-up.

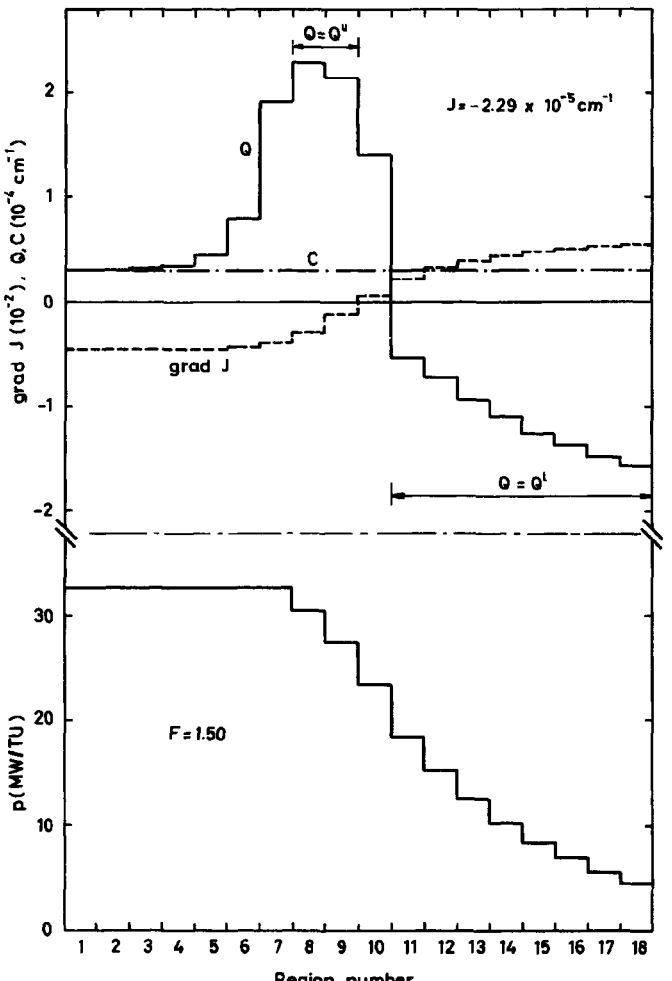

Fig. 17. Ideal Q-distribution for maximum burn-up and form factor limit 1.50. Uniform control poison distribution C.

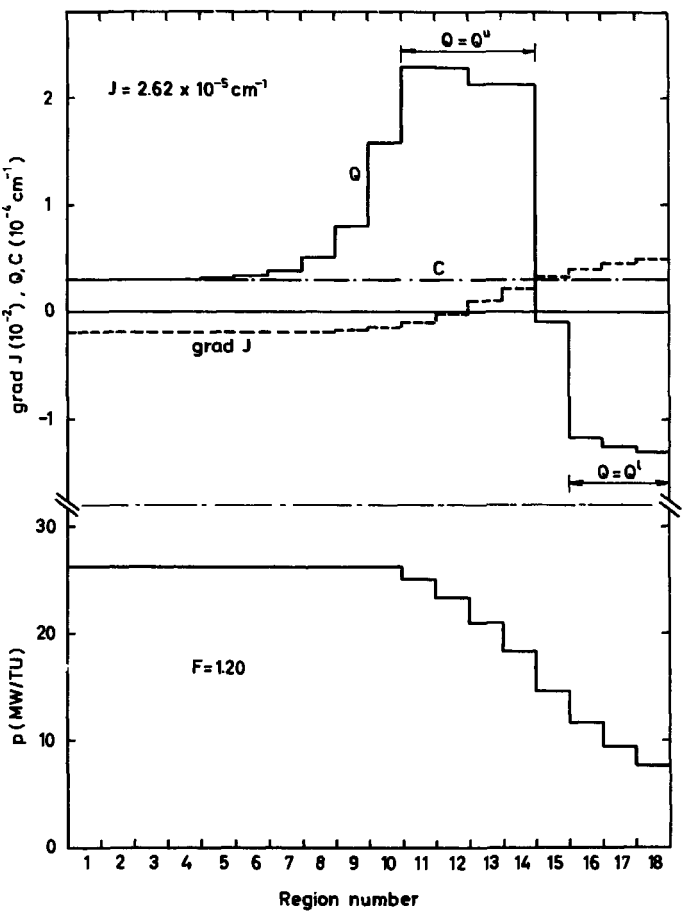

Fig. 18. Ideal Q-distribution for maximum burn-up and form factor limit 1.20. Uniform control poison distribution C.

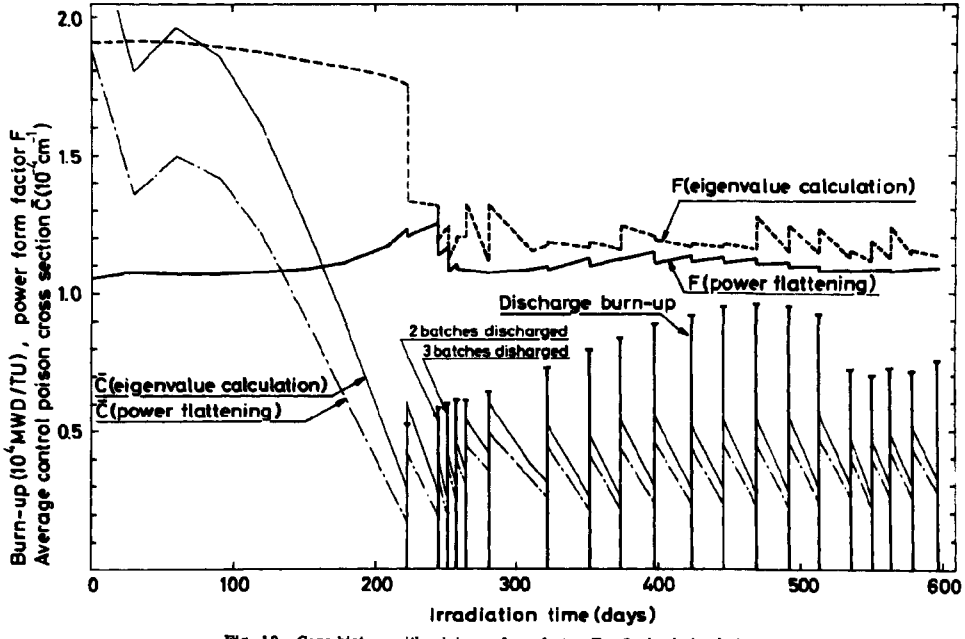

Fig. 19. Core history with minimum form factor F. On-load simulation. Direct shuffling optimization. 5 batch interchanges/cycle.

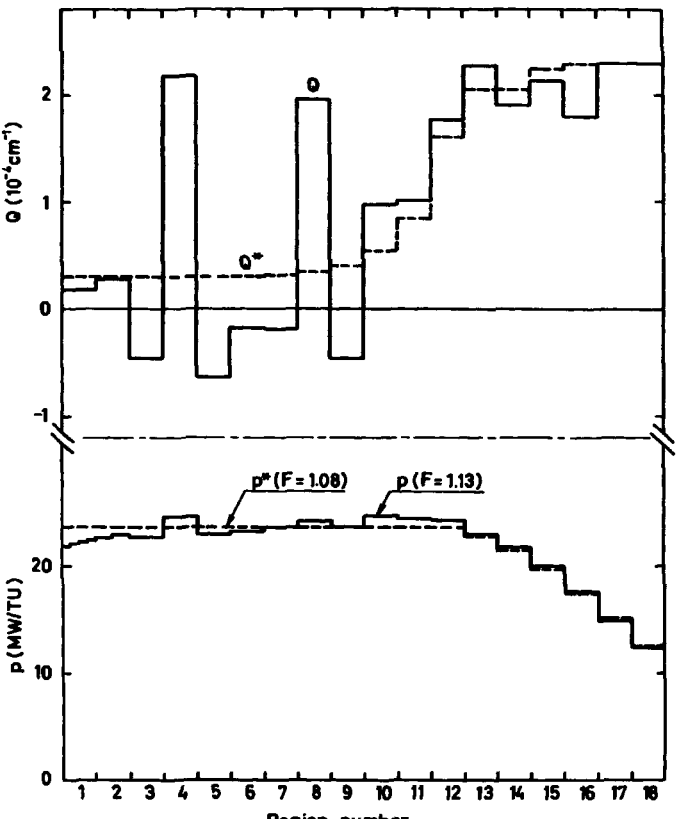

Fig. 20. Comparison of Q-distribution obtained by shuffling and the ideal Q-distribution Q^*. Q-distribution and power distribution p at the end of last cycle in fig. 19.

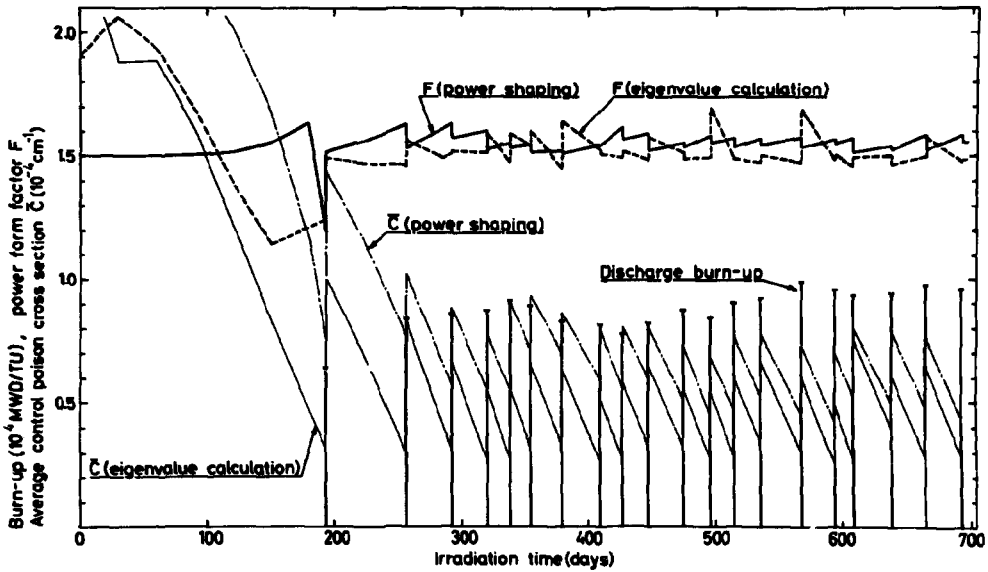

Fig. 21. Core history with maximum fuel burn-up and limited form factor (F_m = 1.50). On-load simulation. Direct shuffling optimization. 5 batch interchanges/cycle.

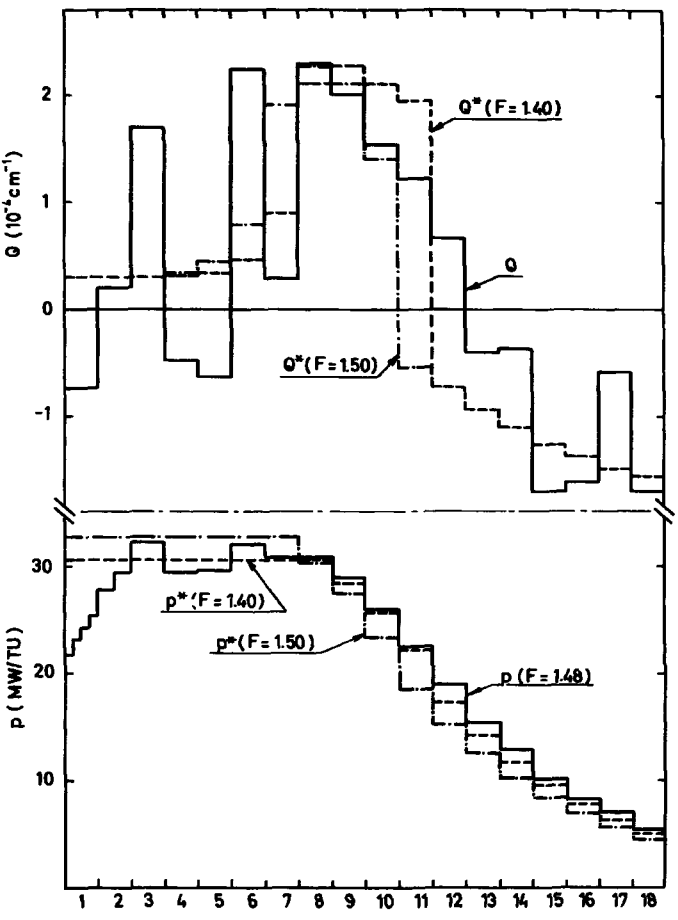

Fig. 22. Comparison of Q-distribution obtained by shuffling and ideal Q-distributions Q^*. Q-distribution and power distribution p at the end of last cycle in fig. 21.

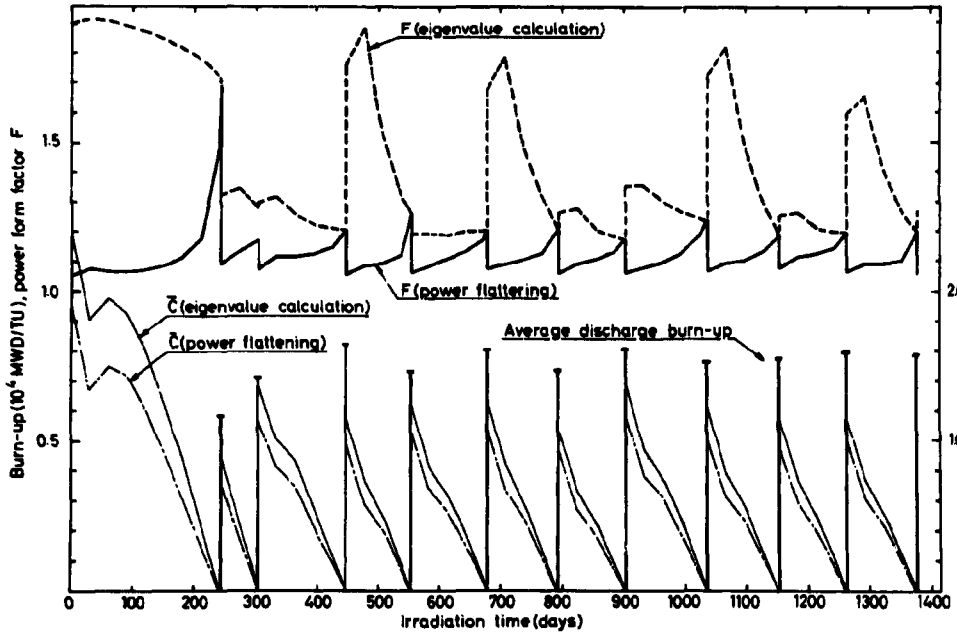

Fig. 23. Core history with minimum form factor F. Off-load simulation. Direct shuffling optimisation. 10 batch interchanges/cycle.

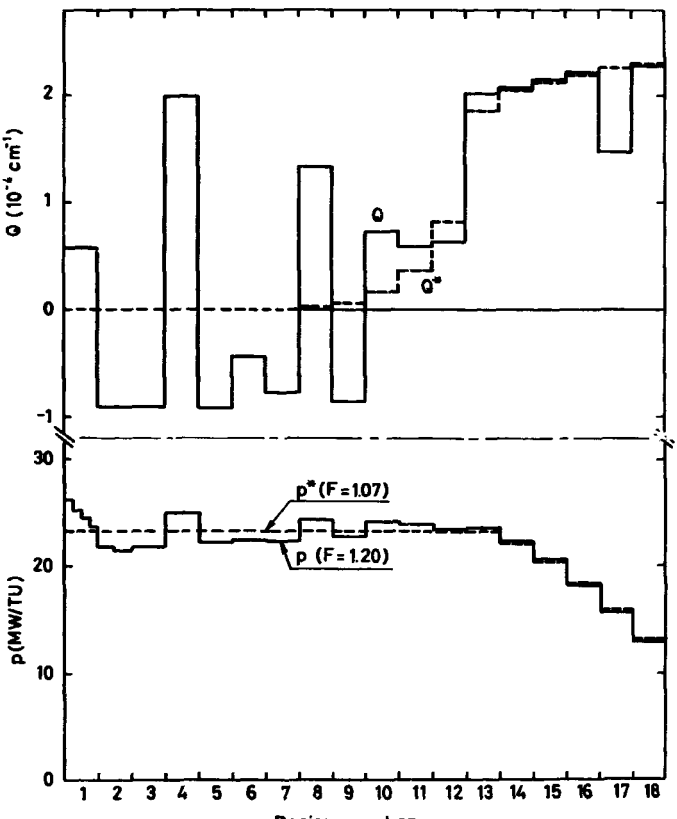

Fig. 24. Comparison of Q-distribution obtained by shuffling and the ideal Q-distribution Q^*. Q-distribution and power distribution p at the end of last cycle in fig. 23.

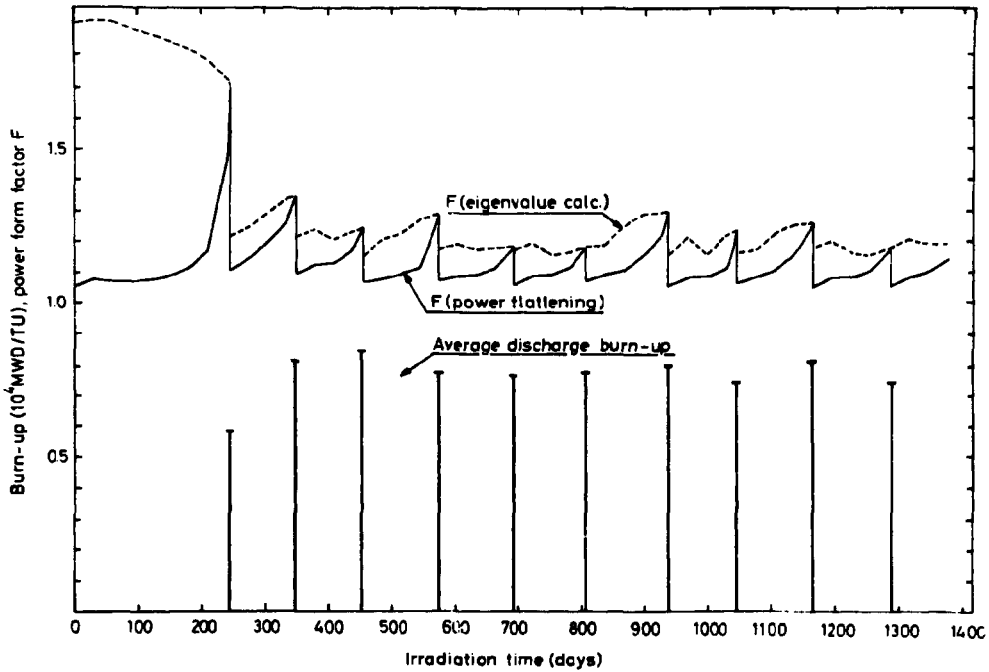

Fig. 25. Core history with minimum form factor at start-of-cycle. Off-load simulation. Direct shuffling optimization. 10 batch interchanges/cycle.

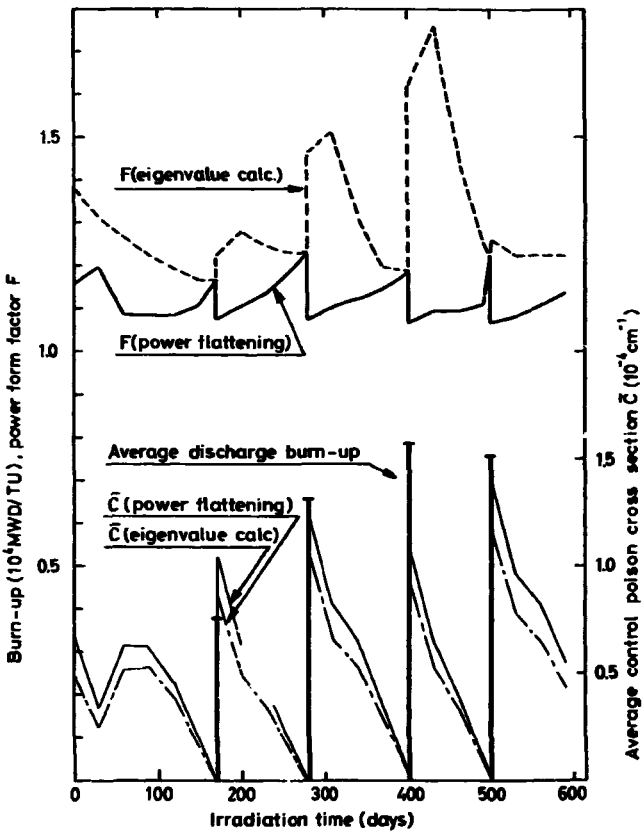

Fig. 26. Initial core history with minimum form factor F. Off-load simulation. 4 enrichments at start-of-life. Direct shuffling optimization. 10 batch interchanges/cycle.

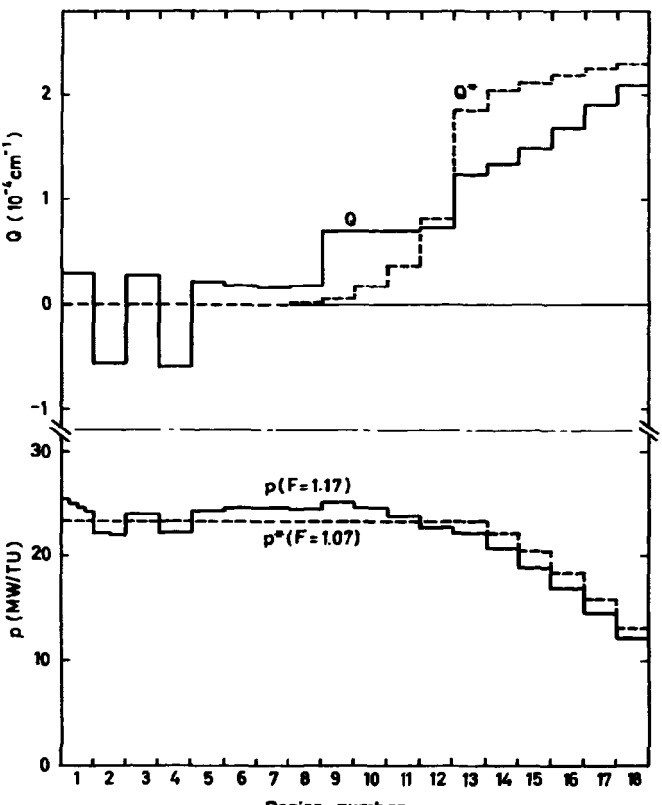

Fig. 27. Comparison of Q-distribution obtained by shuffling and the ideal Q-distribution Q^*. Q-distribution and power distribution p at the end of first cycle in fig. 26 (4 enrichments).

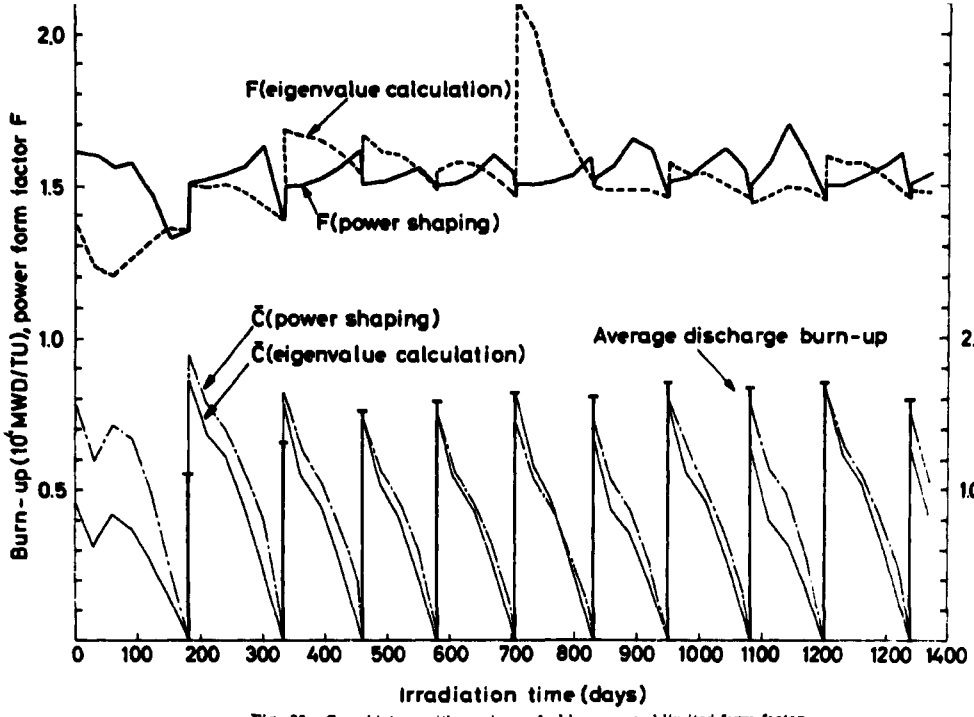

Fig. 28. Core history with maximum fuel burn-up and limited form factor (F_m = 1.50). Off-load simulation. 2 enrichments at start-of-life. Direct shuffling optimisation. 10 batch interchanges/cycle.

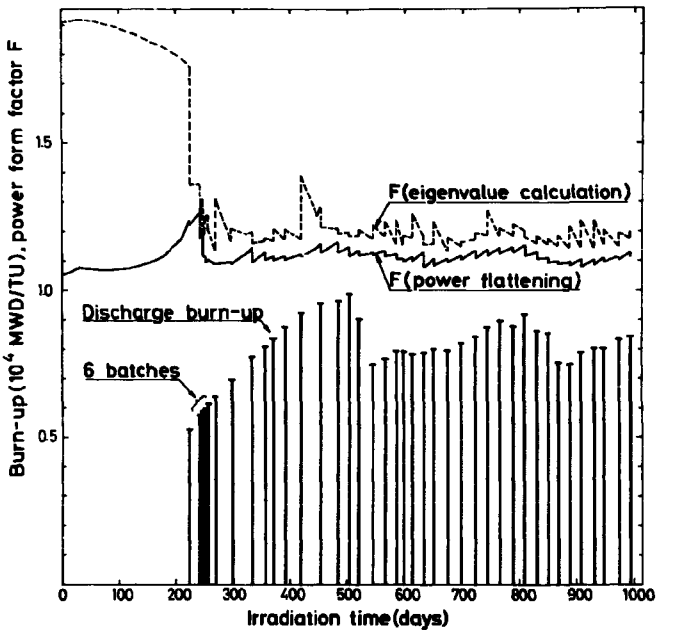

Fig. 29. Core history with minimum form factor F. On-load simulation. Direct shuffling optimization with few trial interchanges. 5 batch interchanges/cycle.

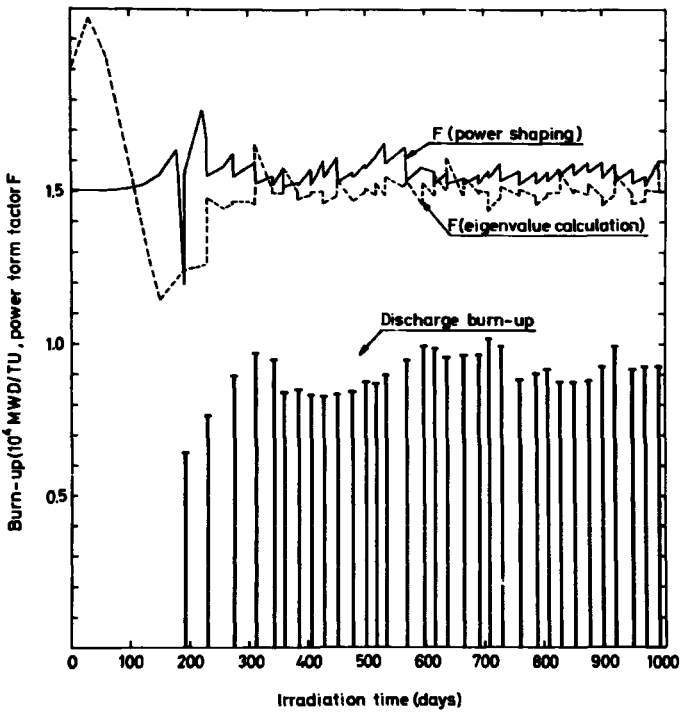

Fig. 30. Core history with maximum fuel burn-up and limited form factor (F_m = 1.50). On-load simulation. Direct shuffling optimisation with few trial interchanges. 5 batch interchanges/cycle.

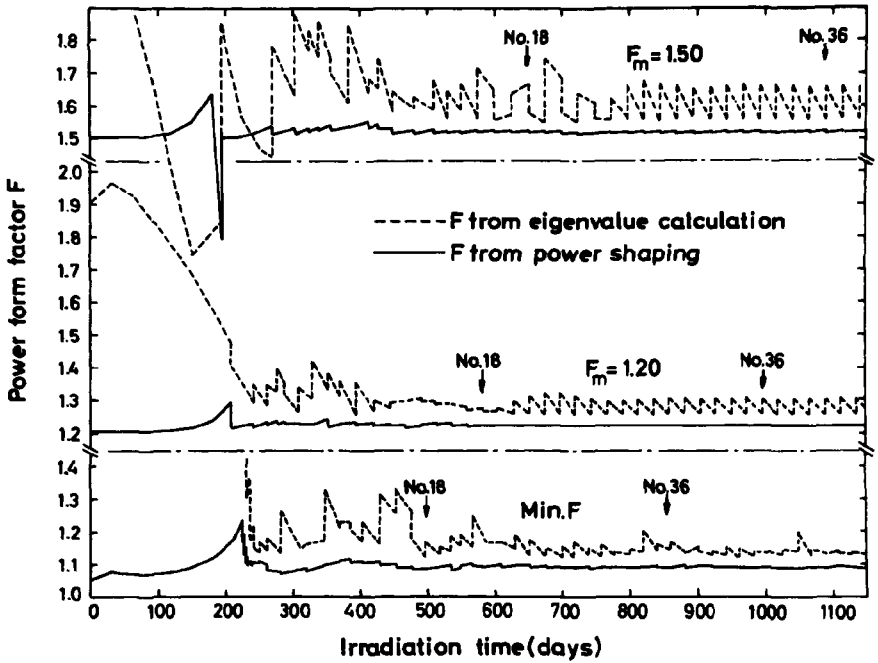

Fig. 31. Form factor histories obtained by the minimum integrated Q-deviations method.

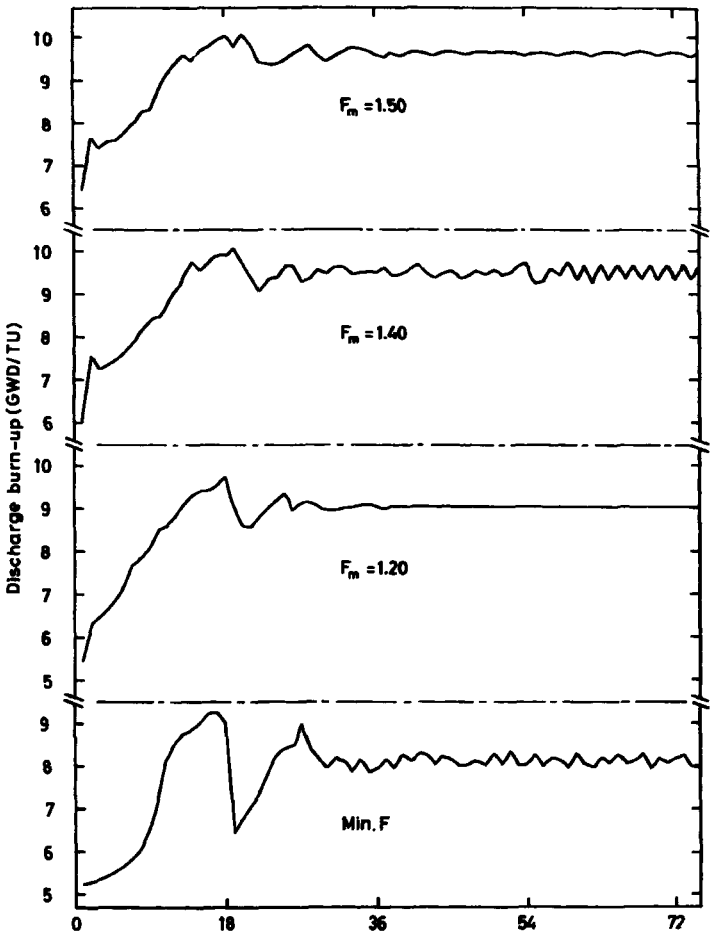

Fig. 32. Discharge burn-up histories obtained by the minimum integrated Q-deviations method. Three curves correspond to fig. 31.

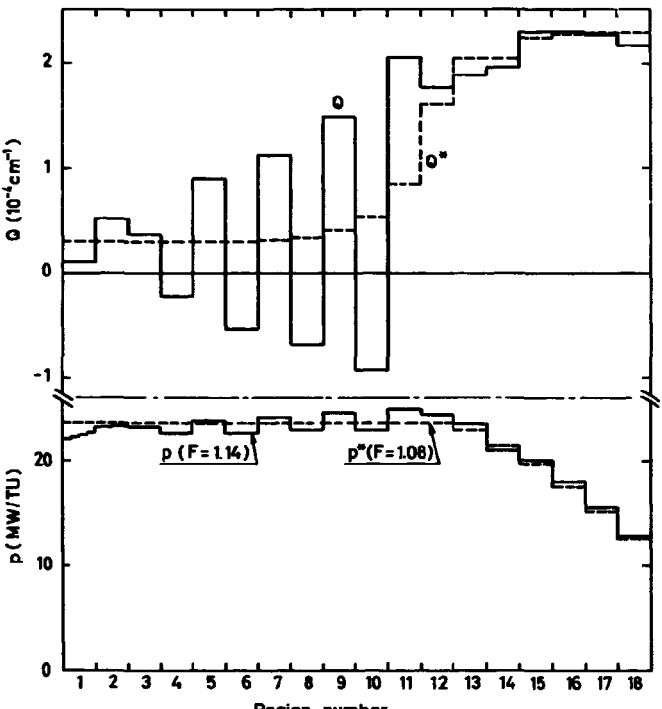

Fig. 33. Q-distribution at end-of-cycle with minimum integrated Q-deviations. Power distribution p approximating p* with minimum form factor.

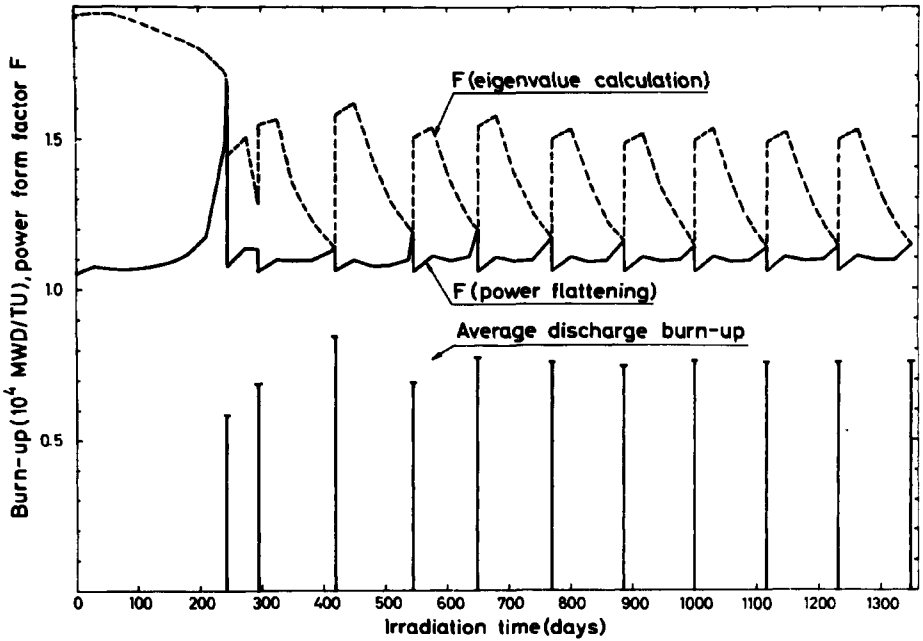

Fig. 34. Core history with minimum form factor F, obtained by the minimum integrated Q-deviations method. Off-load simulation.

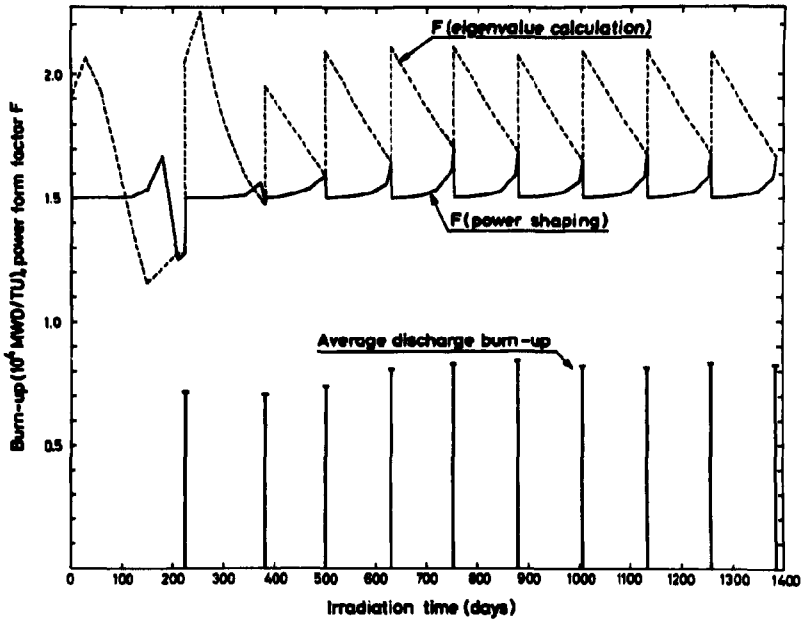

Fig. 35. Core history with maximum fuel burn-up and limited form factor (F_m = 1.50), obtained by the minimum integrated Q-deviations method. Cell-based simulation.

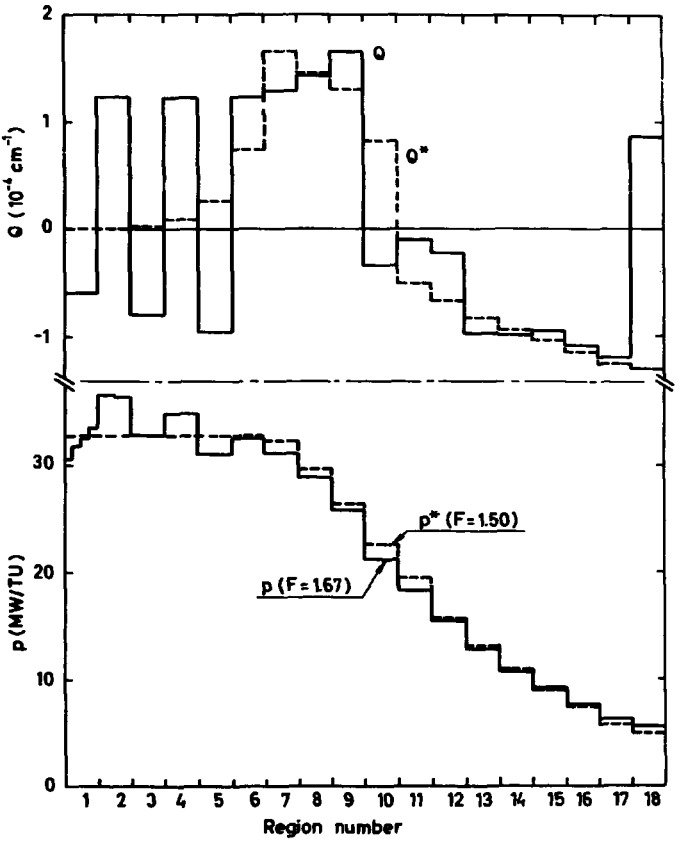

Fig. 36. Q-distribution illustrating bad fit to Q* in the off-load case in fig. 35 with $F_m = 1.50$.

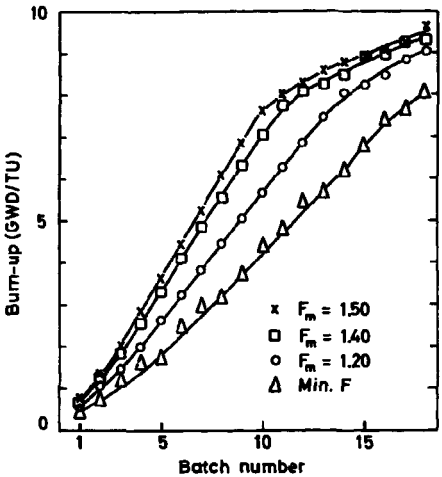

Fig. 37. On-load burn-up spectra.

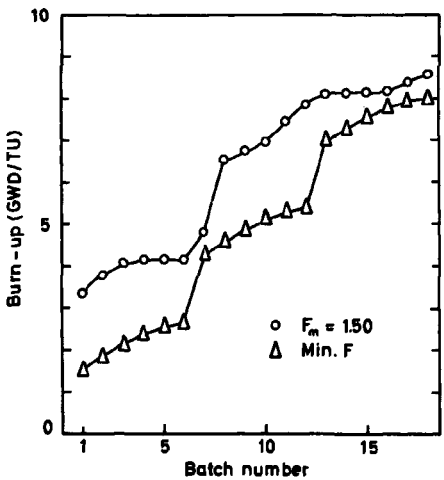

Fig. 38. Off-load burn-up spectra.

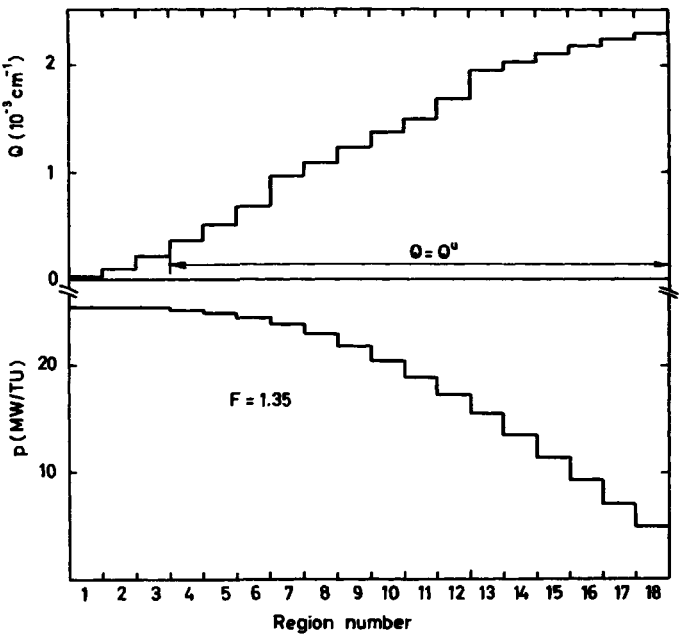

Fig. 39. Ideal Q-distribution with minimum power form factor F for the Yankee reactor. No control poison. Power distribution p unflattened in regions where the upper limit Q^u is reached.

ISBN 87 550 0113 [redacted]